DEVELOPMENT OF A NOVEL MOUSE MODEL FOR HUMAN PULMONARY ARTERIAL HYPERTENSION (PAH)

By

KWON-HO HONG

A DISSERTATION PRESENTED TO THE GRADUATE SCHOOL
OF THE UNIVERSITY OF FLORIDA IN PARTIAL FULFILLMENT
OF THE REQUIREMENTS FOR THE DEGREE OF
DOCTOR OF PHILOSOPHY

UNIVERSITY OF FLORIDA

2007

To my parents, Seoung-Wook Hong and Soon-Im Chung.
To my family, Jung-Ah Um and Jae-Seoung Hong.

ACKNOWLEDGMENTS

I wish to acknowledge all of those who have helped me to complete my graduate studies. Most of all, I would truly like to thank my mentor, Dr. S. Paul Oh, for all of his support throughout my graduate career. He is a great mentor and researcher. His continuing encouragement, guidance and enthusiasm toward science are the reason for my successful graduate studies. Next, I would like to thank my committee members, Dr. Steve Sugrue, Dr. Barry Byrne, Dr. Naohiro Terada, and Dr. Brian Harfe, for their support during my studies. I would also like to thank our collaborators, Dr. Hedeyuki Beppu and Dr. Kenneth Bloch at Massachusetts General Hospital and Dr. En Li at Novartis, for providing us the Bmpr2-floxed mouse line.

I am indebted to all of past and present members of Dr. Oh laboratory for their supports during my studies. In particular, I wish to thank Dr. Tsugio Seki for his help and support in the Alk1 and Alk5 project. I would also like to thank Dr. Young-Jae Lee for his help and advice in the ActRIIB project. I would like to acknowledge Dr. Sung-Ok Park for her support in the Tg(*Alk1-cre*) project. I would like to thank Dae-Song Jang for his help with lung inflation and histology in the Bmpr2 project. I would like to express my gratitude to Donald Lander and Ha-Long Nguyen for their help with English style and grammar of dissertation. Also, I wish to acknowledge the rest of lab members, Eun-Jung Choi, Chul Han, Dr. Hae-Won Han, Eun-Ji Lee, Naime Fliess and Melissa Chen.

I would also like to give my special thanks to my parents, Seoung-Wook Hong and Soon-Im Chung for their constant support during my study. Finally I would like to thank my beautiful wife, Jung-Ah Um, and wonderful son, Jae-Seoung Hong, for being main part of my happiness.

TABLE OF CONTENTS

LIST OF TABLES

LIST OF FIGURES

Figures page

Abstract of Dissertation Presented to the Graduate School
of the University of Florida in Partial Fulfillment of the
Requirements for the Degree of Doctor of Philosophy

DEVELOPMENT OF A NOVEL MOUSE MODEL FOR HUMAN PULMONARY ARTERIAL HYPERTENSION (PAH)

By

Kwon-Ho Hong

August 2007

Chair: S. Paul Oh
Major: Medical Sciences—Molecular Cell Biology

Pulmonary Arterial Hypertension (PAH) is a devastating vascular disorder predisposed by mutation of bone morphogenetic protein receptor type II (*BMPR2*). Given that the heterozygous *BMPR2* mutation incompletely manifests the disease condition of PAH and the endothelial dysfunction has been implicated in PAH individuals, we hypothesized that deletion of *Bmpr2* in the pulmonary endothelial cells (ECs) is sufficient to predispose to PAH. To test this hypothesis, a novel PAH model has been established by using the *Cre/loxP* system.

To the end, first we characterized the dynamic pattern of Alk1 expression via *in vivo* dissection of *Alk1* promoter and intron regions. Based on *in silico* DNA analysis, we isolated a 9.2 kb of *Alk1* fragment which precisely recapitulates the endogenous pattern of Alk1 expression. Transgenic lines carrying the 9.2 kb of *Alk1* promoter/enhancer-*lacZ* gene demonstrated a predominant Alk1 expression in the ECs of large arteries and some capillary beds during development. At adult stage, the level of Alk1 in the systemic ECs was greatly diminished, whereas the Alk1 level in the pulmonary ECs was persistant throughout the stage.

Next, using the 9.2 kb of *Alk1* promoter/enhancer we have developed a novel Cre deleter line, referred as Tg(*Alk1-cre*)-L1, in which an unique pattern of the Cre-mediated DNA excision in the pulmonary ECs was detected. In the Tg(*Alk1-cre*)-L1 line, a uniformly distributed Cre

activity in the pulmonary ECs was detected from E15.5 on. The homogeneous pattern of Cre activity in the pulmonary ECs was persistant, while mosaic or no Cre activity was detected in the systemic ECs during adult stage.

Finally, to investigate cellular impact of the impaired Bmpr2 signaling pathway in pulmonary ECs, the Tg(*Alk1-cre*)-L1 was bred with mice containing conditional Bmpr2 allele. The *Alk1-cre(+);Bmpr2*$^{f/f}$ mice were viable and seemingly indistinguishable from control littermates. In the hemodynamic and morphometric analyses, subsets of *Alk1-cre(+);Bmpr2*$^{+/f}$ and *Alk1-cre(+);Bmpr2*$^{f/f}$ mice revealed an elevation of right ventricular systolic pressure (RVSP) with increases in the number of muscularized distal arteries and thickness of the medial layer. It has been also demonstrated that the frequency of PAH in the groups was increased in an age-dependent manner. Furthermore, some of hypertensive mice exhibited signs of endothelial dysfunctions such as perivascular infiltration of leukocytes and *in situ* thrombosis.

Taken together, we clearly demonstrated that the deletion of *Bmpr2* gene in the pulmonary ECs by itself can predispose to PAH with abnormal vascular remodeling. Because our mouse model is the first genetic model which corresponds to pathophysiological features of human PAH, we believe that mouse lines we developed are useful genetic resources for further studies on elucidating the underlying mechanism of PAH.

CHAPTER 1
INTRODUCTION

Physiology of Pulmonary Circulation

The lung is a vital and highly vascularized organ whose main functions are to provide oxygen (O_2) to peripheral tissues/organs via the bloodstream and remove carbon dioxide (CO_2) from the blood. To fulfill this purpose efficiently, the nature of pulmonary circulation is high flow and low resistance. Pulmonary circulation is very sensitive to any influences affecting the blood flow. This is because the lung is the only organ which accommodates for the whole cardiac output with low blood pressure. The right ventricle, a driving force for pulmonary circulation, is a thin-walled tissue that is poorly prepared for a rapid change in loading condition. The average right ventricular systolic pressure (RVSP) is about 25 mmHg and the average right ventricular diastolic pressure is 0-1 mmHg. The average systolic pressure of the pulmonary artery is the same as the average RVSP. On the other hand, the average diastolic pressure of the pulmonary artery is about 8 mmHg.

Anatomically, pulmonary vessels differ from systemic vessels in that, for a given caliber, the medial layer of pulmonary arteries is much thinner than that of systemic arteries, which reflects the lower resistance in pulmonary circulation. Another difference compared to systemic blood vessels is that arterioles, which generate resistance in systemic circulation, are not present in the pulmonary circulation. The arterioles are replaced by structures called “precapillary arteries”. The lack of arterioles results in transmission of the pressure of the pulmonary artery to alveolar capillaries and pulsatile blood flow.

Perturbations in the homeostasis of cardio-pulmonary vascular physiology result in fatal conditions such as pulmonary arterial hypertension (PAH). PAH is defined as more than 25 mmHg of mean pulmonary artery pressure (mPAP) at rest, or 30 mmHg with exercise (1). PAH

is the third most common cardiovascular disease in persons more than 50 years old, after coronary disease and hypertension (2). Although PAH has been clinically recognized since the late 1800s (3), there are some limitations in studying the underlying mechanism of PAH. One of the biggest limitations is that most of the human lung samples available for studies are from lung biopsies or samples from lung transplants of individuals in the end-stages of PAH. Therefore, there is a gap of knowledge in the pathophysiological progress of PAH. Furthermore, because a blood vessel is a multi-layered and dynamic organ, there is a paucity of knowledge as to the role of each layer in the initiation or procession of PAH. Therefore, the animal model system is considered as an alternative and plausible approach to studying PAH at different pathophysiological stages of the disease. The physiology of a mouse, particularly its pulmonary circulation, is similar to that of a human. For example, the mean systolic PAP of a mouse is about 24 mmHg and the mean diastolic PAP is 8.5 mmHg (4). Thus, the long-term goal of this study is to develop a novel mouse model for studying the underlying mechanisms of human PAH.

Classification of PAH

The current system of classification for pulmonary hypertension (PH) has been established as the result of three World Health Organization (WHO) conferences. The most recent classification of PH followed the results of the 3rd World Conference in Venice in 2003 (5). According to this conference, PH is generally classified as PAH, PH with left heart disease, PH associated with lung diseases and/or hypoxemia, PH due to chronic thromboitic and/or embolic disease (CTEPH), and miscellaneous (Table 1-1).

PAH is subclassified into: 1) idiopathic PAH (IPAH, formerly known as primary pulmonary hypertension, or PPH), 2) familial PAH (FPAH), 3) in association with other pathological conditions (APAH), 4) in association with significant venous or capillary involvement, and 5) persistent PH of the newborn. IPAH is PAH due to an unknown cause.

IPAH is a rare disease with an incidence of 2-3 cases per million per year, and there are twice as many female as male patients (6). The mean age of diagnosis is 37 years (7). Shortness of breath (dyspnea) and fatigue are the most common symptoms of PAH, followed by chest pain, fainting spells (syncope), and heart failure. Although it is dependent on the study, around 10% of PAH individuals are estimated to be FPAH. FPAH is a form of inherited PAH due to mutations of bone morphogenetic protein receptor type II (BMPR2) or activin receptor-like kinase 1 (ALK-1). The symptoms are similar to those of IPAH. Other pathological conditions such as connective tissue diseases (CTD), congenital heart diseases, HIV infection, and some drugs may also lead to the development of PAH. Other occlusive vasculopathy, such as pulmonary occlusive venopathy and pulmonary microvasculopathy, can also cause PAH. The prognosis of survivor and clinical trials of PAH subjects are generally estimated by WHO functional class [formally known as New York Heart Association (NYHA) functional class] (Table 1-2), exercise endurance (distance walked in 6 minutes), and hemodynamics (8).

Pathological Characteristics of PAH

Pathologically, PAH is characterized by obstruction of the small pulmonary arteries in association with medial hyperplasia, neointima formation, plexiform lesions, and occasionally thrombotic lesions.

Remodeling in Intimal Layer

The intimal layer (approximately 1-2 μm of thickness) consists of a base membrane and a single-layered lining of endothelial cells (ECs) localized between the internal elastic laminae and vascular lumen. Pulmonary ECs seem to be a very quiescent cell-type with a doubling time of more than 0.5-1yr. Although the contribution of ECs to PAH is poorly understood, excessive proliferation of ECs is one of the key features of PAH. One remarkable pathological feature of PAH is neointima formation. The term reflects the formation of cell layers with an extracellular

matrix (ECM) between the endothelium and internal elastic laminae in small and large arteries (9). The major cell-type composing the neointima is myofibroblast, which may test positive with some smooth muscle cell (SMC) markers such as α-smooth muscle actin (αSMA) and vimentin. The myofibroblast does not express EC-marker genes such as CD31 and the von Willebrand factor (vWF) (9). The origin of the myofibroblast is currently unknown. In *in vitro* analysis, it has been shown that the myofibroblast isolated neointima exhibited a different response to growth factors compared to cell isolated from vascular SMCs (10). The data suggests that the myofibroblast might be originated from not only SMCs but different cell-types such as transdifferentiation of EC or advantitia cells.

Although the rule of monolayer of endothelium is generally maintained in the PAH lung, studies have shown that tumors or tumorlet-like clusters of ECs contributed by monoclonal endothelial proliferation in plexiogenic-lesions can form (11;12). Plexiform lesion is a hallmark of a severe form of PAH showing intimal proliferation with the formation of multiple capillary-like channels in a pulmonary artery (13). The cell-type responsible for plexiform lesions is still under debate, though it has been suggested that ECs, responding to cytokine, growth factors, or vascular injury, underlie the initiation of the lesions. Cell-types in the plexiform lesion include ECs, myofibroblast, and intermingled connective tissues (11). Interestingly, most pulmonary vessels with plexiogenic lesions show perivascular infiltration of the leukocytes (11;14). Among the cell-types consisting of blood vessel, EC is a dominant cell-type in the plexiform lesion (11). Using the conventional hematoxilin-eosin (H&E) staining, it has been shown that plexiform lesions have been detected in only 10-20% of total pulmonary artery samples (15). The plexiform lesion can be found in any vessel of the lung. One typical example of a plexiform lesion is in the supernumerary artery. If there is a plexiform lesion in the vessel, a concentric

laminar intimal fibrosis (CLIF) is found at the close to branching point, and followed by a plexiform lesion. After the plexiform lesion, an angiomatoid (aneurismal dilation of vessel) lesion is found (13). Although plexiform lesions can occur without CLIF, CLIF is associated with plexiform lesions. A recent study suggested that ECs with a mutation of BMPR2 seem to increase the susceptibility to apoptosis which results in fragile ECs of the precapillary arteries. However, after repeated apoptosis, the remaining apoptosis-resistant ECs seem to undergo massive proliferation and eventually develop plexiform lesions (16).

Remodeling in Medial Layer

Vascular SMCs are major components of the medial layer. Beside the SMCs, elastic laminae are stacked between SMCs. Like ECs, SMCs are also replicatively quiescent and relatively unresponsive to mitogen (17). Hyperplasia in the medial layer is a common feature in all the different forms of PAH. Medial thickening in PAH reflects the role of SMCs in the control of vascular tone. In precapillary vessels, cells inside internal elastic laminae seem to differentiate into SMCs (18). Depending on the location of the blood vessel, the source of SMC differentiation varies. In distal vessels lacking elastic laminae, pericyte and interstitial fibroblast from surrounding lung parenchyma appear to contribute to the process of muscularization (19).

Remodeling in Advantitia Layer

PAH also causes thickening of advetitia layer by increasing the number of fibroblasts. A recent study using a hypoxia model has been shown that CD68-positive circulating mesenchymal precursor of a monocyte/macrophage lineage contributes to the thickening of the advantitia layer (20). Many of the cells produce type I collagen and are αSMA-positive cells. It seems that the induction of many proinflammatory cytokines and chemokines such as monocyte chemoattractant protein (MCP)-1, macrophage inflammatory protein (MIP)-2, interleukin (IL)-1β, IL-6 are involved in the remodeling of the advantitia layer (21).

Treatment of PAH

Basic Treatment

To prevent the worsening of a disease's progress, some lifestyle modifications such as low-level aerobic exercises, avoiding exposure to hypoxic conditions like high altitudes, and restriction from a high-salt diet are recommended (5;22). The hemodynamic changes during pregnancy, labor, and the postpartum period are devastating to PAH patients (23). Diuretic therapy can be used to reduce the right ventricle preload in PAH individual with heart failure. Increases in intracellular calcium and calcium-mediated signals have an effect on muscle contraction (24;25). A study has shown that a high dose of calcium channel blockers have a beneficial effect on the survival rate of some PAH patients (26).

Prostacyclin Therapy

Prostacyclin (Prostaglandin I_2) and thromboxane A_2 (TxA_2) are major metabolites of arachidonic acid in blood vessels. Prostacyclin is a potent vasodilator through production of cyclic AMP (cAMP) and inhibits the growth of SMCs (27). On the other hand, TxA_2 is a potent vasoconstrictor. It has been shown that PAH patients showed a decreased urinary level of prostacyclin metabolites (6-keto-prostacyclin $F_{2\alpha}$), whereas the urinary level of TxA_2 metabolites (TxB_2) has increased (28). The data suggests that the balance between vasodilator and vasoconstrictor is severely impaired in PAH individuals.

The intravenous infusion of epoprostenol (prostacyclin) was first used to treat PAH in the early 1980s (29). Studies showed that continuous intravenous epoprostenol clearly has beneficial effects to WHO functional class III or IV (30;31). Epoprostenol treatment improved exercise tolerance, hemodynamics, and overall survival rates (31). The intravenous treatment of epoprostenol has some side effects such as jaw pain, headache, diarrhea, and nausea (32;33). As

an alterative method to intravenous delivery of prostacyclin, subcutaneous (treprostinil), oral (beraprost), or inhaled (iloprost) delivery of protacyclin analogues are being used (34-36).

Endothelin-1 Receptor Antagonists

Endothelin-1 (ET-1) is mainly released by ECs and exerts its effect in vascular SMC in a paracrine manner. ET-1 works as a vasoconstrictor and has a mitogenic effect on SMC proliferation (37). Its vascular effect is mainly mediated through ET_A and ET_B, which are G protein-coupled receptors (38). ET_B is predominantly expressed in ECs, whereas ET_A is mainly expressed in SMCs (39;40). It has been shown that individuals with PAH exhibit high levels of circulating ET-1 (41;42). Bosentan, a US Food and Drug Administration (FDA) approved drug, is a nonselective ET receptor antagonist which can work on both ET_A and ET_B. Studies demonstrate that the treatment of bosentan on WHO functional class III patient significantly ameliorate hemodynamics and 6MWT (43;44). Because ET_A is the ET-1 receptor expressed in SMCs, selective ET_A receptor blockers such as sitaxsentan and ambrisentan are being investigated for the treatment of PAH (45;46).

Nitric Oxide (NO) Therapy

NO produced by ECs functions as a potent vasodilator through the stimulation of soluble guanylate cyclase and increased production of intracellular cyclic GMP (cGMP) in SMCs (47). The cellular effects of an increased level of cGMP include decreased sensitivity to myosin and the inhibition of calcium released from the sarcoplasmic reticulum (47). The level of cGMP is regulated by phosphodiesterase type 5 (PDE5) (48). Studies have demonstrated that changes in NO pathways were found in lungs with PAH (49;50). It has also been shown that PDE5 is upregulated in the hypoxia-mediated animal model for PAH (51;52).

Inhaled NO gas relaxes pulmonary arteries, which decreases vascular resistance, PA pressure, and RV afterload (53;54). A recent study demonstrated that the oral treatment of

cidenafil citrate (Viagra™), an inhibitor of PDE5, improved exercise capacity, WHO functional class, and hemodynamics in PAH patients (55).

Investigating Therapies

Simvastatin (Zocor™) is a lipid-lowering agent derived from *Aspergillus terreus*. It has been shown that simvastatin has a proapoptotic effect on neointimal SMCs in an experimental PAH model (56). Oral treatment of simvastatin (20-80mg/day) improves exercise endurance and hemodynamics without adverse effects (57).

Studies have also shown that a platelet-derived growth factor (PDGF) receptor antagonist, imatinib mesylate (STI571, Gleevec™) reverses the experimental PAH model and improves exercise capacity, hemodynamics, and cardiac indices (58;59).

Genetics of PAH

Progress has been made in elucidating the cellular impact of a mutation in PAH genes during the development of PAH, since the *BMPR2* gene was first identified as a PAH gene (60;61). Studies show that a mutation of the *BMPR2* gene is responsible for as much as 70% of all FPAH cases and up to 26% of IPAH cases (62). BMPR2 is a member of type II receptors in the transforming growth factor-β (TGF-β) signaling pathway. Recent studies have also demonstrated that other TGF-β receptors, activin receptor-like kinase-1 (ALK-1) and endoglin (Eng), are also related to PAH (63-68). Mutations in ALK-1 and ENG are also linked to another inherited vascular disorder called hereditary hemorrhagic telangiectasia (HHT) (69-72). Interestingly, loss of BMPR2 expression is also found in human prostate cancer cells, suggesting that the BMPR2 signal plays an important role in the regulation of cell proliferation (73).

Transforming Growth Factor-β (TGF-β) Signal Transduction

TGF-β is a large cytokine family that contributes to diverse cellular processes. TGF-β was originally named after its ability to cause a phenotypic transformation of cultured epithelial cells. However, the cellular effects of each member seem to be varied or even opposite, depending upon the cell-type and its developmental stage. Some of these cellular effects include cell proliferation, migration, apoptosis, pattern formation, and immunosupression. TGF-β family members include TGF-βs, bone morphogenic proteins (BMPs)/growth and differentiation factors (GDFs), and activins/inhibin. Each subgroup is categorized by sequence homology and the utilization of cytoplasmic mediator proteins, SMADs (74-76).

TGF-β was initially identified by a finding that a pool of growth factors secreted from a transformed mouse fibroblast was able to induce the formation of foci in the soft agar assay (77). Later, Roberts *et al.* found that TGF-β was one of the active factors in that pool of growth factors (78;79). Since then, the TGF-β superfamily has expanded. In mammals, more than 30 ligands have been identified as members of the TGF-β superfamily.

TGF-β signal transduction is initiated by the binding of a ligand to a heteromeric complex of transmembrane serine/threonine type II and type I receptors. Once ligands bind to a type II receptor, the ligand-type II receptor complex recruits and trans-phosphorylates type I receptor, which, in turn, activates cytoplasmic SMAD proteins. Although most ligands are functionally different, they utilize a limited number of receptors and SMADs. For more than 30 known TGF-β family ligands, only five type II receptors and seven type I receptors have been identified, indicating that each receptor mediates multiple signals. One of the key features of TGF-β signaling pathways is that there is a considerable amount of redundancies in the interaction between ligands and type II receptors, as well as type II and type I receptors (80). Biochemical

studies have determined that activin type II receptors (ACVR2A and ACVR2B) utilize ALK2 (ACVR1), ALK4 (ACVR1B), and ALK7 (ACVRL1C) depending on their interacting ligands including activins (INHBA, INHBB, INHBC, and INHBE), Nodal, BMP7, and GDF11. Activin receptor-like kinase 5 (ALK5) (TβRI; TGFBR1) has been shown to interact with the TGF-β type II receptor (TβRII; TGFBR2) and to mediate TGF-β subfamily signals. Recent studies have implicated ALK5 in mediating other TGF-β family signals, such as GDF8 and GDF11 (81).

Eight SMAD proteins have been identified in mammals so far. The activated type I receptor phosphorylates receptor-regulated SMADs (R-SMADs). R-SMADs then form a complex with a common partner, SMAD4 (Co-SMAD) then enter into the nucleus. Once there, the SMAD complex interacts with diverse transcriptional coactivators or corepressors, according to their genetic makeup and cellular contexts. Depending on which R-SMAD is utilized, TGF-β signaling can be generally separated into two pathways: SMAD 2/3 for TGF-β and SMAD 1/5/8 for BMP.

Bone Morphogenetic Protein Receptor Type II (BMPR2)

Human BMPR2 consisting of a total of 13 exons is localized on chromosome 2q33 (82-84). BMPR2 is comprised of 4 major domains: the extracellular domain (ED), transmembrane domain (TD), kinase domain (KD) and the long cytoplasmic domain (CD). The exons 1-3 encode the ED, exon 4 encodes the TD, exons 5-11 encode the serine/threonine KD, and exons 12 and 13 encode the CD. It has been shown that each domain is highly conserved among species (85). The large C-terminar CD is present only in the BMPR2 among receptors in TGF-β superfamily. Studies have suggested that human BMPR2 is produced by alternative splicing, in which a short form lacks exon 12 encoding a part of CD (84;86). The short form is only 30 amino acids (AA) long compared to 527 AA in the long form after kinase domain (85;87).

Currently, the function of the long CD is largely unknown. Interestingly, a mutation in exon 12 is commonly observed in PAH patients, suggesting that the domain has a specific function; for example, crosstalk with other signaling pathways (88-90). Ramos *et al.* showed that BMPR2 is predominantly expressed in ECs, SMCs, type II pneumocyte, and epithelial cells (91). Studies also demonstrated that BMPR2 is localized in lipid rafts where BMPR2 interacts with caveolin-1α and -1β (91;92).

Atkinson *et al.* demonstrated that BMPR2 mRNA and proteins are markedly reduced in the lung of a PAH individual with a heterozygous mutation of the BMPR2 gene, as compared to normal individuals (14). A lesser reduction of BMPR2 was also found in individuals with secondary PH. The data suggests that reduction of the BMPR2 level primarily contributes to the development of PAH in patients with a BMPR2 mutation.

Mutation of BMPR2 can be found in any of the exons except exon 13 (90). The types of mutations that can be found in BMPR2 include missense, nonsense, frameshift, deletion, duplication, abnormal splicing, and single nucleotide polymorphism (SNP) (88-90). More than 50% of BMPR2 mutations are predicted to lead to protein truncation through a premature termination codon and that there is an age variability for the initial onset of PAH (93).

One of the key genetic features of PAH is that a mutation of any of the PAH genes incompletely manifestates PAH. Studies have revealed that a BMPR2 mutation develops PAH in around 20-30% of individuals with heterozygous BMPR2 mutations, suggesting that other factors might be involved in the development of PAH (62;94). Studies also showed that Bmpr2 null or hypomorphic mice are embryonic lethal due to defects in mesoderm formation and outflow tract formation of the heart (95;96).

So far, more than 20 BMP/GDF ligands have been identified in humans (97). In biochemical studies, some of the BMPs/GDFs such as BMP2, 4, 6, 7, 9, 15, and GDF-5 can bind to BMPR2 and utilize ALK-1, -2, -3, -5, or -6 as a type I receptor (98-101). Depending on the utilization of a type I receptor, signals through BMPR2 are mediated by either SMAD2/3 or SMAD1/5/8. BMP signaling through BMPR2 has been implicated for various biological processes such as cardiac development, bone and cartilage formation, craniofacial development, and reproduction (98;102-104). Cellular effects of the BMPR2 signal in the vasculature seem to be heterogeneous rather than homogeneous, depending on the cell-type. For example, BMPR2 signal by BMP2, 4, or 7 seems to cause apoptosis in the human pulmonary artery SMC by downregulating Bcl-2 and in a caspases (caspase 3, 8, or 9)-dependent manner (105;106). Studies have shown that the reduction of the BMPR2 resulting from knockdown or overexpression of the mutant form of BMPR2 can rescue from BMP7-mediated apoptosis in SMCs (106). Even in the pulmonary artery SMC, the cellular effect of BMPR2 seems to be dependent upon the BMP protein. Frank *et al.* showed that BMP4 has an effects of proproliferation and promotion of cell migration of pulmonary artery SMCs, whereas BMP2 has an opposite effect (107).

A more complicated model of BMPR2 signaling in SMC was recently reported (108). The authors showed that in the absence of Bmpr2, BMP2/4 can utilize ActRIIa and Alk2 or Alk3, and BMP7 can utilize ActRIIa and Alk2. The redundancy can partially explain why a BMPR2 mutation incompletely develops PAH. On the other hand, a BMPR2 mutation in the pulmonary artery ECs initially causes an increase in apoptosis (16). The study suggested that after a certain amount of apoptosis has occurred, the surviving ECs proliferate in an uncontrolled manner, which in effect causes increased cellularity in the intimal layer. Although a dependence on cell-type for the biphasic function of BMPR2 seems to exist, cell-cell interaction between ECs and

SMCs can also contribute to the development of PAH. A recent study has shown that SMCs exhibit a marked increase in cell proliferation in the presence of a conditioned medium from ECs from PAH individuals (109). The authors have demonstrated that one of the factors contributing to SMCs proliferation is an increased level of serotonin (5HT) due to elevated level of tryptophan hydroxylase (TPH), a required enzyme for 5HT production pathway, in ECs associated with PAH.

Activin Receptor-Like Kinase-1 (ALK-1)

ALK-1 is encoded by 10 exons and is localized on chromosome 12q11-q14 (110;111). It has been shown that a mutation of ALK-1 is responsible for HHT2 (72). Although some geographical regions may show a higher rate of incidence for HHT than others (110), the disease affects more than 1 in 10,000 individuals world-wide (112). It is characterized by recurrent epistaxis, mucocutaneous telangiectasia, gastrointestinal hemorrhage, and arteriovenous malformation (AVM) in the pulmonary, cerebral, or hepatic vasculature (112).

Homozygous deletion of Alk1 causes embryonic lethality by embryonic day (E) 10.5 with severe defects in vascular development (113;114). Recently, Srinivasan *et al.* has shown that heterozygous Alk1 mice display the human HHT phenotype in a number of features showing age-dependent disease penetrance, vascular lesions in the specific organs and pathohistological similarity of the lesions (115). Interestingly, blood vessel malformation in the female uterus was also evident in aged $Alk1^{+/LacZ}$ mice with 129/Sv background (Unpublished observation). The observation is reminiscent of a vascular defect in $Eng^{+/-}$ mice with 129/Ola background (116). Seki *et al.* showed that arterial ECs show a robust Alk1 expression over venous ECs during embryonic and early postnatal stages, but a greatly diminished level of Alk1during adult life, except in pulmonary ECs (117).

Recently, studies have shown that some HHT patients with heterozygous mutation of ALK-1 exhibit pathophysiological conditions of PAH (63;65;66;68). These patients exhibit an increase in mPAP and plexiform lesions in the pulmonary vasculature in addition to HHT phenotypes. The result is paradoxical because the pulmonary pathophysiologys of PAH and HHT are considered to be in opposition. For example, HHT patients carrying pulmonary arteriovenous malformation (PAVM) suffer severe dilation in the pulmonary vessels, which may lead to a decrease in pulmonary resistance. On the other hand, PAH patients exhibit obliteration of small pulmonary arteries, which result in markedly increased pulmonary vascular resistance (63). The molecular mechanism by which heterozygous mutation of ALK-1 develops such opposite vascular phenotypes remains unknown.

Endoglin

Eng, which is encoded by 14 exons, is a type III receptor in TGF-β signaling pathways. Eng is localized on chromosome 9q33-q34. It has been shown that a mutation of Eng is responsible for HHT1 (70;71). A recent study demonstrated that a mutation of Eng can cause HHT phenotypes as well as PAH (68). The study showed that a substitution of a nucleotide is identified within the putative splicing site of intron 12 of Eng, 22 bp upstream of exon 13. The substitution seems to cause a loss of exon 13 without disruption of the reading frame of the Eng.

Another study showed that an HHT individual with a mutation in Eng developed PAH after taking an appetite suppressant, dexfenfluramine (67). Although the underlying mechanism of PAH in a person with an Eng mutation is completely unknown, the studies suggest that the mutation of Eng influences other TGF-β signaling pathways, which then display PAH phenotypes, rather than Eng mutation alone causing PAH.

Animal Models for PAH

Experimental Models

Physiological models

A hypoxia-caused mismatch in the ratio between ventilation (V) and perfusion (Q), is a potent factor in the development of PAH. The hypoxia-induced vasoconstriction is a unique feature of pulmonary physiology. Thus, if the lung is exposed to a hypoxic condition which then causes low partial pressure of arterial oxygen (P_aO_2), pulmonary vascular resistance (PVR) is increased to match the V/Q ratio. Although acute hypoxia might be beneficial to enhance the oxygenation of peripheral blood vessels, chronic hypoxia causes elevation in mPAP. According to the Poiseuille's equation, PVR is inversely proportional to the fourth power of the radius of the pulmonary arteries. Therefore, small changes in the radius of a pulmonary artery can cause a drastic increase in pulmonary arterial pressure. Such chronic hypoxia is followed by vascular remodeling (118). Medial thickness is a remarkable feature of hypoxia-induced PH. Persons who dwell at high altitudes show an increase in hemodynamics, the number of red blood cells (polycythemia), right ventricular hypertrophy, and vascular remodeling (119). Although the molecular mechanism underlying hypoxia-mediated vascular remodeling is not clearly defined, the oxygen sensor(s)-mediated change of ion channels has been implicated as being involved in the vascular remodeling and constriction of SMCs (120;121). It has been shown that hypoxia causes change in the production of mitochondrial reactive oxygen species (ROS), which then results in an increase in cytoplasmic calcium ($[Ca^{2+}]_{cyt}$) concentration via increased influx and the release of Ca^{2+} (122;123). The increased $[Ca^{2+}]_{cyt}$ results in phosphorylation of the myosin light chain, which causes an increase in vascular tone. Hypoxia is also followed by depolarization of the membrane by inhibition of voltage-gated K^+ channel (Kv) activity (120). Recently, Takahashi *et al.* showed that sustained exposure to hypoxic conditions causes a

reduction in the BMPR2 level in the experimental model (124). It seems that a loss of BMPR2 in SMC causes a reduction of Kv expression, which results in depolarization of the membrane (125). A recent study demonstrated that sustained hypoxia causes perivascular accumulation of CD45, CD11b, CD14, and CD68-positive cells, termed fibrocytes, in pulmonary artery advantitia. The study suggests that circulating mesenchymal precursor cells play an important role in remodeling of pulmonary arteries with a hypoxic condition (20).

In contrast to V/Q mismatch with hypoxia, an over-perfusion of pulmonary circulation due to congenital heart diseases can cause PAH. Studies have shown that an over-circulation-induced experimental model is sufficient to develop PAH with abnormal vascular remodeling, increases in ET1, inducible NOS (iNOS), and vascular endothelial growth factor (VEGF) expressions (126;127). The studies also showed that PAH by induction of over-circulation in a porcine model could be prevented by administration of bosentan and sidenafil.

Monocrotaline (MCT) model

Monocrotalline (MCT) is a pyrrolizidine alkaloid plant toxin derived from the seed of the *Crotalaria spectabilis*. Like the hypoxia-induced PAH animal model, administration of MCT to a rodent is a widely investigating model system in the PAH field. Because the pyrrolizidine alkaloid needs to be bioactivated to a pyrrolic derivative [MCT pyrrole (MCTP)] by cytochrome P450 in the liver, it often causes hepatic damage as well (128). It has been shown that treatment of MCTP causes megalocytosis of ECs and SMCs, characterized by markedly enlarged cells with enlarged nuclei and organelles (129). Studies have indicated that the endothelial golgi is a main target of the MCTP by disruption of the Caveolin-1/raft function due to blockage in trafficking of the raft scaffolding proteins (129;130). An *in vitro* study demonstrated that treatment of MCTP to cultured pulmonary arterial ECs causes apoptosis with an increase in permeability (131). The administration of MCT or MCTP causes, initially, an increase in cardiac output with

the muscularization of small arteries, followed by a gradual increase in vascular resistance. After three weeks of MCT treatment, cardiac output is dropped and pulmonary arterial pressure is further increased. Accumulating data suggests that MCT or MCTP injures both ECs and SMCs, which results in a dysfunction in both cell-types. A recent study also suggests that administration of MCT causes marked downregulation of Bmpr2, Alk1, Alk6, and Smad4, 5, 6, and 8 expressions (132). The study suggests that MCT causes not only the dysfunction of vascular cells, but also downregulation in the expression of PAH genes.

Genetic Models

BMPR2 signaling pathway

The significance of the heterozygous Bmpr2 mouse is still considered controversial as far as being a model system for human PAH is concerned. Beppu *et al.* has observed a mild elevation of pulmonary arterial pressure with mild muscularization of small pulmonary arteries in heterozygous Bmpr2 null mice (133). The *Bmpr2*$^{+/-}$ mice do not exhibit vascular lesions such as neointima formation or plexioform, except in the muscularization of precapillary arteries. However, once *Bmpr2*$^{+/-}$ mice were challenged with a hypoxic stimulus, there was no difference observed in the hemodynamics between *Bmpr2*$^{+/-}$ mice and the wild-type mice. Paradoxically, a hypoxic condition in a *Bmpr2*$^{+/-}$ mouse causes less muscularization of the pulmonary arteries (133). On the other hand, with the same mouse, other independent groups failed to observe an elevation of pulmonary arterial pressure (134;135). They did demonstrate that an adenovirus-mediated pulmonary overexpression of 5-lipoxygenase (5LO), a mediator of inflammation, and a chronic infusion of serotonin (5HT) develops PAH in *Bmpr2*$^{+/-}$ mice. The result suggests that subjects carrying mutations in the BMPR2 gene are predisposed to the development of PAH, but not sufficient for development of PAH-associated vascular lesions. The studies raised the possibility that an additional genetic and/or environmental "second hit" is necessary to reach

clinical manifestation of PAH in subjects with heterozygous BMPR2 mutation. The *Bmpr2*$^{+/-}$ mice and human studies suggested that a mechanistic model of PAH, called haploinsufficiency of the *BMPR2* gene in the onset of PAH, does not seem to be the precise mechanism for the development of PAH (89;90;93).

A study highlighted the role of the Bmpr2 gene in SMCs by showing an elevation of RV pressure in transgenic mice by overexpressing a dominant-negative form of Bmpr2 in SMCs (136). In the study, the authors employed a method called inducible transgenesis in that a truncated Bmpr2, by insertion of a base pair at a kinase domain, was designed to be overexpressed by a SMC-specific SM22-α promoter under the regulation of tetracycline. The transgenic mice exhibited elevated RV pressure with muscularization of pulmonary arteries. However the mouse line does not show any of the other vascular injuries observed in the severe form of PAH such as neointima formation and plexiogenic lesions. The data suggests that impairment of the Bmpr2 signal in SMC is sufficient to cause elevation of pulmonary arterial pressure, but not to further other pathological conditions.

A recent study demonstrated that Bmp4 plays a role in the development of hypoxia-related PAH (107). Frank *et al.* showed that mice in a hypoxic condition experience selective upregulation of Bmp4 with reduction of phosphorylation of Smad1/5/8 and Id1, a downstream gene of the Smad1/5/8, expression. However, the hypoxia-mediated hypertension was less severe in Bmp4 heterozygous mice (*Bmp4*$^{+/lacZ}$) compared to wild-type mice. Further analysis suggested that Bmp4 derived from ECs plays an important role in the migration and proliferation of SMCs in the hypoxia-induced PAH model. The study showed that Bmp4 is one of the factors involved in the development of PAH under certain conditions.

Serotonin transporter (5HTT)

Serotonin (5-hydroxytryptamine, 5HT) is known to function as a vasodilator in the systemic vessel, and vasoconstrictor in pulmonary blood vessels (137;138). 5HT is also known as a potent mitogen to SMCs (139). It has been implicated that 5HT is capable of causing PAH after an outbreak of the disease in individuals who used aminorex fumarate, an appetite suppressant that inhibits 5HT reuptake by platelet (138). Plasma levels of 5HT are normally low because most of the 5HT in the body is metabolized by the liver and stored by platelets (140). 5HT is synthesized from L-tryptophan, an essential amino acid (109). Over 95% of 5HT is produced from enterochromaffin cells in the gut, whereas the remaining amount is synthesized in the other cell-types in the brain and lung (141). The synthesis is regulated by an enzyme called typtophan hydroxylase (TPH). There are two different isotypes of PTH, PTH1 and PTH2, involved in the synthesis of 5HT (109). Eddahibi *et al.* showed that TPH1 is more widely expressed in different organs such as intestine, brain and lung, whereas TPH2 is predominantly expressed in the brain. 5HT mediates its signal through at least five classes of 5HT receptors which belong to G protein-coupled receptor (GPCR) and serotonin transporter (5HTT). Because aminorex fumarate is a substrate for 5HTT, the outbreak of PAH after taking the drug has opened a new avenue of investigating the involvement of 5HT in the development of PAH. It also has been shown that a polymorphism in the human 5HTT promoter alters the level of gene expression (142). Generally, the polymorphism is composed of two alleles: a 44-bp insertion or deletion, designated the L and S alleles. In PASMCs with the L/L genotype, 5-HTT expression is 1.5-fold higher than that in LS or SS cells under basal conditions, and this difference is even more marked when 5-HTT expression is increased by external stimuli (143;144). Interestingly, the ECs from an IPAH individual showed high levels of TPH1 mRNA. On the other hand, 5HTT is upregulated in the SMCs from an IPAH individual (109). In recent studies, however, two

independent groups failed to find any correlation between 5HTT polymorphism and BMPR2 in the age at diagnosis or survival interval of PAH patients (145;146). It has been shown, however, that 5HTT is upregulated in different forms of PAH in the remodeled SMCs (147). Furthermore, Guignabert *et al.* demonstrated that an early increased level of 5HTT after MCT treatment was observed, and an administration of fluoxetine, an inhibitor of 5HTT, prevented and reversed MCT-induced PAH (148). It has been shown that a null mutation of 5HTT results in a less severe PAH with sustained hypoxia (143). Recent studies have demonstated that an overexpression of 5HTT causes elevated RV pressure with muscularization of pulmonary arteries (149;150). In the same line of evidence, Long *et al.* observed that *Bmpr2*$^{+/-}$ mice exhibited an increase in susceptibility upon the administration of 5HT (135). However, the authors found that the synergistic effect was mediated by both $5HT_2$ and $5HT_1$ receptors. Although some discrepancies exist, previous in vitro and in vivo studies suggest that 5HT, through 5HTT, plays an important role in the remodeling of pulmonary vasculature.

Endothelial nitric oxide synthase (eNOS)

It has been shown endothelial nitric oxide synthase (eNOS) is strongly expressed in the pulmonary ECs and the epithelium of normal lungs (49). In the same study, it was also shown that the expression of eNOS (NOS3) is severely impaired in a PAH individual. Giaid *et al.* demonstrated that the staining intensity of eNOS was negatively correlated with the severity of pathological condition. Interestingly, the study showed that there was an inverse correlation between the level of eNOS expression and total vascular resistance of pulmonary vessels in PAH patients with plexiform lesion. Steudel *et al.* showed that deletion of eNOS causes pulmonary arterial pressure to elevate, with a decrease in vasodilatory response to acetylcholine (151). However the authors failed to find any morphometric changes in *eNOS*$^{-/-}$ mice, suggesting that eNOS modulated vascular tone rather than vascular remodeling. Another study demonstrated that

the muscularization of pulmonary arteries was more severe than normal in both female and male *eNOS*$^{-/-}$ mice during embryonic stages and at birth, but the abnormal muscularization was persisted only in the male *eNOS*$^{-/-}$ mice, suggesting a gender bias in *eNOS*$^{-/-}$ mice (152). Paradoxically mice with hypoxia-induced PH displayed an increased level of the eNOS protein without a concomitant increase in NO bioactivity (153;154).

Recent studies highlighted that a co-factor for eNOS, tetrahydrobiopterin (BH_4), plays an important role in the pulmonary vessel homeostasis (155;156). The studies demonstrated that a hyperphenylalaninemic mutant mouse (hph-1) exhibits a 90% reduction in GTP-cyclohydrolase 1 (GTP-CH1), which catalyzes the rate-limiting step for the *de novo* production of BH_4. BH_4 functions as an essential co-factor for several enzymes, including phenylalanine-4-hydroxylase (PAH), tyrosine-3-hydroxylase (TH), tryptophan-5-hydroxylase (TPH), all three forms of nitric oxide synthase (NOS1, NOS2, and NOS3), and glyceryl-ether mono-oxygenase (157). Interestingly, the elevation of RV pressure and muscularization of pulmonary arteries with a reduction of NOS activity were evident in *hph-1* mice compared wildtype mice. The hypertensive phenotype in *hph-1* mice can be rescued by crossing them with a transgenic line selectively overexpressing GTP-CH1 in ECs. The data suggests that an impairment in BH_4 production of the ECs can cause PAH, presumably through the eNOS pathway.

Atrial natriuretic peptide (ANP)

ANP, a member of natriuretic peptides, is a cardiac hormone with potent diuretic, vascular relaxant, and antiproliferative properties. In systemic circulation, it modulates intravascular volume and the hypertensive response to salt loading (158). Like other natriuretic peptides, ANP acts on a membrane-bound receptor that activates particulate guanylate cyclase and promotes cGMP accumulation (159).

In pulmonary circulation, ANP seems to play a role as a physiological modulator in the regulation of vascular resistance and vascular remodeling. Klinger *et al.* showed that ANP-deficient mice have moderately elevated RV systolic pressures (22 ± 2 vs. 15 ± 1 mmHg) and thickened RV walls when compared to heterozygous or wild-type mice. After 3 weeks of hypoxia, the mean RV systolic pressures for homozygous mutants were higher (29 ± 3) than heterozygous or wild-type mice (23 ± 1 and 22 ± 2 mmHg, respectively). There was a greater degree of vascular remodeling of the distal pulmonary vessels in homozygous mice than in heterozygous or wild-type mice under both hypoxic and normoxic conditions (158).

Vasoactive intestinal peptide (VIP)

Studies demonstrated that VIP plays an important role as a vasodilator, an inhibitor of SMC proliferation, an anti-inflammatory and an anti-apoptotic agent in pulmonary vessels (160;161). A recent study demonstrated that deletion of the VIP gene leads to a mild elevation of RV pressure with right ventricular (RV) hypertrophy and pulmonary vascular remodeling (162). Immunohistochemical analysis showed that a thickening of the medial layer resulted from an increase in SMCs and collagen deposition. However the study failed to show the massive proliferation of ECs which is typically seen in the severe form of the disease. Another feature of $VIP^{-/-}$ mice is that a perivascular infiltration of inflammatory cell was observed surrounding affected vessels.

S100A4/Mts1

The S100 family members are known to be involved in multiple cellular processes including cell motility, intercellular adhesion, extracellular signal transduction, and cell proliferation and differentiation (163). S100A4/Mts1, a member of the S100 family of calcium-binding proteins, has been implicated as being induced in malignant metastatic breast cancer and in the stimulation of angiogenesis (163;164). Ambartsumian *et al.* demonstrated that the

S100A4/Mts1 protein is capable of enhancing the endothelial cell motility *in vitro* and stimulating the corneal neovascularization *in vivo* (163). Lawrie *et al.* showed that S100A4/Mts1 can facilitate both the proliferation and migration of the human pulmonary artery SMC through receptor for advanced glycation end products (RAGE). Furthermore, it has been shown that a subset of transgenic mice (~5%) overexpressing S100A4/Mts1 could develop plexogenic arteriopathy with intimal hyperplasia which led to the occlusion of the vessel lumen (165). The study also showed that the expression of S100A4/Mts1 was induced in the medial layer of vessels with plexiogenic lesions and neointima formation.

Unanswered Questions in PAH

Although much progress has been made in the PAH field, a number of questions are yet to be answered. First, one debating issue in the etiology of PAH still exists regarding the vascular components underlying the initiation and process of the pathological condition of PAH. Because all blood vessel components exhibit abnormal remodeling in a PAH individual, there is a paucity of information about the cell-type initiating the abnormal vascular remodeling. Studies show that a subset of PAH individuals possess endothelial dysfunctions including perivascular infiltration of leukocytes, an increase in inflammatory cytokines, and *in situ* thrombosis (3;14;166-168). The data has raised the possibility that dysfunction in the endothelium may lead to an imbalance in vasodilators *vs.* vasoconstrictors, which then triggers the aforementioned abnormal vascular remodeling. Nevertheless, no part of the study has clearly demonstrated that the cellular impact of the mutation of PAH genes are in a specific cell-type of pulmonary blood vessels.

Secondly, an emerging body of evidence has implicated that an additional factor (modifier) might be necessary to reach the pathophysiological condition, along with a heterozygous mutation of BMPR2 gene. In this vein, another issue needing to be answered in the BMPR2 signaling pathway is which downstream mediator impaired by BMPR2 mutation causes PAH.

SMAD is known as a canonical mediator of the BMPR2 signal. A study shows that phosphorylation of Smad1/5 was reduced in the pulmonary arterial SMCs of PAH individuals with BMPR2 mutation (169). The study suggests that not only BMPR2 expression is reduced, but additionally, the activation of the SMAD pathway is severely impaired by a mutation of BMPR2 in PAH individuals. On the other hand, because the BMP signaling pathway has a crosstalk with other pathways, there is a mounting evidence that the mitogen-activated protein kinases (MAPKs), including $p38^{MAPK}$, $p42/44^{MAPK}$ (ERK1/2), and c-Jun-N-terminal kinase/stress-activated protein kinase (JNK/SAPK), are regulated by BMPs and TGF-βs in certain cell-types (92;170). Recent studies have shown that exogenous BMP ligands affect phosphorylation of $p38^{MAPK}$ and $p42/44^{MAPK}$, and have a proliferation effect on SMCs (108;169). The studies suggest that those MAPK pathways somehow interact with SMAD pathways. However, no data has demonstrated which pathway(s), ie. SMAD-dependent or SMAD-independent, is responsible for PAH due to BMPR2 mutation.

Thirdly, because the plexiogenic lesion seems to be due to monoclonal proliferation of ECs, as shown in the previous studies (12;171), the possibility of a loss of heterozygosity (LOH) of BMPR2 gene in those cells has been suggested. The idea is that the monoclonal cell growth within such lesions is considered to be akin to neoplasia. Because homozygous null of Bmpr2 results in early embryonic lethality, it has been suggested that a mutation of one allele of the BMPR2 gene is transmitted through the germ line, whereas a mutation of the other allele is brought about by somatic mutation. Although there was a limitation in the number of samples, Machado *et al.* failed to find out the LOH of the BMPR2 gene in the plexiform lesion of a PAH lung (172). Nevertheless, to test the observation made in humans, the conditionally homozygous deletion of the BMPR2 gene in an animal would answer the issue.

Lastly, the current mechanism for the hyperplasia in the vascular wall is based on the finding of a resistance to apoptosis and proproliferation in SMCs of the MCT model and in PAH patients (16;173;174). Besides the hypothetic model based on proliferation *vs.* apoptosis, recent studies have shown that circulating EC progenitor cells or bone marrow-derived cells (BMDCs) can also contribute to, to some degree, vascular remodeling (175-178). Although the physiological effects of transplanted BMDCs in the experimental model are controversial or various, the studies do demonstrate that the BMDCs or circulating EC progenitor cells can be incorporated into remodeling medial and intimal layers. Based on the above findings, one important question that can be raised is which cell-type, ie. preexisting SMCs or ECs *vs.* circulating progenitor cells or BMDCs, is the dominant player in the abnormal vascular remodeling. The studies suggest that both may occur in the process of PAH individuals. Nevertheless, none of the studies have demonstrated the issue.

Table 1-1. Diagnostic classification of pulmonary hypertension (PH)

Pulmonary arterial hypertension
Idiopathic
Familial
Associated with
Collagen vascular disease
Congenital left-to-right shunt
Portal hypertension
Infection with human immunodeficiency virus
Drugs and toxins
Other conditions
Associated with substantial venous or capillary involvement
Pulmonary veno-occlusive disease
Pulmonary capillary hemangiomatosis
Persistent pulmonary hypertension of the newborn
Pulmonary hypertension with left heart disease
Left-sided atrial or ventricular heart disease
Left-sided valvular heart disease
Pulmonary hypertension associated with lung disease or hypoxemia or both
Chronic obstructive pulmonary disease
Interstitial lung disease
Sleep-disordered breathing
Alveolar hypoventilation disorders
Chronic exposure to high altitude
Developmental abnormalities
Pulmonary hypertension due to chronic thrombotic or embolic disease or both
Thromboembolic obstruction of proximal pulmonary arteries
Thromboembolic obstruction of distal pulmonary arteries
Nonthrombotic pulmonary embolism (tumor, parasites, foreign material)
Miscellaneous
Sarcoidosis, pulmonary Langerhans'-cell histocytosis, lynphangiomatosis, and compression of pulmonary vessels (adenopathy, tumor, and fibrosing mediastinitis)

This classification is adapted from Humbert *et al*., 2004 (5)

Table 1-2. Functional classification of pulmonary arterial hypertension (PAH)

Class	Description
Class I	Pulmonary arterial hypertension witout a resulting limitation of physical activity. Ordinary physical activity does not cause under dyspnea or fatigue, chest pain, or near syncope
Class II	Pulmonary arterial hypertension resulting in a slight limitation of physical activity. The patient is comfortable at rest, but ordinary physical activity causes under dyspnea or fatigue, chest pain, or near-syncope
Class III	Pulmonary arterial hypertension resulting in a marked limitation of physical activity. The patient is comfortable at rest, but less than ordinary activity causes under dyspnea or fatigue, chest pain, or near-syncope
Class IV	Pulmonary arterial hypertension resulting in an ability to carry out any physical activity without symtoms. Dyspnea, fatigue, or both may be present even at rest, and discomfort is increased by any physical activity.

This classification is adapted from Humbert *et al.*, 2004 (5)

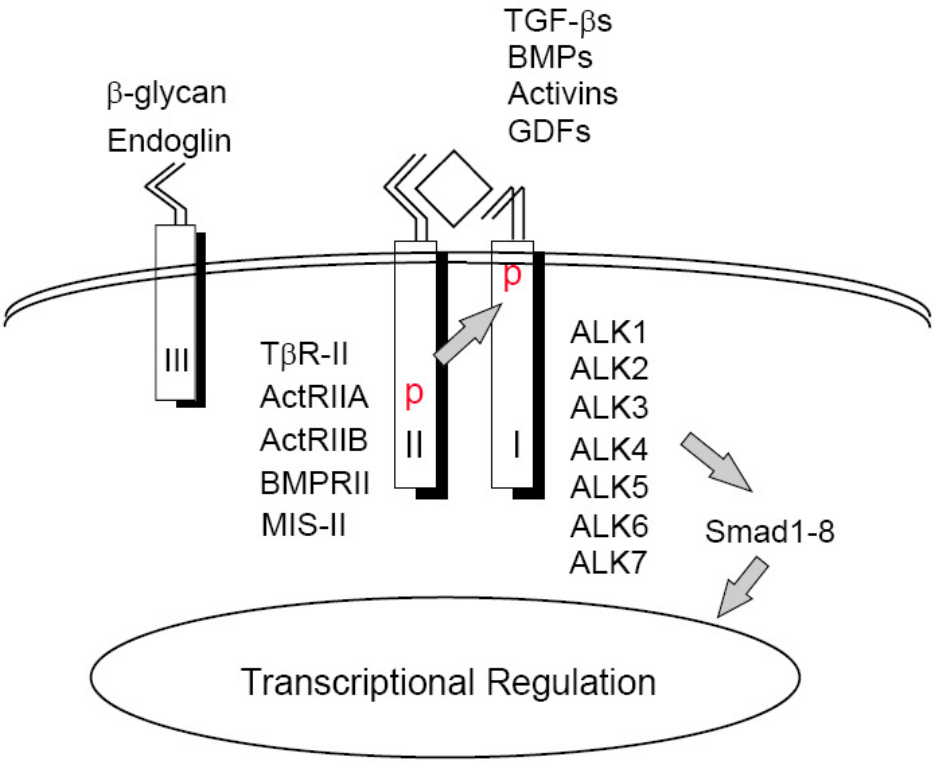

Figure 1-1. Signal transduction of TGF-β. There are more than 30 known ligands in the TGF-β superfamily. TGF-β̲ family members include TGF-βs, bone morphogenic proteins (BMPs)/growth and differentiation factors (GDFs), and activins/inhibin. The ligand starts signaling by binding to and phosphorylating the serine/threonine kinase receptors, and then the signal is propagated through phosphorylation of the cytoplasmic SMAD proteins. There are seven type I, five type II and two type III receptors in the signaling pathway. The type II receptor includes TGF-β type II receptor (TβRII), activin type II receptors (ActRIIA and ActRIIB), bone morphogenetic protein type II receptor (BMPR2), and Müllerian inhibiting substance type II receptor (MISR2). The type I receptors include activin receptor-like kinase (ALK) 1-7. The type III receptors include β-glycan and endoglin. Eight SMAD proteins have been identified in mammals so far. The activated type I receptor phosphorylates receptor-regulated SMADs (R-SMADs). The R-SMADs then form a complex with a common partner SMAD 4 (Co-SMAD), and enter into the nucleus. The inhibitory (I)-SMADs, SMAD 6 and SMAD 7, negatively modulate TGF-β signaling by inhibiting the interaction between R-SMADs and type I receptor or SMAD 4 and by targeted degradation of receptors.

CHAPTER 2
MATERIALS AND METHODS

Sequence Comparison Analyses

Mouse and human *ALK1* genomic DNA sequences were obtained from the UCSC Genome browser (http://genome.ucsc.edu). To visualize the mouse and human *ALK1* genomic sequence homology, dot-plot sequence comparisons were performed by using the Dot Matcher program available at European Molecular Biology Open Software Suite (http://p8090-bioinfo.pbi.nrc.ca.lp.hscl.ufl.edu/EMBOSS/), and DNA sequence homology alignment was conducted using the Blast 2 Sequences program (http://www.ncbi.nlm.nih.gov.lp.hscl.ufl.edu/gorf/bl2.html). Blast 2 Sequences was also used to search for common regulatory elements between *Alk1* and endothelium- or artery-specific genes. The following genes were included: *Tek (Tie-2)*, *Nos3 (eNOS)*, and *Cdh5 (VE-cadherin)*, for endothelium-specific genes; and *Efnb2 (Ephrin-B2), Bmx, Nrp (Neuropilin-1), Dll4, Notch1, Notch3,* and *Notch4*, for artery-specific genes. Full-length gene sequences as well as 10 kb 5' regulatory regions from each gene were used as queries, and comparisons against 9.2 kb pXh4.5-in2 sequence were performed with default settings.

In Silico Analysis of Alk1 Promoter

To identify potential transcriptional factor binding sites (TFBSs) in the pXh4.5-in2 sequence, the rVISTA 2.0 program provided by Lawrence Livermore National Laboratory was utilized (http://rvista.dcode.org/). The program matches a TFBS consensus matrix from the TRANSFAC 7.3 database (http://www.biobase.de) to query sequences and tests whether matched consensus matrixes are conserved between two query sequences. Some transcriptional factors (TFs) have multiple consensus matrixes with different names in the database. Therefore, the number of potential TFBS consensus matrixes is usually greater than the number of potential

TFs. In addition, the number of TFBSs is usually greater than the number of TFBS consensus matrixes because each TFBS consensus matrix can be matched to multiple locations in the query sequences. For the *Alk1* regulatory element analysis, the same set of sequences used for the dot-plot analysis were inputted into the rVISTA 2.0 program. Potential TFBSs that were conserved between the mouse and human sequences were then obtained. The program located 471 conserved potential TFBSs in the 9.2 kb mouse sequence, where each TFBS was matched to one of the 112 TFBS consensus matrixes. Among these112 matrixes, 16 TFBS consensus matrixes for the 12 TFs were known to regulate EC-specific genes.

Generation of Transgenic Mouse Lines

The pXh4.5-SIBN and pBam9-SIB constructs were generated from 4.5 kb of *Xho* I and 9.2 kb of *Bam* HI fragments of *Alk1*, which contain 2.7 kb and 8 kb of the promoter regions, respectively, as well as exon 1 through a 5' region of intron 2. For the third construct, pXh4.5-in2-SIB, the 3' end of the 4.5 kb of *Xho* I fragment was extended to 3' region to include the rest of intron 2, exon 3, and a 5' region of intron 3, for a total length of 9.2 kb. Each *Alk1* genomic fragment was connected to either the SIBN or SIB cassette, which contained SV40 splicing donor/acceptor signals (SD/SA), internal ribosomal entry sequence (IRES), β-galactosidase gene, poly A signal, and with or without a neomycin resistant gene cassette driven by the PGK promoter. The DNA constructs were microinjected into the male pronuclei of fertilized eggs from the FVB strain using the established procedures. The founder lines were screened by genomic Southern blot or PCR analyses. Several founder lines from pXh4.5-SIBN, pBam9-SIB and pXh4.5-in2-SIB were further examined for their transgene expression by whole-mount X-gal staining of F1, F2, or F3 embryos. Consequently, four pXh4.5-SIBN, one pBam9-SIB, and two

pXh4.5-in2-SIB mouse lines were established. The mouse lines from the pXh4.5-in2-SIB construct will be referred as Tg(*Alk1-lacZ*) hereafter.

For the generation of Tg(*Alk1-cre*) lines, the 9.2 kb of *Alk-1* promoter/enhancer element was used. The 9.2 kb of *Alk1* fragment was connected to a Cre transgene. For proper splicing and initiation for transcription, the Cre cassette also contained SD/SA, IRES and Cre genes. Two independent founder lines, Tg(*Alk1-cre*)-E and Tg(*Alk1-cre*)-L1, were obtained from the pAlk1-Cre construct. To test the ability of the Cre-mediated DNA excision, the Tg(*Alk1-cre*) F1 mouse was crossed with a Cre tester line, R26R, and subsequently X-gal staining and histology were carried out.

Mouse Breeding

All procedures performed on animals were reviewed and approved by the University of Florida Institutional Animal Care and Use Committee. The mice used for the procedures were wild-type C57BL/6J and FVB mice, which were purchased from Harlan (Indianapolis, Ind). The establishment of $Alk1^{+/lacZ}$, $Alk5^{+/lacZ}$, and $Flk^{+/lacZ}$ reporter lines were described previously (81;117;179).

The pregnant female mice were sacrificed at specific gestational days. To examine the expression pattern of Alk1 in embryos, male Tg(*Alk1-lacZ*) mice were crossed with either the C57BL/6J or FVB wild-type mice. Once a vaginal plug was found, the stage of the embryo was considered as at embryonic days (E) 0.5. The pregnant female mice were dissected at various embryonic stages such as E7.75, 8.5, 9.5, 10.5, 11.5, 12.5, 13.5, 15.5, and 18.5 embryos. The harvested embryos were then subjected to X-gal staining. To examine the expression pattern of Alk1 at postnatal stages, various organs such as lung, heart, intestine, eyes, brain, kidney, and skin were isolated and used for X-gal staining.

For examination of the expression pattern of *Alk1, Flk1, or Alk5* gene in the placenta, female Tg(*Alk1-lacZ*), $Alk1^{+/lacZ}$, $Alk5^{+/lacZ}$, or $Flk1^{+/lacZ}$ mice were intercrossed with wild-type C57BL/6J male mice. The embryos and uteri/placentas were used for examining expression patterns of LacZ in the maternal and fetal blood vessels in the placenta and umbilical vessels. To generate Alk1-null embryos, male and female $Alk1^{+/lacZ}$ mice were intercrossed. At E9.5 and 10.5, placentas with embryos were harvested, fixed and stained with an X-gal solution.

To test the Cre-mediated DNA excision, a male Tg(*Alk1-cre*) F1 mouse was crossed with a female R26R mice. At E9.5, 10.5, 11.5, 13.5 and 15.5 embryos were harvested, fixed and stained with an X-gal solution. To examine the Cre-mediated DNA excision in a germ cell, male or female Tg(*Alk1-cre*);R26R bigenic mice were crossed with wild-type C57BL/6J mice. At various embryonic stages, embryos were harvested and subjected to X-gal staining.

Conditional allele of *Bmpr2* was generated in a previous study (180). Mice carrying *Bmpr2* conditional allele were bred with the Tg(*Alk1-cre*)-L1 line. After multiple rounds of the breeding process, the following mouse groups containing different genetic combination were generated: *Alk1-cre(+);*$Bmpr2^{f/f}$, *Alk1-cre(+);*$Bmpr2^{+/f}$,and *Alk1-cre(-);*$Bmpr2^{f/f}$. To visualize the Cre-mediated *Bmpr2* deletion, an R26R transgene was introduced into a few of the mice in each group, and a PCR analysis was carried out with a primer set flanking two *loxP* sequences.

X-Gal Staining

For examination of the embryonic expression pattern of *Alk1*in the Tg(*Alk1-lacZ*) line, the pregnant female mice were euthanized by cervical dislocation. Mouse uteri with embryos were removed, placed in PBS, and opened to expose the embryos. The residual uterine wall and yolk sac were carefully removed. If the embryos were older than E12.5, chest and abdominal walls of the embryos were opened, and internal organs were isolated and processed together with the embryos. The isolated embryos were subjected to fixation with a fixative solution (1%

formaldehyde, 0.2% glutaraldehyde, 2 mM $MgCl_2$, 5 mM EGTA, and 0.02% NP-40) for 10 minutes at room temperature. After fixation, the embryos were washed with PBS for 5 minutes. The washing was repeated three times on a rocker. Next the embryos were put into an X-gal solution [5 mM $K_3Fe(CN)_6$, 5 mM $K_4Fe(CN)_6$, 2 mM $MgCl_2$, 0.01% NaDeoxycholate, and 0.5 mg/ml X-gal]. The embryos were incubated in the X-gal solution overnight at 37℃. The next morning, the stained embryos were washed with PBS, fixed with 4% paraformaldehyde for 2hrs, washed again with PBS and kept at 4℃ for future use. To examine the LacZ expression in organs at postnatal stages, each organ was removed, sliced to 1-2 mm thickness and stained with the same X-gal staining procedure as the embryos.

To examine the β-galactosidase activities in the extraembryonic proper of Tg(*Alk1-lacZ*), $Alk1^{+/lacZ}$, $Alk5^{+/lacZ}$, or $Flk1^{+/lacZ}$ embryos, the uterine wall and yolk sac were opened, and the placenta with the embryo attached were fixed for 15 minutes in the X-gal fixative solution. For E12.5 - 15.5 stages, placentas were sagittally dissected to 1-2 mm thickness for better penetration of X-gal solution. After washing with PBS, the same X-gal staining procedure that was employed on the embryos was applied. The stained samples were either embedded in paraffin for histology or cleared with organic solvent (Bezyl alcohol:Benzyl benzoate = 1:1) for whole mount imaging.

PCR Analysis

Tail biopsies were carried out at three weeks post-delivery. A small piece of the yolk sac was used for the genotyping of embryonic stages. The clipped tail or yolk sac was lysed in lysis buffer [50 mM Tris (pH 8.0), 0.5% TritonX-100] with proteinase K (1 mg/ml) for overnight at 55℃. The next morning the lysed tail samples were centrifuged at 12000 rpm for 10 minutes to precipitate tissue debris. The PCR reaction mixture consisted of the following: 2.5 μl of 10X

buffer, 3 μl of $MgCl_2$ (25 mM), 0.5 μl of dNTPs (25 pM), 0.5 μl of each primer, 1 μl of genomic DNA, and 15 μl of H_2O. Mineral oil was overlaid to prevent the PCR mixture from evaporation. A "hot start" PCR reaction was prepared under the following directions: the mixture was stayed at 94℃ for 10 minutes then the temperature was lowered to 72℃. Once the temperature reached 72℃, 2 μl of a *Taq* polymerase was added. After adding the *Taq* polymerase, the PCR cycle was run in the following way: 35 cycles at 94℃ for 45 seconds, 1 cycle at 60℃ for 45 seconds, and 1 cycle at 72℃ for 1 minute. The primers used for genotyping are summarized in the Table 2-1.

Wound Healing Study

Four-month-old mice were anesthetized with an intraperitoneal (I.P.) injection consisting of 0.015 mL of 2.5% Avertin per gram of body weight. The back of the mouse was shaved and swabbed with Betadine. Three 4mm-diameter full-thickness excisional wounds were placed on the mid-dorsum using a biopsy punch. The wounds were not sutured and were treated with Betadine. The wounded areas were completely recovered after 14 days, in most cases. The mice were euthanized at six different time points (3, 5, 8, 10, 12, and 14 days after wounding), and full dorsal-side skins were removed and stained with X-gal, followed by fixation and clearing.

Histology and Immunohistochemistry

The pieces of tissue and embryo samples were dehydrated with increasing concentrations of ethanol (70 %→ 95 %→ 100 %) for 15 minutes each and incubated in an organic solvent for another 15 minutes. After incubation in the organic solvent, the samples were incubated in paraffin for at least 2 hrs. The embedded embryos, placentas, and adult tissue samples were cut into 6-7 μm of thicknesses. For morphometric analysis after hemodynamic study, the left lobe of lung was transversely cut to 5 μm thickness. Tissue sections were deparaffinized in CitrosolV for at least 15 minutes and sequentially rehydrated with an ethanol series (100 % → 95 %→70 %, 15

minutes/each) and water. Some of the sections were subjected to hematoxylin and eosin (H&E) staining. To determine the X-gal positive cells, the sections were counterstained with nuclear fast red (NFR).

For immunohistochemistry, the standard ABC method was used with a Vector staining kit (Vector laboratories, Inc., CA). Briefly, sections were hydrated and endogenous peroxidase activity was blocked by treating them with 3% (v/v) hydrogen peroxide (H_2O_2) at room temperature for 10 minutes. After two times of washes with PBS, the sections were incubated with blocking serums corresponding to their secondary antibodies species for 1 hour at room temperature, followed by an incubation of primary antibodies. Biotinated secondary antibodies were incubated for thirty minutes after being washed with PBS. After secondary antibody incubation, sections were treated with peroxidase-conjugated avidin/biotin complex for thirty minutes followed by two PBS washes. Color development was carried out with a DAB^+ substrate chromogenic solution (Vector laboratories, Inc., CA). The antibodies used for immunohistochemistry are the following: αSMA (clone: 1A4; Sigma, 1:800), Pecam1 (clone: Mec13.3; PharMingen, 1:200), phosphor-Smad1/5/8 (Cat. # 9511; Cell Signaling Tech., 1:300), CD68 (clone: M-20; Santa Cruz Biothech., 1:400), cytokeratin (Cat. #: Z0622, DAKO, 1:600), Ki-67 (clone: M-19 Santa Cruz Biothech., 1:400) von Willebrand factor (Cat #: A0082; DAKO, 1:400), fibrin(ogen) (Cat. #: A0080; DAKO, 1:400), Tenascin-C (Cat. #: AB19013; Chemicon, 1:200), cleaved caspase-3 (clone: 5A1; Cell Signaling Tech., 1:400), and Serotonin transporter (clone: C-20; Santa Cruz Biotech., 1:200) antibodies.

Hemodynamic Analysis

Indirect systemic pressure was recorded by using the tail-cuff method. A pneumatic pulse sensor was distally placed on the tail to an occlusion cuff controlled by a Programmed Electro-

Sphygmomanometer (PE-300, Narco Bio-Systems, TX). To evaluate pulmonary pressure, right ventricular systolic pressure (RVSP) was measured by right heart catheterization through the right jugular vein. Briefly, each mouse was anesthetized with Ketamine (100 mg/kg)/Xylazine (15 mg/kg) and placed in a supine position. A 2-3 cm incision was made to expose the right jugular vein. A Mikro-Tip pressure transducer (SPR-835, Millar Instrument, TX) was inserted into the right external jugular vein and advanced into the right ventricle. All electrical outputs from the tail cuff, the pulse sensor and transducer were recorded and analyzed by a Powerlab 8/30 data acquisition system and the associated Chart software (ADinstrument, CO). After the hemodynamic study, the mouse was euthanized, and the organs, including the heart and lungs, were isolated for further analyses. The outflow tract and atria were removed prior to the weighing of the right and left ventricle plus the septum.

Morphometric Analysis

After the hemodynamic analysis, the left lung was then inflated with 20-25 cmH_2O of gravity for 20 minutes followed by flow with 4% paraformaldehyde for another 20 minutes. The trachea of the inflated lung was tied up with suture silk and fixed with 4% paraformaldehyde overnight. The next morning, the lung sample was washed two times with PBS for 10 minutes each, then transversely sliced into 0.5 cm sections. To determine the muscularized peripheral vessels and wall thickness, immunostaining with αSMA was performed. In each section, αSMA-positive vessels were categorized by their locations such as vessels at the level of terminal bronchioli, respiratory bronchioli, alveolar ducts, or alveolar sac. To determine muscularization of pulmonary vessels, peripheral blood vessels ranging from 30-70 μm of diameter were counted in at least four fields at X20 magnification. The counted vessels were categorized as fully muscularized (75-100% of medial layer is covered by αSMA staining), partially muscularized

(1-74% of medial layer is covered by αSMA staining), or non-muscular vessels at the level of alveolar duct and alveolar sac. The percentage of pulmonary vessels in each category was calculated by dividing the number of vessels in the category by the total number of counted vessels in the same field. To calculate the percentage of wall thickness (WT), circular and fully muscularized vessels with ranges of 30-70 μm of diameter were selected. A thickness (WT1) between the outer boundary and the inner boundary of the αSMA-positive medial layer was measured. Another thickness (WT2), the diametrically opposite point of the vessel, was measured. At the same time, the external diameter (ED) was also measured. The percentage medial thickness for these vessels were calculated as [(WT1 + WT2) X 100]/ED.

Western Blotting

One of the right lung lobes were used for Western blot analysis. Once removed from a -80℃ freezer, the lung lobe was placd into a Chemicon lysis buffer [50 mM Tris (pH 6.8), 1 mM EDTA and 2% SDS], disrupted with a pestle until the lung tissue was able to move freely, sonicated three times for 5 seconds and spun at 13000 rpm for 15 minutes. The concentration of protein was determined using the Biorad DC Assay kit. Forty micrograms of total proteins were fractionated by 12% of SDS-PAGE, transferred to PVDF membranes and incubated with the primary antibody for BMPR2 (Cat #: 612292; BD Transduction Lab., 1:500). After incubation with horseradish peroxidase-linked anti-mouse IgG, a chemiluminescent detection reagent (ECL Plus™, Amersham Pharmacia Biotech Inc, NJ) was used to detect the protein. The antibodies used for the other Western blotting analysis's are the following; phospho-ERK (clone: E-4; Santa Cruz Biothech., 1:800), total ERK (p44/42) (Cat #: 9102; Cell Signaling Tech., 1:800), Smad 1 (clone: T-20; Santa Cruz Biothech., 1:400), Alk1 (clone: D-20; Santa Cruz Biothech., 1:400),

eNOS (Cat #: 610296; BD Transduction Lab., 1:800), GAPDH (Cat. #: ab8245; abcam, 1:10,000), and β-actin (clone:A5441; Sigma, 1:10,000).

Statistics

Data were described as mean ± SEM. The difference between groups was determined by the Student's t-Test or Two-way ANOVA. A value of $p < 0.05$ was considered as a statistically significant.

Table 2-1. Primers used for PCR reactions

Genes	Forward primers	Reverse primers
Bmpr2 (floxed)	CACATATCTGTTATGAAACTTGAG	CACATATCTGTTATGAAACTTGAG
Bmpr2 (null)	CACATATCTGTTATGAAACTTGAG	TTATTGTAAGTACACTGTTGCTGTC
Cre	GCTAAACATGCTTCATCGTCGGTC	CAGATTACGTATATCCTGGCAGCG
LacZ	GTCGTTTTACAACGTCGTGACT	GATGGGCGCATCGTAACCGTGC
Alk1 (wildtype)	CAGCACCTACATCTTGGGTGGAGA	ACTGTTCTTCCTCGGAGCCTTGTC
Alk1 (mutant)	CAGCACCTACATCTTGGGTGGAGA	CGGGTACAATTCCGCAGCTTTTAG
Alk5	TGCCAAATGAAGAGGATCCATCAC TAG	AAGACCACTTGCTGTGGACAGAG

CHAPTER 3
IDENTIFICATION OF ARTERIAL ECS-SPECIFIC ALK1 PROMOTER

Note

The work presented in this chapter was published in "Isolation of a Regulatory Region of Activin Receptor-Like Kinase 1 Gene Sufficient for Arterial Endothelium-Specific Expression" by Seki T, Hong KH, Yun J, Kim SJ, Oh SP, 2004 Circulation Research;94:e72., and "Activin receptor-like kinase 1 (ALK1) is essential for placental vascular development in mice" by Hong KH, Seki T, and Oh SP, 2007 Laboratory Investigation; 87(7):670-679.

Introduction

Blood vessels consist of a network of arteries, capillaries, and veins. Recent discoveries of artery- or vein-specific genes, such as ephrinB2 and its receptor EphB4, and some molecules involved in the Notch-delta signaling pathway have contributed to a significant advancement in understanding the mechanisms by which arteries and veins gain their distinct identities during vascular development (181). In contrast to the long-standing belief that the acquisition of arterial and venous identities is largely determined by different physiological parameters (eg, blood flow, blood pressure, and shear stress), genetic studies in mice and fish suggest that arterial and venous ECs acquire their distinct molecular identities before the establishment of blood flow (182;183). Studies have shown that the aforementioned artery- or vein-specific genes play crucial roles in angiogenesis and segregation of the two blood vessel types (182;184;185). It remains unclear, however, whether those genes are directly involved in the morphogenesis of vessel type–specific architecture during development.

ALK1 is a TGF-β type I receptor in vascular ECs (113;186). Haploinsufficiency of ALK1 in a human causes HHT2, also known as Osler-Weber-Rendu syndrome, which is characterized by recurrent epistaxis, localized mucocutaneous telangiectases, and arteriovenous malformations

(AVM) in the lungs, liver, and brain (187;188). Mutations on the gene include nonsense, missense, frameshift, and interference of splicing, all of which seem to result in loss-of-function mutations (188). Clinical and genetic data have demonstrated that 60% of HHT cases are caused by such exonic mutations; however, types of mutation in the remaining 40% of the cases are still inexplicable (189;190). Although there has been significant progress in understanding the genetics of HHT, an etiological role of non-exonic mutations of *ALK1* in HHT still remains to be studied.

Pathologically, the telangiectasia is divided into three stages. In the first stage, the cutaneous vascular bed is obvious with the dilation of postcapillary venule followed by a thickening of vessel walls resulting from accumulation of excessive pericytes. In the second stage, dilated arterioles are observed with intervening capillary beds. In the end stages, the venule becomes gradually dilated and spreaded throughout the skin in a tortuous pattern. The capillary network is no longer observed and is replaced by direct connections between arterioles and venules. The arteriole and venule portions of each arteriovenous connection appear to maintain characteristics of their origins (191).

Our lab and another group have reported that Alk1 plays an important role in vascular development and remodeling (113;114;117). Homozygous Alk1 mutant mice show embryonic lethality around E10.5 with severe vascular defects characterized by hyperdilation of large vessels, and failure in recruitment of VSMCs sheathing ECs tube (113). Consistent with this result, a mutation in the zebrafish *Alk1* gene, *vbg*, resulted in an increased number of ECs within the affected vessel, suggesting the role of Alk1 in vascular remodeling (192). It has also been shown that *Alk1* heterozygous mice display HHT-like phenotypes in a number of characteristics including age-dependent penetrance, lesions in specific anatomical locations, histological

similarities between the lesions, and even the recapitulation of the secondary phenotype of cardiac pathology (115).

Using *Alk1-lacZ* "knock-in" mice ($Alk1^{+/lacZ}$), we have previously observed a dynamic spatiotemporal expression pattern of *Alk1*: *Alk1* is expressed predominantly in arterial ECs throughout the developmental and postnatal growth stages, and its expression is diminished in the adult stage; *Alk1* expression is induced in reconstructing and remodeling arteries during angiogenesis prompted by either wound healing or tumorigenesis (117). The data from these expressions together with the VSMC defect in *Alk1*-deficient embryos suggest that ALK1 may be directly involved in the morphogenesis of arterial development and remodeling. As proposed in the earlier study, HHT has been generally considered as a disease that is initiated in the vein (112). However, our demonstration, which shows predominant Alk1 expression in arterial ECs, suggests that the artery is the primary vessel affected, and the remodeling of the vein could be a secondary effect caused by hemodynamic changes (117).

The placenta is a vital organ for exchanging gases, nutrients, waste products, and various cytokines as a maternal and fetal interface (193;194). Morphogenesis of the chorioallantoic placenta begins with formation of the chorion from extra-embryonic ectoderm and the allantois from mesoderm at the posterior end of the embryo during gastrulation. Subsequently, allantois reaches to the chrionic plate, and feto-placental blood vessels are established by E8.5 (195). Extensive branching morphogenesis by the allantoic mesoderm and the chorionic trophoblasts (syncytiotrophoblasts) takes place to structure the labyrinth (Lab) layer at which the maternal-fetal exchange occurs. Both mouse and human placentas are similar because both belong to the hemochorial placenta, in that the lining of the fetal trophoblast cells are in direct contact with the maternal blood. Trophoblasts from the ectoplacental cone contribute to the spongiotrophoblast

(Sp) layer, in which maternal arterial endothelial cells are eroded away and replaced by fetal trophoblast cells. This replacement step is important because it makes the maternal arteries low resistant vessels (194).

The main goal of this chapter is to characterize the nature of the spatiotemporal pattern of Alk1 expression using the conventional transgenic approach, and to further analyze both embryonic and extraembryonic Alk1 expression in the transgenic line.

Results

Generation of Transgenic Constructs and *In Silico* Analysis of the Alk1 Promoter

To investigate the *cis*-acting elements required for the spatiotemporal expression of the *Alk1* gene (Figure 3-1A), three different transgenic constructs containing various regions/lengths of putative regulatory sequences connected to the *lacZ* gene were generated (Figure 3-1B). The first construct, pXh4.5-SIBN, contained a 2.7 kb promoter, exon 1, and a part of 5' region of intron 2. Five independent founder lines were established from this construct, and the transmission of the transgene to F1 offspring was confirmed via genomic Southern blot analyses. None of the embryos from these lines, however, displayed the vascular-specific expression of the *lacZ* gene. To investigate whether the essential regulatory elements resided in upstream sequences, the 2.7 kb promoter region was extended to a total length of 8 kb in the second construct, pBam9-SIB. As in the first case, a mouse line from this construct did not exhibit a vascular-specific expression pattern of the transgene either.

These results prompted us to search for the potential regulatory elements by comparing DNA sequences between the human and mouse *ALK1* gene loci. Intriguingly, dot plot and blast analyses revealed the presence of highly conserved sequences at the 3' region of intron 2 (Figure 3-1C). The span of a 1.8 kb conserved region in the 3' region of intron 2 consisted of at least five homologous regions ranging from 37 to 145 bp in length, and each sequence cluster showed more

than 80% identity (data not shown). Based on these results, a third construct, pXh4.5-in2-SIB, which was similar to the first construct, pXh4.5-SIBN, but with the extension of the 3' region to include the remaining intron 2, exon 3, and approximately 300 bp of 5' region of intron 3, for a total length of 9.2 kb were generated (Figure 3-1B). Two founder lines from this construct showed artery-specific expression of the *lacZ* gene (Figure 3-2A), which recapitulated the pattern seen in $Alk1^{+/LacZ}$ embryos (Figure 3-2B).

To examine detailed regulatory activities of the 9.2 kb *Alk1* sequences, a pattern of X-gal stainings in various stages of embryos, adult organs, as well as in wounded skins, were prepared and compared to the results to those of the $Alk1^{+/lacZ}$ mice.

Expression Pattern of LacZ in Tg(*Alk1-lacZ*) Mice

Two transgenic mouse lines from the pXh4.5-in2-SIB construct, Tg(*Alk1-lacZ*)*C2* and *K1*, showed identical expression patterns with slightly different intensity [thus, will be collectively referred as Tg(*Alk1-lacZ*) hereafter]. In embryos, the transgene expression pattern of Tg(*Alk1-lacZ*) was virtually indistinguishable from $Alk1^{+/LacZ}$ except for the intensity levels (Figure 3-2). Strong expressions in the capillaries of perineural tissues in E10.5 to 13.5 embryos were consistently observed (Figure 3-2C and 2D). The transgene expression in Tg(*Alk1-lacZ*) was detected in developing arterial ECs, but neither in VSMCs nor in venous ECs (Figure 3-2E and 2F). The artery-specific expression was also clearly shown in internal thoracic arteries (Figure 3-2G and 2H), mesenteric arteries (Figure 3-2I), and descending aorta and intercostal arteries (Figure 3-2J and 2K). Strong expression in the pulmonary vessels (Figure 3-2L and 2M), and the lack of staining in the liver (data not shown) were also consistent with those in $Alk1^{+/LacZ}$.

The X-gal staining patterns of Tg(*Alk1-lacZ*) mice during postnatal life were, to a large extent, identical to the ones of $Alk1^{+/LacZ}$ mice, in which the intense *Alk1* expression in arterial vessels during the postnatal growth phase was greatly diminished in most of the tissues except for

the lungs at the adult stage. Consistent with these observations, Tg(*Alk1-lacZ*) mice showed intense vascular staining, such as in the brain and the iris (Figure 3-3A and 3B), during the early postnatal growth phase. In the adult stage, however, positive staining was barely detectable in the capillary-like small vessels throughout the body, except for a moderate amount of expression in the lungs (Figure 3-3C through 3E). In the skin, the Tg(*Alk1-lacZ*) mice showed intense staining of arteries at the newborn stage (Figure 3-3F) as observed in $Alk1^{+/LacZ}$. Unlike $Alk1^{+/lacZ}$ mice, however, the expression was greatly reduced in the 2-week-old mice.

Next, a transgene expression during induced angiogenesis in adult mice using a skin wound healing model was also examined. Although overall X-gal staining intensity in the skin was lower in Tg(*Alk1-lacZ*) mice when compared with the $Alk1^{+/lacZ}$ mice, the expression pattern was comparable. During wound healing in the adult stage, the transgene expression was induced in arterial vessels in a similar fashion as the $Alk1^{+/lacZ}$ mice, although the staining was significantly lighter and limited in both duration and area (Figure 3-3G through 3J). Although the vascular staining in the wounded area of the $Alk1^{+/lacZ}$ mice was present from days 3 to 12 after wounding, staining of the transgenic mice was observed only from days 3 to 8. Also, the staining was restricted to the vessels adjacent to the wounds and did not extend to distant arteries that fed the wound lesion in the transgenic mice.

Identification of Regulatory Elements in the Homologous Regions

Our transgenic studies indicate that the conserved intronic regions may contain the enhancer element(s) for the artery-specific Alk1 expression. To investigate whether the 9.2 kb regulatory fragment of the *Alk1* gene contains common regulatory elements, DNA sequence homology alignments between the 9.2 kb regulatory sequence and regulatory regions of other known endothelium- or artery-specific genes were performed. Extensive homology searches, however, did not reveal any significant continuous homology region.

To identify potential transcriptional factor binding sites (TFBSs) in the 9.2 kb regulatory fragment, comprehensive *in silico* analysis with the rVISTA 2.0 program was performed. In the analysis, 16 conserved TFBSs for 12 transcriptions factors known to regulate EC-specific genes within the 9.2 kb regulatory fragment were found (Table 3-1, Figure 3-4). The *in vivo* relevance of the conserved intronic regions and TFBSs remains to be investigated.

Alk1 Is Expressed in the Primitive Blood Vessels During Early Chorioallantoic Placenta Development

Utilizing *Alk1*$^{+/lacZ}$ as well as Tg(*Alk1-lacZ*) lines, the expression pattern of Alk1 during early chorioallantoic placental development was investigated. The first detectable Alk1 expression was observed in the allantoic bud at around E7.75 (Figure 3-5A). At the subsequent stages when the allantoic mesoderm forms primitive umbilical vessels and reaches to the chorionic plate, Alk1 expression was detected in these primitive vascular beds formed in the allatoic mesoderms as well as in the embryonic blood vessels (Figure 3-5B). Most Alk1-positive cells in these extra-embryonic tissues were positive for Pecam1, a mature endothelial cell-specific marker (Figure 3-5C and 5D). Alk1 expression was apparent in patent blood vessels formed in the chorio-allantoic connection of E9.0 embryos (Figure 3-5E and 5F).

Alk1 Is Differentially Expressed in Umbilical Arterial Endothelium, and Required for the Distinctive Umbilical Artery and Vein

To further investigate whether the arterial endothelium-specific expression pattern that we have observed in the embryo proper is conserved in extraembryonic vessels, we examined the X-gal staining pattern in the umbilical vessels of E15.5 *Alk1*$^{+/lacZ}$ and Tg(*Alk1-lacZ*) mice and compared it with that of *Flk1*$^{+/lacZ}$ and *Alk5*$^{+/lacZ}$ mice. X-gal-positive cells were found mostly in the umbilical arterial endothelium of *Alk1*$^{+/lacZ}$ mice (Figure 3-6A and 6B). No X-gal positive cells were found in the vascular smooth muscle or adventitial layers, and the venous endothelial cells had a very weak X-gal positive staining. Tg(*Alk1-lacZ*) mice exhibited the same expression

pattern with the *Alk1*$^{+/lacZ}$ mice, except that the X-gal staining intensity in the venous endothelium was stronger than that of *Alk1*$^{+/lacZ}$ mice (Figure 3-6C and 6D). In contrast, X-gal-positive cells were found in both the arterial and venous endothelium as well as in the capillaries in the advantitial layer of the umbilical artery in *Flk1*$^{+/lacZ}$ mice (Figure 3-6E and 6F). Interestingly, the X-gal staining intensity in the venous endothelium was stronger than that of the arterial endothelium (Figure 3-6E). In addition, X-gal-positive staining in the microvessels surrounding medial layer of arteries were detected in *Flk1*$^{+/lacZ}$ (Figure 3-6E), but not in *Alk1*$^{+/lacZ}$ mice (Figure 3-6C). These results demonstrate heterogeneity of expression of endothelial-specific genes in a vessel type-dependent manner. The Alk5 expression was predominantly detected in the medial layers but not in the endothelium of both umbilical arteries and veins (Figure 3-6G and 6H). The non-overlapping expression patterns of these TGF-β type I receptors are consistent with our previous study in embryonic vessels, suggesting that TGF-β might be involved in vascular morphogenesis utilizing two distinct type I receptors: ALK1 in ECs and ALK5 in vascular SMCs.

The vessel type-specific expression patterns as well as the function of Alk1 were investigated with *Alk1*$^{+/lacZ}$ and *Alk1*$^{lacZ/lacZ}$ embryos at E9.5 and 10.5 stages. The differential expression pattern was not obvious at the E9.5 stage (Figure 3-7A), but became noticeable by the E10.5 stage (Figure 3-7C). Umbilical arterial and venous lumens were clearly separated in *Alk1*$^{+/lacZ}$ mice along the entire length of umbilical vessels (Figure 3-7A and 7C), whereas only one large lumen was found in the *Alk1*-null embryos at both E9.5 (four out of four embryos) and E10.5 (three out of three embryos), especially around the middle of umbilical vessels (Figure 3-7B and 7D).

Alk1 Is Expressed in the Arteries and Capillaries in the Labyrinth Layer of Placenta

Next, the Alk1 expression in the mid- and late gestational stages of placentas was examined. Expression patterns in both Tg(*Alk1-lacZ*) and *Alk1*$^{+/lacZ}$ placentas were essentially identical, although the overall staining intensity appeared to be higher in the Tg line (Figure 3-8A – 8F). A murine placenta is a multiple layered organ consisting of an endometrium-derived deciduas (Dec), a junctional zone containing trophoblast giant cells, a spogiotrophoblast (Sp), and a labyrinth (Lab) where physiological exchanges occur (193). The Lab layer contains multiple cellular barriers: a single layer of mono-nucleated cytotrophoblasts, two layers of multi-nucleated syncytiotrophoblasts, and fetal capillary endothelial cells (194). Predominant arterial staining was again manifested, and fetal arteries projecting to the Lab layer of the definitive placenta were distinctively highlighted by the X-gal staining. On the other hand, X-gal staining was not detected in the Sp as well as Dec layers of placentas in the Alk1 reporter lines. Dissimilar from Alk1 reporter lines, X-gal-positive fetal arteries projecting into the Lab layer were unobservable in the *Flk1*$^{+/lacZ}$ mice (Figure 3-8G – 8I). In addition, Flk1 expression was detected from maternal vessels in the decidua and uterine walls (Figure 3-8G).

Histological sections of X-gal stained *Alk1*$^{+/lacZ}$ placenta confirmed the restricted Alk1 expressions in the umbilical vessels and the Lab layer (Figure 3-9A – 9D). No detectable X-gal staining was observed from fetal and maternal vessels in the Sp and Dec layers. To determine the cell type expressing Alk1 in the Lab layer, we stained E12.5 placenta sections with anti-Pecam1 or cytokeratin (CK) antibodies. We used E12.5 placentas because the villus density in the Lab layer is less compact than that of E15.5, and thus different cell layers can be identified more easily. The X-gal-positive cells in the Lab layer appeared to be Pecam1-positive, but mostly non-overlapping with CK-positive cells, showing that Alk1 is expressed in endothelial cells but not in syncytiotrophoblasts.

Alk1-Deficiency Results in Impairment of Umbilical and Placental Blood Vessel Formation

To investigate the role of Alk1 in placental development, Alk1-null placentas at E9.5 stage were examined. The branching morphogenesis of the chorionic ectoderm and invasion of allantoic mesoderm into the Lab layer of *Alk1*$^{lacZ/lacZ}$ placentas were largely unaffected (Figure 3-10A and 10B). In Alk1-null placentas, however, the chorionic vessels were severely dilated and showed signs of fusions, similar to the vascular abnormality observed in Alk1-null embryos (113).

Discussion

In this chapter, we have demonstrated, using transgenic mice, that the 9.2 kb fragment of the *Alk1* gene contains essential regulatory elements for its spatiotemporal expression and that heterogeneous Alk1 expression is conserved in extra-embryonic vasculature and is restricted to fetal ECs. Also implicated, an intriguing possibility is that the conserved region in intron 2 may contain the enhancer elements for the artery-specific gene expression. This result suggests that intron 2 contains a potential regulatory element(s) which directs its arterial EC-specific expression.

Supporting this notion, a homology study between mouse and human *ALK1* revealed that at least five homologous regions ranging from 37 to 145 bps exist at the 3' end of intron 2. Each homologous region shows more than 80% homology between the two species. The data also demonstrated that 16 conserved transcriptional factor binding sites (TFBSs) for 11 transcription factors known to regulate EC-specific genes within the homologous regions of 3' end of intron 2. The *in silico* data suggests a potential role of the intronic sequence in the spatiotemporal regulation of Alk1 expression during vascular development. Thus, the analysis of role of the homologous intronic sequences in the regulation of Alk1 expression may provide novel genetic insights in arteriogenesis. This study also suggests that the expression pattern observed in the

Alk1$^{+/lacZ}$ mice was not a consequence of *Alk1* haplo insufficiency. The presented 9.2 kb regulatory fragment, as the first regulatory elements specific for arterial endothelial cells, would provide invaluable information regarding regulatory mechanisms of *Alk1*, as well as other artery-specific genes. Furthermore, this regulatory fragment can be used to activate or silence a gene in developing arteries to study its function in arteriogenesis and in the remodeling of arterial vessels.

We also showed that Alk1-deficiency results in severe dilation and fusion of chorioallantoic and umbilical vessels, suggesting a vasodilatory phenotype of the Alk1-null embryos. The variance of expression patterns between Tg(*Alk1-lacZ*) and *Alk1*$^{+/lacZ}$ mice in the skin wounds may be due to either the strain differences, or a lack of additional *cis*-acting elements involved in the Alk1 expression during wound-induced angiogenesis.

Using lacZ reporter lines we also demonstrated heterogeneous Alk1 expression patterns in umbilical and fetal placental vessels and that Alk1-deficiency leads to persistent umbilical vessels and extensive dilation of chorioallantoic vessels. Alk1 expression was first detected in the allantoic bud and then in the allenochorionic primitive vessels when allantois reaches to the chorion. Alk1-null embryos formed a large persistent vessel instead of a separated umbilical artery and vein. At present it is not clear whether the two umbilical vessels might have been formed and then laterally fused, or that separation had not occurred during development of the umbilical vessels of the mutant embryos.

At later stages, Alk1 was shown to be expressed predominantly in the arterial endothelium of umbilical vessels. This result is consistent with our previous findings in embryonic vessels (117), indicating that oxygen concentration is not the underlying basis of the vessel type-specific differential Alk1 expression. Recent studies suggest that arterial and venous endothelial cells have distinct molecular identities prior to patent vessel formation. Ephrin-B2 was expressed in

both arterial ECs and SMCs, whereas EphB4 (a putative receptor for Ephrin-B2) was expressed almost exclusively in venous ECs prior to the onset of circulation (196;197). More recently, several other artery-specific genes have been reported in vertebrate embryos, including a Notch ligand *Delta* (Dll4) (198;199) and a Notch-Delta downstream transcription factor (Gridlock) (200). Studies have clearly shown that these genes are involved either in early lineage determination between arterial and venous ECs or in segregating two vessel identities at the capillary level. However, it is unclear whether these artery- or vein-specific genes are involved in creating a structural and functional distinction between arterial or venous vasculature.

Unlike *Ephrins* and *Delta* ligands, which are membrane-bound and thus require cell-to-cell contact, Alk1 interacts with TGF-β ligands as paracrine or endocrine signals. It has been demonstrated that Alk1-deficiency leads to impaired differentiation or recruitment of SMCs and severe dilation and fusion of embryonic and extra-embryonic vessels (113;114). With the correlation between the thickness of smooth muscle layers and the level of Alk1 expression in the artery and vein, we speculate that ALK1 may play an important role in arteriogenesis and in the remodeling of arteries. Temporal deletion of the Alk1 gene at later stages of development would provide a direct answer to this hypothesis.

Alk1-null embryos exhibited severe dilation of blood vessels with an elevated VEGF mRNA label (113). A question was raised as to whether such vascular defects were a response to a hypoxic condition. In the study, we presented evidence that the process of establishing the labrynthine layer was unaffected in Alk1-null placenta, yet chorionic vessels were severely dilated to the same degree to the embryonic vessels. This result suggests that the phenomenon of blood vessel dilation is primarily due to Alk1-deficiency per se rather than a secondary response to hypoxia.

ALK1 shares numerous common characteristics with ENG. Both ALK1 and ENG are plasma membrane proteins mediating TGF-β family signals, are involved in the same genetic disease, and are expressed in vascular endothelial cells. Recent reports have suggested that elevated sENG in conjunction with sFLT1 of placental origin might be a major pathogenetic marker and cause of preeclampsia (201;202). Preeclampsia is characterized by hypertension and proteinuria in the third trimester of pregnancy and occurs in 5% of all pregnancies (203;204). Deficiency or incompletion of replacing maternal arterial endothelium with trophoblasts increases vascular resistance and maternal blood pressure, and thus may contribute to the pathogenesis of preeclampsia. Unlike Flk1 (VEGF receptor 2) whose expression is limited to endothelial cells, a strong fetal Flt expression was observed in spongiotrophoblasts and syncytiotrophoblasts in addition to ECs (205). Eng was also shown to be highly expressed in the syncytiotrophoblasts (206). Since both ALK1 and ENG interact as a signaling partner and are involved in the same genetic disease, there is an emerging question whether ALK1 is also involved in preeclampsia (207).

In the study, a difference in the expression pattern of Alk1 from those of Eng or Flt1 in the placenta has been found: Alk1 expression was restricted to fetal endothelial cells while Eng and Flt1 were shown to be expressed in the placental trophoblast cells (205;206). This difference suggests that Alk1 is most likely not involved in preeclampsia at the level of placenta.

Table 3-1. List of transcription factors of which TFBSs were found in the *Alk1* regulatory fragment and their respective EC-specific target genes

Binding sites		
TFs	In promoter	In enhancer
SP1	VEGFR2, VE-cadherin, ICAM2, eNOS	
SP3	VE-cadherin	
AP2	VEGFR2	
CREB	VEGFR1	
NF-κB	VEGFR2, PECAM, ICAM2	
GATA	vWF	VEGFR2
GATA1	ICAM2	
GATA2	PECAM, endothelin1, ICAM2, eNOS	
ETS	ICAM2	Tie2, VEGFR2
ETS1	VEGFR1, VEGFR2, VE-cadherin, vWF	
ETS2	VEGFR1, VEGFR2	
ELF1	Tie2	

SP1 indicates specific protein 1; SP3, specific protein 3; AP2, adaptor protein 2; CREB, cyclic-AMP response element binding protein; NF-κB, nuclear factor-κB; ELF1, E74-like factor 1; VEGFR, vascular endothelial growth factor receptor; VE-cadherin, vascular endothelial cadherin; ICAM2, intercellular adhesion molecule; eNOS, endothelial nitric oxide synthase; PECAM, platelet/endothelial cell adhesion molecule; and vWF, von Willebrand factor.

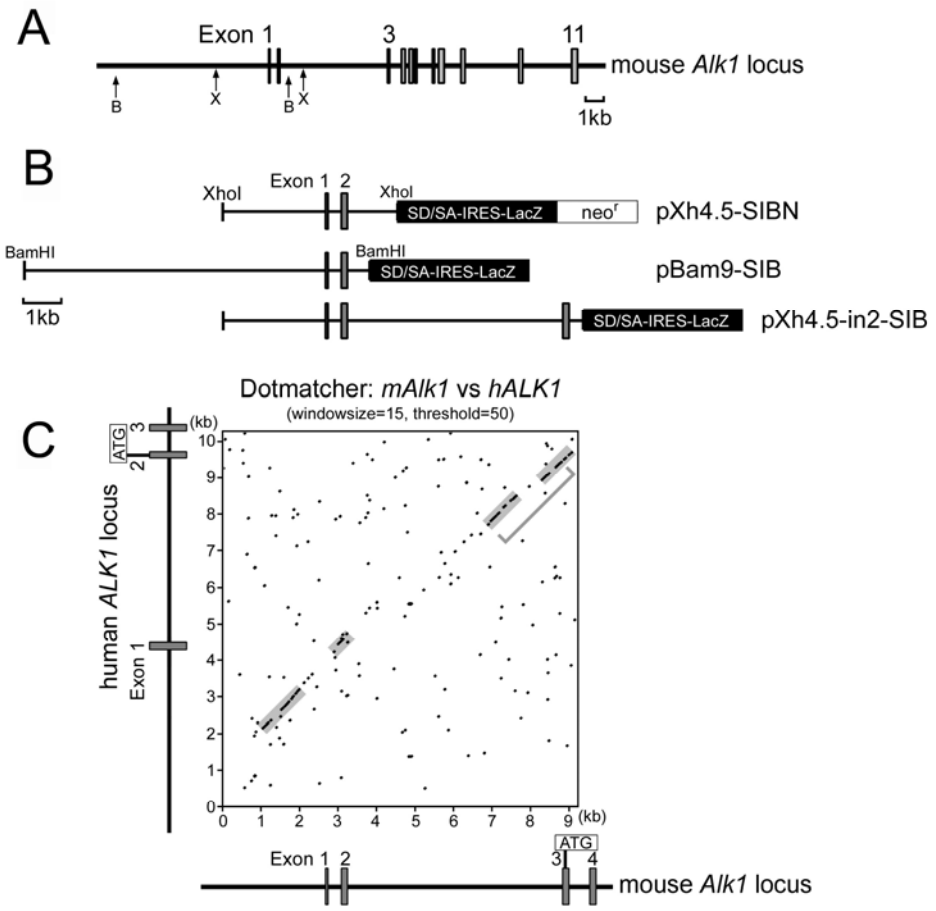

Figure 3-1. Transgenic constructs and the dot plot analysis between human and mouse *ALK1* genomic sequences. A) Full mouse *Alk1* gene structure. Restriction enzyme sites used for generating the transgenic constructs are indicated by X (*Xho*I) and B (*Bam*HI). Boxes represent exons, and exon numbers are indicated above. B) Schematic representations of 3 transgenic constructs. Detailed construct information is available in the Materials and Methods. C) Dot plot analysis between partial genomic sequences of human (y-axis) and mouse (x-axis) *ALK1* gene. Exon 1 of the human *ALK1* gene is split in 2 exons (1 and 2) in the mouse *Alk1* gene. Continuous sequence homologies are highlighted by gray shaded areas. Note that the 3' regions of mouse intron-2 and human intron-1 are highly conserved (gray bracket).

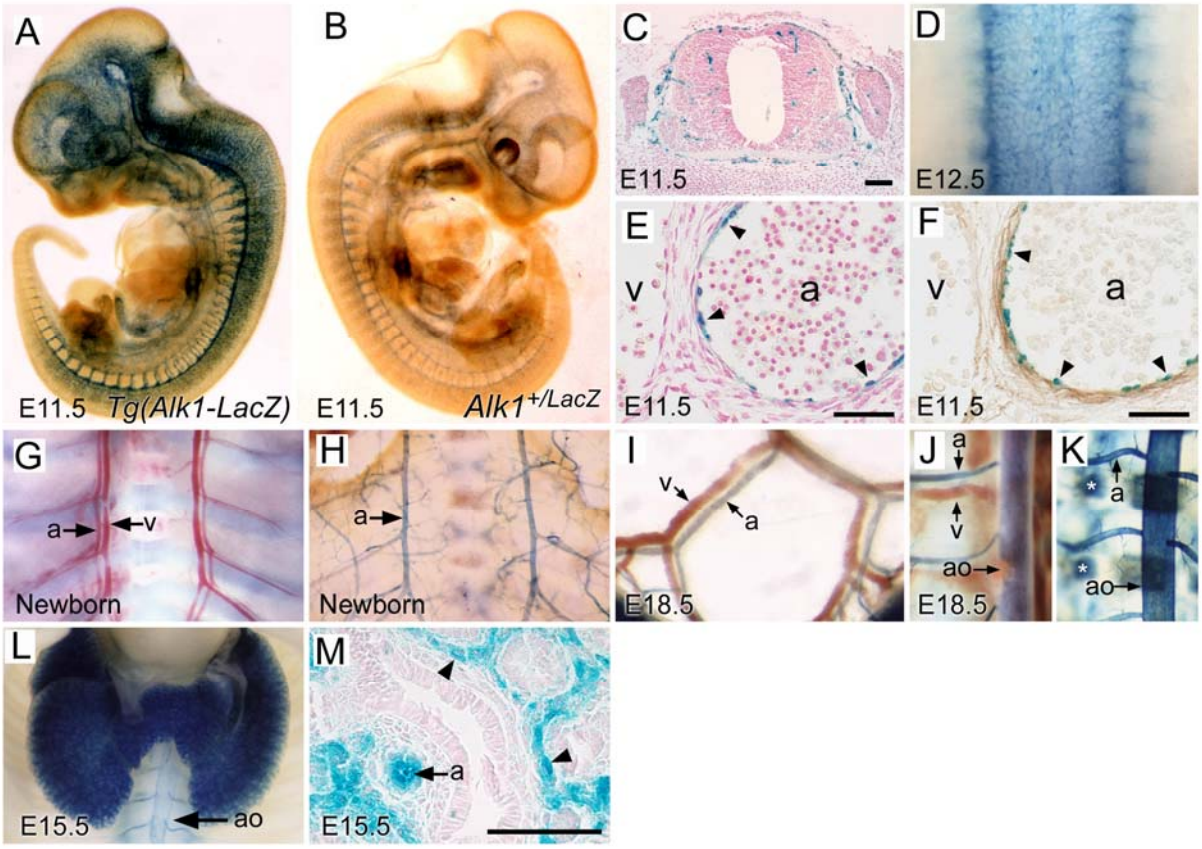

Figure 3-2. Artery-specific lacZ expression in the blood vessels of Tg(*Alk1-lacZ*) embryos. A) and B) Whole-mount X-gal–stained E11.5 *Tg(Alk1-lacZ)* and *Alk1*$^{+/LacZ}$ embryos, showing the identical staining pattern but with much higher intensity in *Tg(Alk1-lacZ)*. C) and D) Strong *LacZ*-positive capillary-like vessels in the developing neural tube; C) the section of E11.5 embryo and D) a dorsal view of E12.5 neural tube. E) and F) Sections of X-gal–stained E11.5 *Tg(Alk1-lacZ)* embryos counterstained with nuclear fast red (NFR) or immunostained with anti-αSMA. Note that the X-gal–positive cells were found in a single layer of endothelium in the artery (a, arrowheads), but not in the vein (v), and were not concomitant with SMCs. G) and H), Blood vessels on the thoracic wall of newborn pups before and after X-gal staining, showing that only arteries and connecting small arteries were X-gal positive. I) Whole-mount X-gal–stained mesenteric vessels of E18.5 fetuses. Only mesenteric artery (a) but not vein (v) showed the transgene expression. J) and K) X-gal–stained aorta and intercostal blood vessels before and after clearing with the organic solvents. Similar sizes of intercostal arteries (a) and veins (v) were running side-by-side J), whereas only arteries and dorsal aorta (ao) were X-gal positive. X-gal–positive staining in the rib skeleton (*) is from the endogenous β-gal activity. L) Intense X-gal staining in the lungs and aorta (ao) of E15.5 *Tg(Alk1-lacZ)* embryos. M) NFR counterstained section of E15.5 lungs showed X-gal–positive arteries (a) and capillaries (arrowheads). Note that bronchial epithelial cells were X-gal negative. Scale bars in C, E, F, and M = 50 μm.

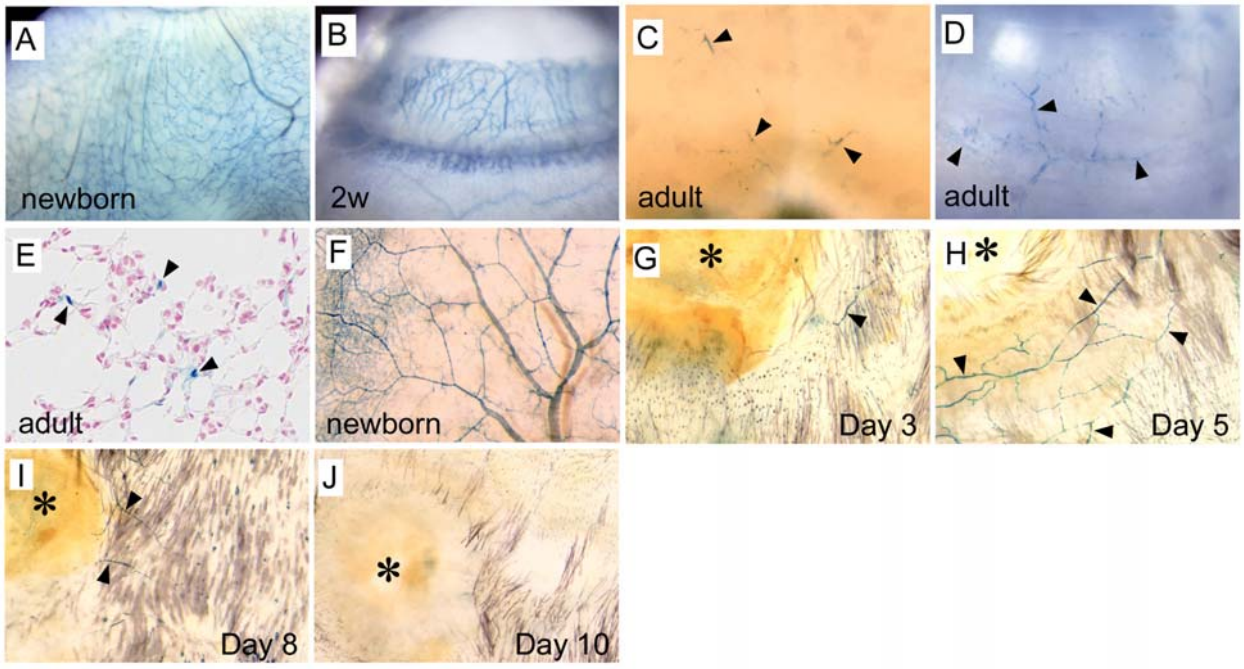

Figure 3-3. Postnatal transgene expressions in Tg(*Alk1-lacZ*) mice. A) - D) X-gal–stained blood vessels in the brain and the iris. A) and B) Intense transgene expression in newborn brain and 2-week-old iris were greatly diminished in the adult stage. C) and D) Only speckled staining in small branches (arrowheads) was observed. E) Adult lung section counterstained with NFR. Alveolar capillaries expressed the transgene in the adult stage. F) Intense staining in the arteries of newborn skin. G) - J) X-gal staining in the skin during days 3, 5, 8, and 10 after wounding. LacZ expression was induced during wound healing (arrowheads), but in a limited extent. Number and intensity of X-gal–positive vessels peaked at day 5 after wounding and diminished completely by day 10. Asterisks (*) in G) through J) indicate the wounds.

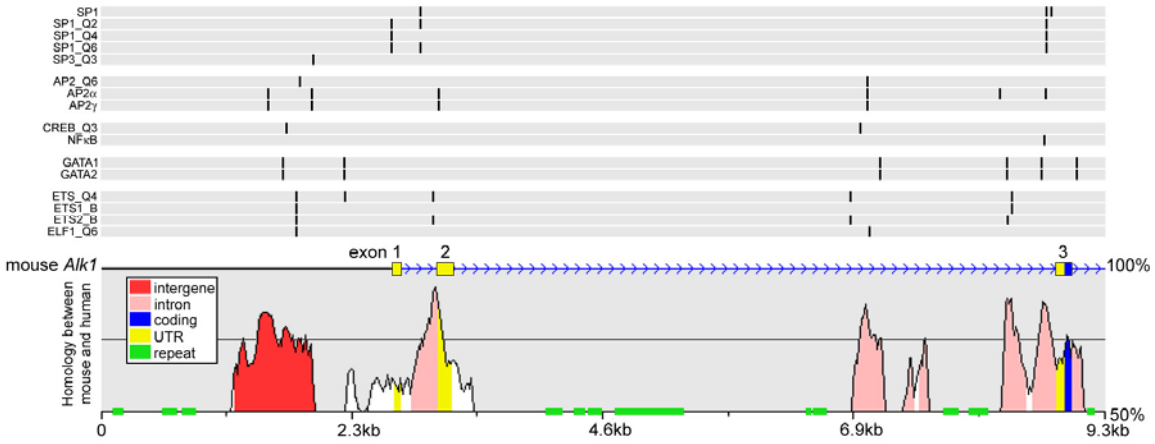

Figure 3-4. Potential transcriptional factor binding sites identified in the mouse Alk1 pXh4.5-in2 fragment by the rVISTA analysis. Top, 16 TFBS matrixes, which represent TFBSs for 12 different transcription factors. Some transcription factors have multiple TFBS matrixes. For example, SP1 has 4 different TFBS matrixes (SP1, SP1_Q2, SP1_Q4, and SP1_Q6). Positions of each conserved TFBS are indicated as a bar within the matrix. Bottom, Mouse *Alk1* gene structure (the top line), and the sequence homology between *mAlk1* and *hALK1* sequences. Color legends in the boxed area indicate the nature of the highly homologous regions. Repetitive sequences are indicated by green boxes on the bottom line. Only the transcriptional factors known to have active roles in regulating EC-specific genes are shown.

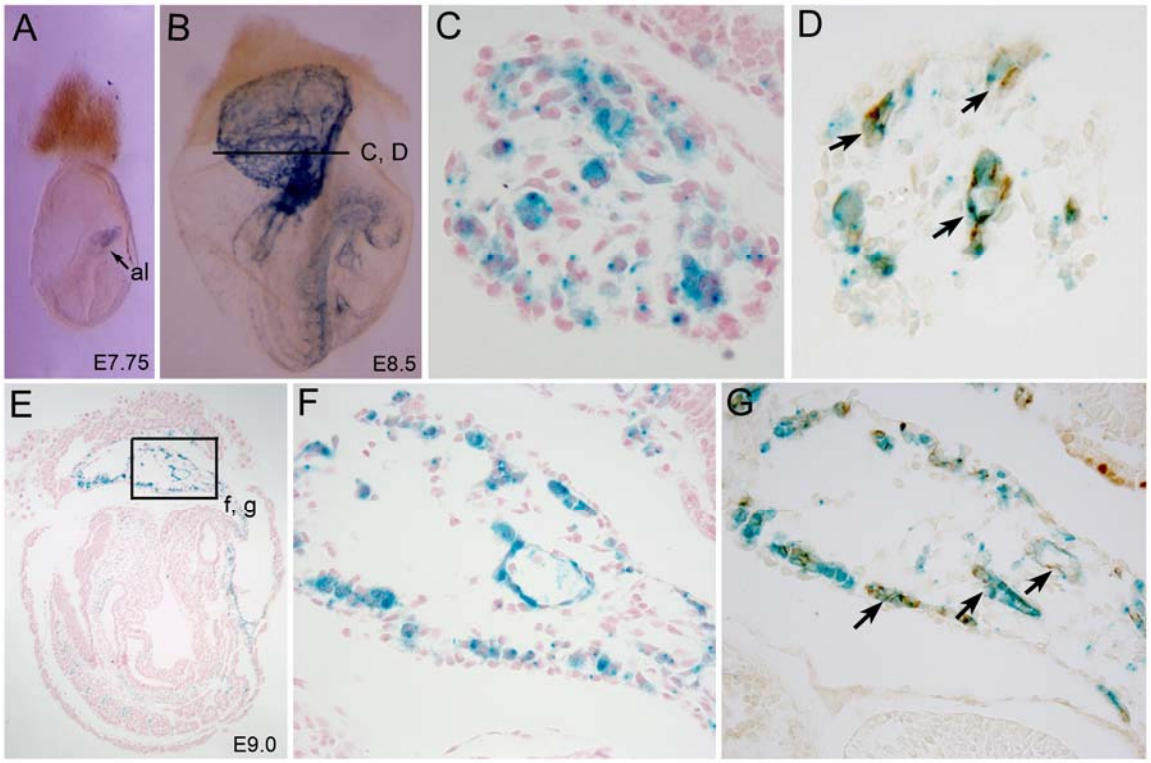

Figure 3-5. Whole-mount X-gal staining of Tg(*Alk1-lacZ*) embryos at days E7.75–E9.0 during early chorioallantoic development. A) The first detectable Alk1 expression was found in the allantoic bud of E7.75 embryos. al, allantois. B) - D) X-gal staining was detected in the developing blood vessels of the embryo proper as well as in the primitive chorioallantoic vessels of E8.5 embryos. C) Transverse sections of X-gal stained E8.5 embryos at the level of the allantois were counterstained with NFR or D) immunostained with Pecam1 antibodies, showing that the majority of X-gal-positive cells are Pecam1-positive. E) - G) Longitudinal section of E9.0 embryos shows X-gal staining in embryonic and extra-embryonic ECs. F) and G) Higher magnification views of allantoic mesoderm, showing development of patent blood vessels positive for X-gal and Pecam1. Arrows in D) and G) indicate some representative cells positive for both X-gal and Pecam1.

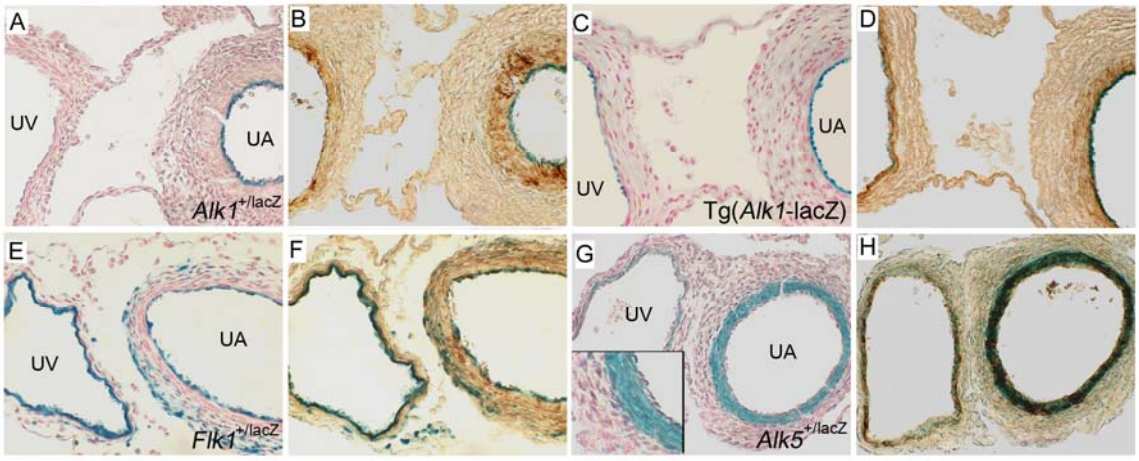

Figure 3-6. Expression patterns of Alk1, Flk1, and Alk5 in E15.5 umbilical vessels. Transverse sections of whole-mount X-gal-stained umbilical vessels of *Alk1*$^{+/lacZ}$; A) and B), Tg(*Alk1-lacZ*); C) and D), *Flk1*$^{+/lacZ}$; E) and F), and *Alk5*$^{+/lacZ}$; G) and H) embryos were counterstained with NFR in A), C), E), and G) or immunostained with αSMA antibody in B), D), F), and H). A) – D) Note that X-gal-positive cells were mostly detected in the endothelium of the umbilical artery (UA) of *Alk1*$^{+/lacZ}$ and Tg(*Alk1-lacZ*) embryos. E) and F) X-gal-staining intensity was stronger in the umbilical vein (UV) than in the UA, and capillaries in the medial and adventitial areas were also X-gal-positive in *Flk1*$^{+/lacZ}$ mice. G) and H) X-gal-positive cells were localized in smooth muscle layers, but not in endothelium of the UA and UV in *Alk5*$^{+/lacZ}$. A high-magnification view of the UA is shown as an inset in G).

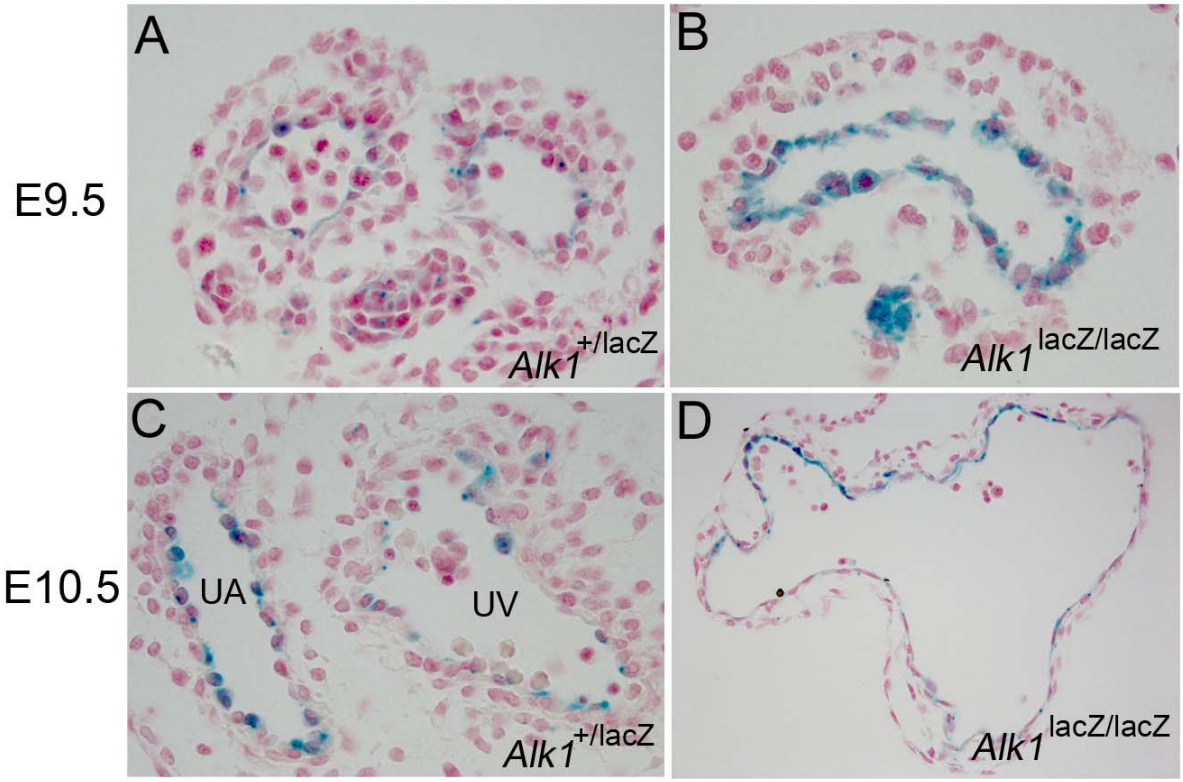

Figure 3-7. Impaired formation of two distinct umbilical vessels in Alk1-null embryos. A) and C) Histological analysis of umbilical vessels of *Alk1*$^{+/lacZ}$ and B) and D) *Alk1*$^{lacZ/lacZ}$ embryos at E9.5 and E10.5. Transverse sections of whole-mount X-gal-stained umbilical vessels were counterstained with NFR. Two distinct blood vessels were apparent in *Alk1*$^{+/lacZ}$, whereas only one large persistent vessel was present in *Alk1*$^{lacZ/lacZ}$ embryos. C) It is interesting to note that the UA-predominant Alk1 expression became evident in E10.5 embryos.

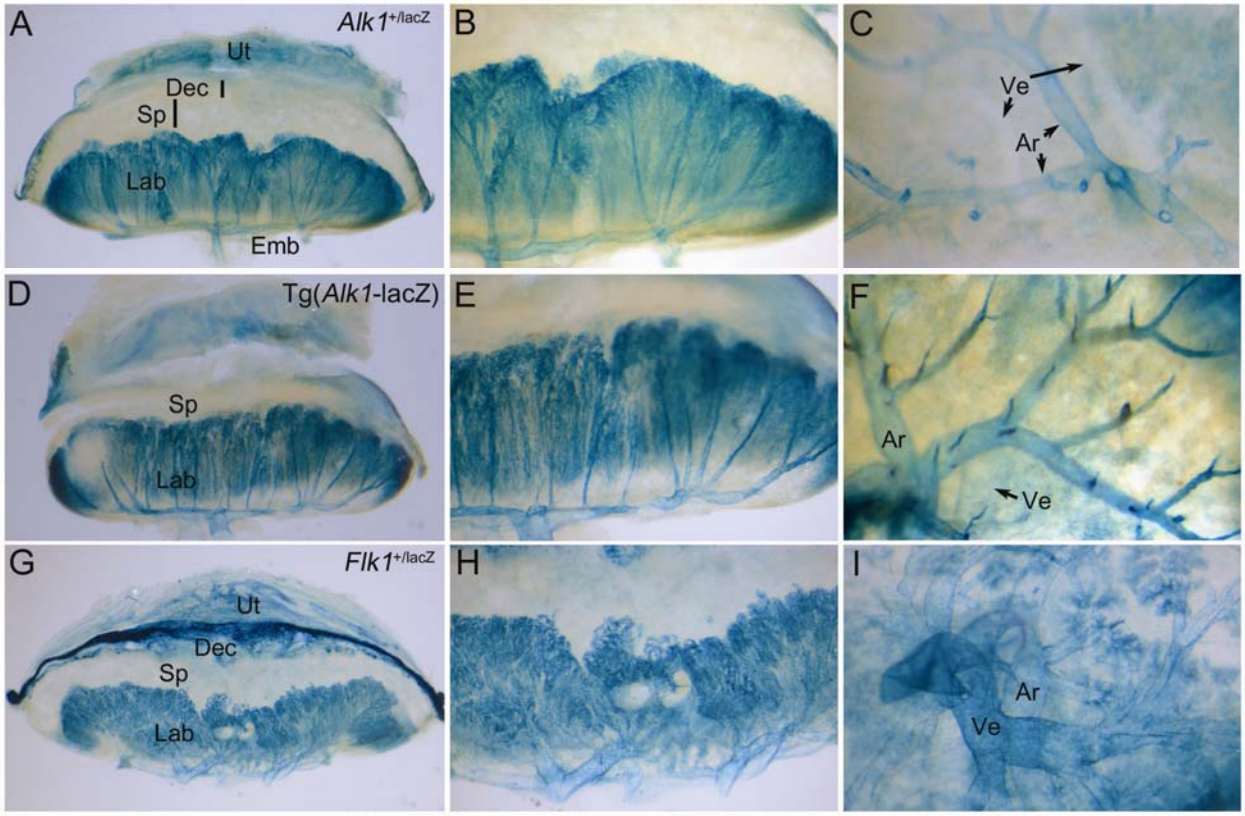

Figure 3-8. Comparison of Alk1 and Flk1 expression patterns in the definitive placentae. A) – I) Whole mount X-gal-stained placentae of E15.5 *Alk1*$^{+/lacZ}$, Tg(*Alk1-lacZ*), and *Flk1*$^{+/lacZ}$ embryos were cleared with organic solvents. B), E) and H) Higher magnification of longitudinal views of A), D) and G) C), F) and I) Horizontal views of X-gal-stained placenta from fetus side. Note that Alk1 expression is limited to the Lab layer and strong in fetal arteries projecting into the Lab layer. Ar, fetal arteries; Dec, decidua basalis; Emb, embryonic side; Lab, labyrinth layer; Sp, spongiotrophoblast layer; Ut, uterine wall; Ve, fetal veins.

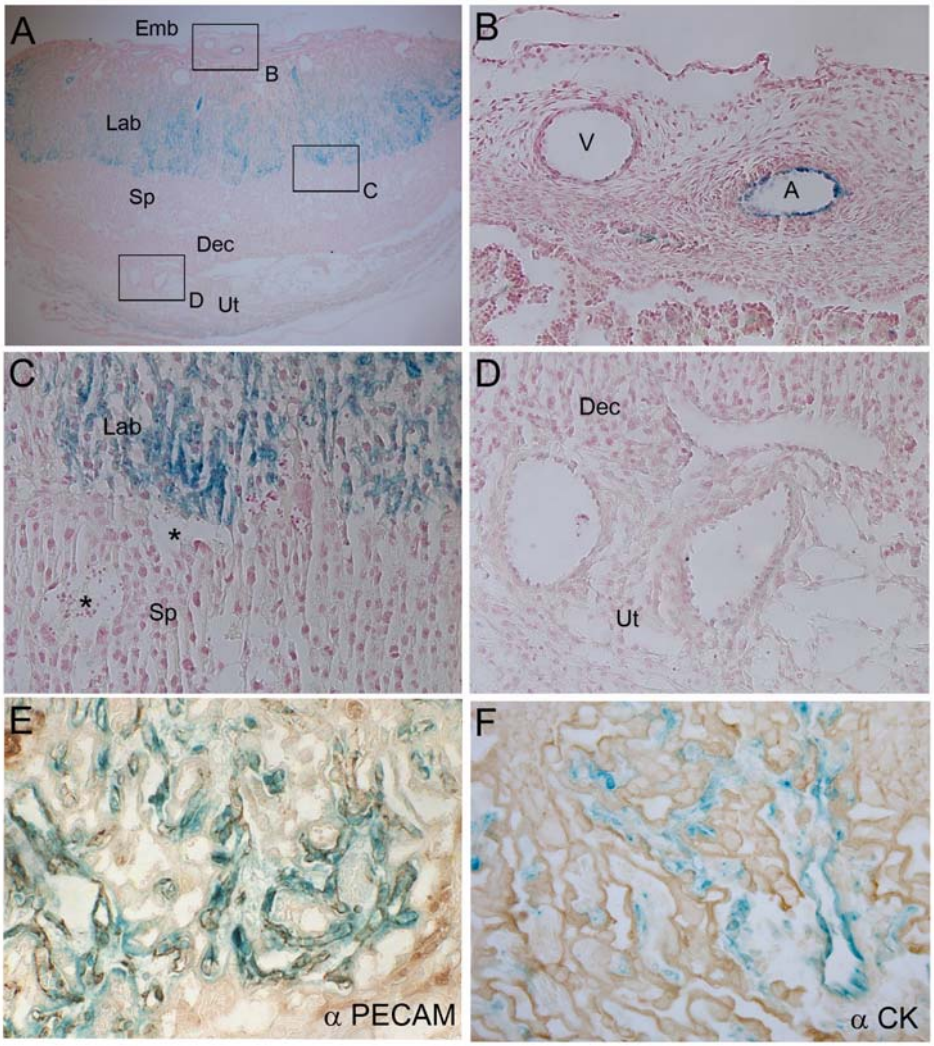

Figure 3-9. Longitudinal sections of X-gal-stained *Alk1*$^{+/lacZ}$ placenta. A) - D) Histological sections of E15.5 placenta shows that X-gal-positive cells are localized mostly in fetal blood vessels at umbilical arteries and capillaries in the Lab layer, whereas no X-gal-positive cells are detected in the Sp and Dec layers or in the uterine wall. E) and F) Immunostaining (shown as brown color) of the Lab areas of X-gal-stained E12.5 placenta with Pecam1) or CK) antibodies, showing that EC, but not syncytiotrophoblasts, are X-gal positive.

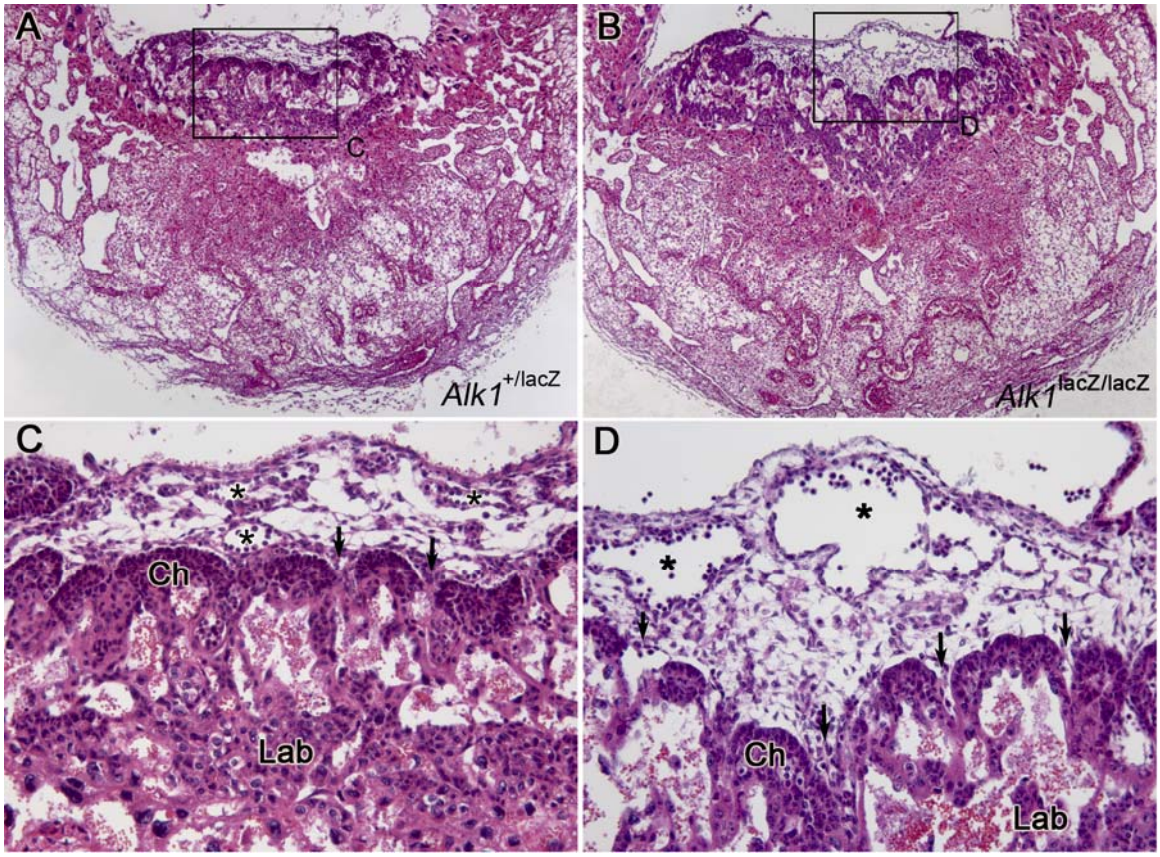

Figure 3-10. H&E staining of histological sections of E9.5 placentas from A) and C) *Alk1*$^{+/lacZ}$ mice, and B) and D) *Alk1*$^{lacZ/lacZ}$ mice. Asterisks and arrows in C) and D) indicate chorioallantoic blood vessels and areas of allantoic mesodermal invasion into developing Lab, respectively. Ch, chorionic ectodermal cells.

CHAPTER 4
DEVELOPMENT OF A NOVEL TRANSGENIC LINE EXPRESSING CRE RECOMBINASE IN ENDOTHELIAL CELLS

Notes

The work presented in this chapter will be published in part with "*In vitro* dissection of TGF-β signal transduction pathways reveals ALK5- and TGFβR2-independent role of ALK1 for pathogenesis of hereditary hemorrhagic telangiectasia 2 (HHT2)." by Park SO, Lee YJ, Seki T, Hong KH, Flies N, Jiang Z, Park A, Wu X, Karlsson, S, Kaartinen V, Moses HL, Raizada MK, Roman BL, and Oh SP, 2007 (submitted) and "Genetic ablation of the *Bmpr2* gene in pulmonary endothelium is sufficient to predispose pulmonary arterial hypertension." by Hong KH, Lee YJ, Beppu H, Bloch K, Li E, Raizada MK, and Oh SP (in preparation).

Introduction

Using a mouse as a model system for studying human genetic diseases has been considered to be advantageous for multiple reasons. First, mice have a relatively short lifecycle. Second, its genome has been completely sequenced and gene delivery methods using microinjection, electroporation, chemicals, viruses, and naked DNA to different developmental stages of mice gamete have been well established with high efficacy. Third, embryonic stem (ES) cells showing germ-line transmission are available from various mouse strains including inbred strains (129 and C57BL/6) or hybrid strains between 129 and C57BL/6. Forth, mouse ES cells have a high efficiency of homologous recombination compared to other species. Lastly, mouse physiology is comparable to human physiology (http://www.informatics.jax.org/mgihome/other/mouse_facts3.shtml).

Much progress in the manipulation of the mouse genome has been made since the *Cre*/*lox*P system was firstly used (208). Although some limitations in the *Cre*/*lox*P system still exist, one of the biggest advances contributed by the *Cre*/*lox*P system is that it allows us to bypass

embryonic lethality due to the lack of a gene, and study the role of a gene of interest in a specific cell-type or tissue. On the other hand, one of the critical limitations of the *Cre/lox*P system is that once genomic DNA is recombined by the Cre recombinase in a cell type, the progenitor cells, which might have an ability to differentiate into other cell types, also contain the recombined allele. Even though the main feature of the *Cre/lox*P system is beneficial for some lineage tracing or fate-mapping studies during development, there is a possibility that the loss of a gene in unwanted cell types or tissues may then cause phenotypes in those cell types or tissues. To overcome this drawback of the *Cre/lox*P system, it is required that a better gene manipulation system need to be found or multiple mouse lines showing different patterns of Cre-mediated DNA excisions need to be developed.

The cardiovascular system, in mammals, includes the heart, blood and blood vessels. These three components are anatomically and functionally closely related to maintain the homeostasis of our body system. Because of the close relationship, one of the difficulties in studying the etiology of a particular cardiovascular disease lies in which type of cell, in a certain component, is primarily responsible for the disease. For example, an endothelium, which displays functional and morphological heterogeneity depending on its location or subcellular environments, is a continuum tissue from the heart to peripheral organs. Developmentally, the origin of ECs seems to be various. Initially, it has been proposed that only the mesodermal cells that migrated from the primitive streak into the yolk sac produces ECs and hematopoietic stem cell (HSC) progenitors *in situ* in mammals (209). However, subsequent studies have shown that such progenitors also arose intraembryonically, specifically in the para-aortic mesoderm serving as the precursor to the aorta-gonad-mesonephros (AGM) region (210). The placenta has also been implicated as an organ presenting both EC and hematopoietic precursor cells (211).

Although the exact time of specification of the mesodermal cells to ECs remains to be answered, it is generally accepted that the vasculogenesis, a process of blood vessel formation occurring by a *de novo* production of ECs, begins first in the yolk sac, followed by the AGM region, and then the placenta, in mammalian embryos (212). At the stages of ECs specification, EC precursors and cardiac progenitor cells seem to share some common markers such as fetal liver kinase-1 [Flk1 or vascular endothelial growth factor receptor-2 (VEGFR-2)] and LIM-homeobox transcription factor islet-1 (Isl1), and can be trans-differentiated between each other. Mice lacking Flk1 exhibited embryonic lethality between E8.5 and 9.5 with defects in the development of haematopoietic cells and ECs. Yolk-sac blood islands were absent at E7.5 days, organized blood vessels were not observed in the embryo or yolk sac at any stage, and haematopoietic progenitors were severely reduced (179;213). In a recent study, it has been shown that Flk1-positive cells have an ability to be differentiated to cardiomyocytes, SMCs, and ECs as well (214). Another fate-mapping study demonstrated that the Isl1 delineating the second cardiogenic progenitor field can mark cell populations that contribute to myocardial cells, subsets of endocardium, and aortic endothelium (215;216).

So far, multiple transgenic (Tg) and knockin (KI) lines expressing the Cre in ECs have been developed. Those mice include Tg(*Tie2-cre*), Tg(*Tie1-cre*), Tg(*Flk1-cre*), $Flk1^{+/cre}$, and Tg(*Vecad-cre*). Among them, the most commonly used mouse line is the Tg(*Tie2-cre*) line (217). A recent study demonstrated that Tie2-cre-mediated β-galactosidase activity was found in the endocardium, the mesenchyme of the atrioventricular (AV) cushions as well as ECs (218). Indeed, the onset of Cre-mediated recombination in the ECs and the mesenchyme of AV cushions of the Tg(*Tie2-cre*)*;*R26R mice was readily detected at E9.5 (217). During early heart valve formation, a subset of ECs which specifies the cushion-forming regions delaminates and

invades into the cardiac jelly, a mass of connective tissue, where they subsequently proliferate and complete their differentiation into mesenchymal cells (219;220). Although the Tg(*Tie2-cre*) line is widely using to delete a gene of interest in the ECs, it possibly deletes a gene in the AV cushion, which then causes defects in the cardiac valve. Supporting this possibility, recent studies showed that conditional abolition of some genes using the Tg(*Tie2-cre*) line lead to defects in the valve formation as well as minor or detrimental phenotypes in the blood vessel (221-223). The studies suggest that the Tg(*Tie2-cre*) line is a useful model for studying the function of a gene in the entire ECs or for fate-mapping studies, but is not suitable for studying functions of genes in the ECs of specific vascular beds.

It has been shown that the Tg(*Flk1-cre*) line exhibits strong Cre activity in the hematopoietic cells as well as ECs of developing blood vessels. Aside from that, Cre activity is very weakly detected in the pulmonary vasculature (224). Furthermore, Cre-mediated lineage tracing study using $Flk1^{+/cre}$ mice have shown that both vascular endothelium and cardiac muscle arise from Flk1-positive mesodermal progenitors during development (225).

Like the Tg(*Tie2-cre*) line, the Tg(*Tie1-cre*) line also exhibits the Cre-mediated DNA excision in the mesenchymal cells in the cardiac cushion (226;227). Song *et al.* showed that the Tie1-cre-mediated β-galactosidase activity in the Tg(*Tie1-cre*)*;*R26R bigenic mice was readily detected at E9.5 with whole-mount staining (227). Histological analysis revealed that the Tie1-Cre-mediated β-galactosidase activity was detected in the endocardial cells, mesenchymal cells in the AV cushion and ECs, indicating that the Tie1-Cre-mediated DNA recombination occurred prior to endothelial-mesenchymal transition (EMT) during AV cushion formation.

As described above, the current Cre deleter lines used in endothelial biology have multiple advantages and disadvantages simultaneously. Therefore, the goal of this chapter is to establish a

stable transgenic line expressing Cre in arterial and pulmonary ECs using the 9.2 kb of *Alk1* promoter/enhancer. Because the Tg(*Alk1-cre*) line developed in this study will be used in the development of a mouse model for PAH, the primary focus of this chapter lies in the development and screening of the Tg(*Alk1-cre*) line(s) which exhibits an activity of Cre-mediated DNA excision in the lung ECs dominantly during late gestation and adult stages.

Results and Discussion

Expression Pattern of Alk1 During Lung Development

To examine the detailed expression pattern of endogenous Alk1 in the lung, lungs from various stages of the Tg(*Alk1-lacZ*) embryos were subjected to X-gal staining and histological analysis. Mouse lung development has been proposed to be divided into five stages based on epithelial processes: 1) embryonic (or lung bud) stage, 2) (pseudo)glandular stage, 3) canalicular stage, 4) saccular stage, and 5) alveolar stage (228;229). The lung bud stage (E8.0 - 9.0) occurs as the lung primordium is budded out from the foregut endoderm and subsequently envaginated into surrounding splanchnic mesenchyme. The endodermal bud branches and differentiates within the surrounding mesoderm, which ultimately gives rise to the airways, blood vessels, and alveoli of the mature lung together. The glandular stage (E9.0 - 16.0) is characterized by rapid and further branching of epithelial cells. The primary phase of vessel formation occurs during the canalicular stage (E16.0~) as blood vessels extend more peripherally following the airway branches. During maturation stages, the saccular and the alveolar stages (E17~), are characterized by formation of thick-walled saccules that are capable of respiratory function and eventually become the delicate septae of mature alveoli (230). As shown in Figure 4-2A, the Alk1-positive cells were readily detected in the primordial lung bud at E9.5. Using Tg(*Tie2-lacZ*) line, it has been shown that already at E9.5 - 10.0, ECs expressing Tie2 was part of the splanchnic plexus surrounding the developing esophagus and airways (231). In the study, Parera

et al clearly showed that ECs expressing other markers such as Flk1, Pecam1 and Fli1 were present surrounding lung epithelial cells.

As shown in Figure 4-1A, the branching of primordial lung to both left and right sides was obvious at E10.5. The whole mount X-gal staining of the lung revealed that a continuum of Alk1-positive cells was present at the proximal pulmonary vessels, whereas some patchy or speckled Alk1-positive cells were seen at the distal part of the lung (Figure 4-1A). The Alk1-positive cells in the forming of the proximal or branching pulmonary vessels were readily identified in the X-gal stained sections (Figure 4-2B). In the analysis, the forming afferent vessel, in which only the proximal part of the vessel contained erythrocyte-filled lumen, was continuous from the 6^{th} aortic arch (Figure 4-2B). Although the Alk1-positive cells were weakly stained with anti-Pecam1, most of the X-gal stained cells were overlapped with the marker (Figure 4-2C).

At E11.5, the Alk1-positive cells were further extended into the distal lung and formed efferent vessels which would give rise to the pulmonary vein (Figure 4-1B). Histological analysis showed that most of the Alk1-positive cells were overlapped with Pecam1 staining, and distal vessels were evident of formation of erythrocyte-containing lacunae (Figure 4-2F). It is interesting to note that the αSMA-positive cells started to sheathe the proximal part of the airway but not the vessels (Figure 4-2E). The data suggests that although the ECs expressing Pecam1 and Alk1 form the architecture of primitive lung blood vessels, the vessels are not mature yet.

In the E12.5 and 13.5 lungs, Alk1-positive cells started to delineate lines of connection from the pulmonary artery to the pulmonary vein ECs (Figure 4-1C and 1D). A cross section of an E13.5 lung showed that Alk1-positive cells extended further to the distal lung and surrounded the epithelial cells (Figure 4-3A).

In the E15.5 lung, the immunohistochemistry clearly indicated that the Alk1-positive cells were limited in the ECs (Figure 4-3B and 3C). The αSMA staining clearly marked SMCs surrounding epithelial cells and Alk1-positive ECs (Figure 4-3D). The pattern of X-gal staining in the lung was comparable with immunostaining with Pecam1 in the wildtype lung (Figure 4-3E and 3F).

In the present study, the expression pattern of Alk1 during lung development was examined. As discussed in Chapter 3, Alk1 is continuously expressed in pulmonary ECs, whereas other systemic vessels exhibit reduced or no Alk1 expression during adult stages. The data presented in this chapter suggest that pulmonary ECs start to express Alk1 from E9.5 and continue to express Alk1 throughout the rest of the developmental stages and adult life. Using vascular casting and electron microscopy, it has been proposed that pulmonary vessel formation is established by two distinct processes: the central (proximal) vessels formation is occurred by angiogenesis and peripheral (distal) vessels by vasculogenesis (232). The study suggested that the connection between the central and peripheral vascular lumen is established around E13.0-14.0 where the pulmonary circulation starts. However, Schachtner *et al.* showed that the connection between proximal vessels containing lumen and distal vessels lacking lumen was already formed by E10.5, indicating that the distal vessel is also formed in angiogenesis (230). Consistent with the finding, a recent study also demonstrated that using the Tg(*Tie2-lacZ*) line, the proximal and distal vessels are connected to each other during the lung bud stage (231).

Although in the presented study we can not completely rule out the possibility that Alk1 is expressed in the angioblasts, endothelial progenitor cells, Alk1-positive cells were present with a patchy and discontinuous cluster in the distal lung. The data, although it is substantial, suggests that Alk1 plays a role in the vasculogenesis during lung development. Another important finding

made known through this study is that like umbilical venous ECs, pulmonary venous ECs also express Alk1 from at least E12.5.

Generation of Tg(*Alk1-Cre)* Line

To develop the mouse line expressing the Cre recombinase in the arterial ECs, we constructed a p*Alk1-cre* vector which contained the 9.2 kb of *Alk1* promoter, SV40 splice donor and acceptor (SDSA), the internal ribosome entry site (IRES), and the Cre recombinase gene (Figure 4-4). By using the standard DNA injection technique, two founder lines were obtained (data not shown). The founders were screen by PCR analysis. The founder lines were mated with C57BL/6J mice to generate F1 offspring. To determine the tissue-specificity of the Cre-mediated DNA excision (which will be referred to as Cre activity hereafter), the F1 Tg(*Alk1-cre*) lines were intercrossed with a Cre tester line, R26R mice containing stop codon flanked by *loxP* sequences and a gene encoding β-galactosidase in the ROSA26 locus (233). Then, to determine whether the Cre activity could be seen in germ cells, some of the *Alk1-cre(+);*R26R bigenic mice were crossed with wild type C57BL/6J mice. Interestingly, one of the Tg(*Alk1-cre*) line, called Tg(*Alk1-cre*)-E, exhibited an ectopic onset of Cre activity in the germ cells. From the mating scheme, E10.5 embryos genotyped *Alk1-cre(+);*R26R, *Alk1-cre(-);*R26R, *Alk1-cre(+)*, and wild type were obtained. After X-gal staining and PCR genotyping, like *Alk1-cre(+);*R26R embryo, embryos genotyped *Alk1-cre(-);*R26R displayed Cre activity throughout their entire body, suggesting that the Cre-mediated DNA excision had occurred during germ cell formation in the Tg(*Alk1-cre*)-E line (data not shown).

In contrast to the Tg(*Alk1-cre*)-E line, the other line called Tg(*Alk1-cre*)-L1 exhibited an onset of Cre activity during the late embryonic stages. In this line, the patchy X-gal staining was observed in E13.5 lung as shown in Figure 4-5A. A histological sectioning of the lung displayed

discontinuous X-gal staining in the pulmonary vessels. Immunostaining with anti-Pecam1 showed incomplete colocalization of the immunostaining on the X-gal stained ECs (Figure 4-5B and 5C). At E15.5, however, the Tg(*Alk1-cre*)-L1 showed a uniform X-gal staining in the pulmonary ECs (Figure 4-5D). As shown in Figure 4-5E and 5F, the X-gal staining was completely overlapped with Pecam1 immunostaining. Interestingly, Cre activity in the Tg(*Alk1-cre*)-L1 line was dominant in the pulmonary vessel whereas mosaic or no activities were observed in the systemic vessels.

Newborn pups from the Tg(*Alk1-cre*) and R26R cross were obtained. As shown in Figure 4-6A, whole-mount X-gal staining was seen in the dorsal aorta and branching intercostal arteries in the *Alk1-cre(+);*R26R bigenic mouse, but not in the *Alk1-cre(-);*R26R monogenic mouse (Figure 4-6B). In the histological analysis, however, a mosaic Cre activity judged by discontinuous X-gal staining was detected in the cross section of the dorsal aorta (Figure 4-6C).

Next, the pattern of X-gal staining during postnatal life was carefully examined. As shown in Figure 4-6D, the staining intensity and pattern of X-gal staining was robustly and evenly detected in most of the ECs at 2 week-old lungs. The Cre activity in the Tg(*Alk1-cre*)-L1 line was detected in most likely all of the pulmonary ECs including arteries, capillaries and veins.

In this study, we presented a novel Tg(*Alk1-cre*)-L1 line which exhibited uniform and persistent Cre activity in the pulmonary ECs from E15.5 on. The immediate goal of this chapter was to develop a novel Tg(*Alk1-cre*) line for the development of an animal model of human PAH in Chapter 5. As discussed in Chapter 3, because it has been shown that Tg(*Alk1-lacZ*) line displays the absence of LacZ expression in the endocardiac ECs, there are clear advantages of using the Tg(*Alk1-cre*)-L1 line over already established Cre lines driven by other endothelial cell-specific promoters, such as *Tie2-Cre*, *Tie1-Cre*, *Flk1-Cre*, and $Flk1^{+/cre}$ KI lines. To

overcome any early developmental defects in cardiogenesis and pulmonary blood vessel formation, the Tg(*Alk1-cre*)-L1 line is useful because of pulmonary EC-dominant Cre activity. Moreover the deletion of Bmpr2 by crossing with the Tg(*Tie2-cre*) line can cause severe cardiac defects (personal communication). The presented Tg(*Alk1-cre*)-L1 line will be a unique mouse line for studying the underlying mechanism of Bmpr2-related PAH in ECs.

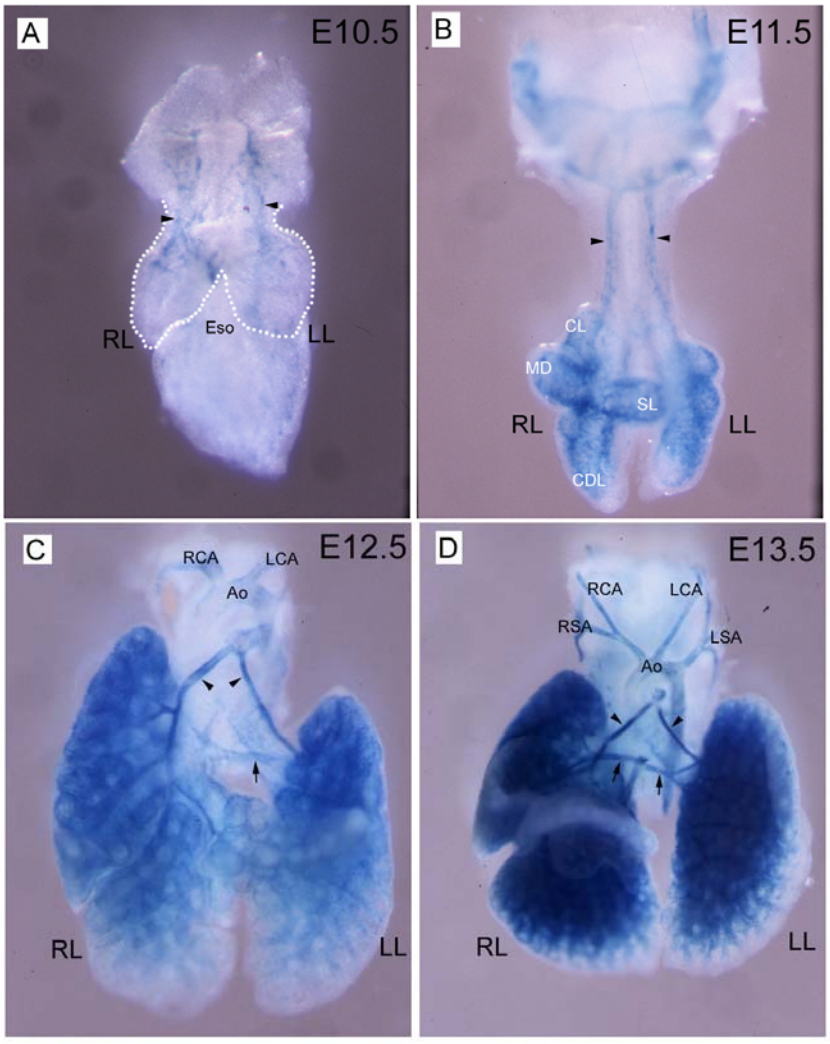

Figure 4-1. Dynamics of Alk1 expression during mouse lung development. The whole mount view of X-gal stained Tg(*Alk1-lacZ*) lungs at E10.5 - 13.5. A) At E10.5, lung branching to left and right lobes were readily detected (marked white dot line) and continuous distributions of Alk1-positive cells were evident in the afferent vessels (arrow head). On the other hand, a patchy distribution of Alk1-positive cells was detected in the distal lung. B) At E11.5, the primitive lung lobes were obvious. Alk1 expression is further extended to the distal lung. C) and D) At E12.5 and 13.5, Alk1 expression was detected in the large vessels such as aorta (Ao) and branching left and right common carotid arteries (LCA and RCA, respectively) and right and left subclavian arteries (RSA and LSA, respectively). At the stages, Alk1 expression is detected in the pulmonary arteries and veins (arrow). Eso; esophagus, RL; right lobe, LL; left lobe, CL; cranial lobe, ML; medial lobe, CDL; caudal lobe, SL; sacral lobe.

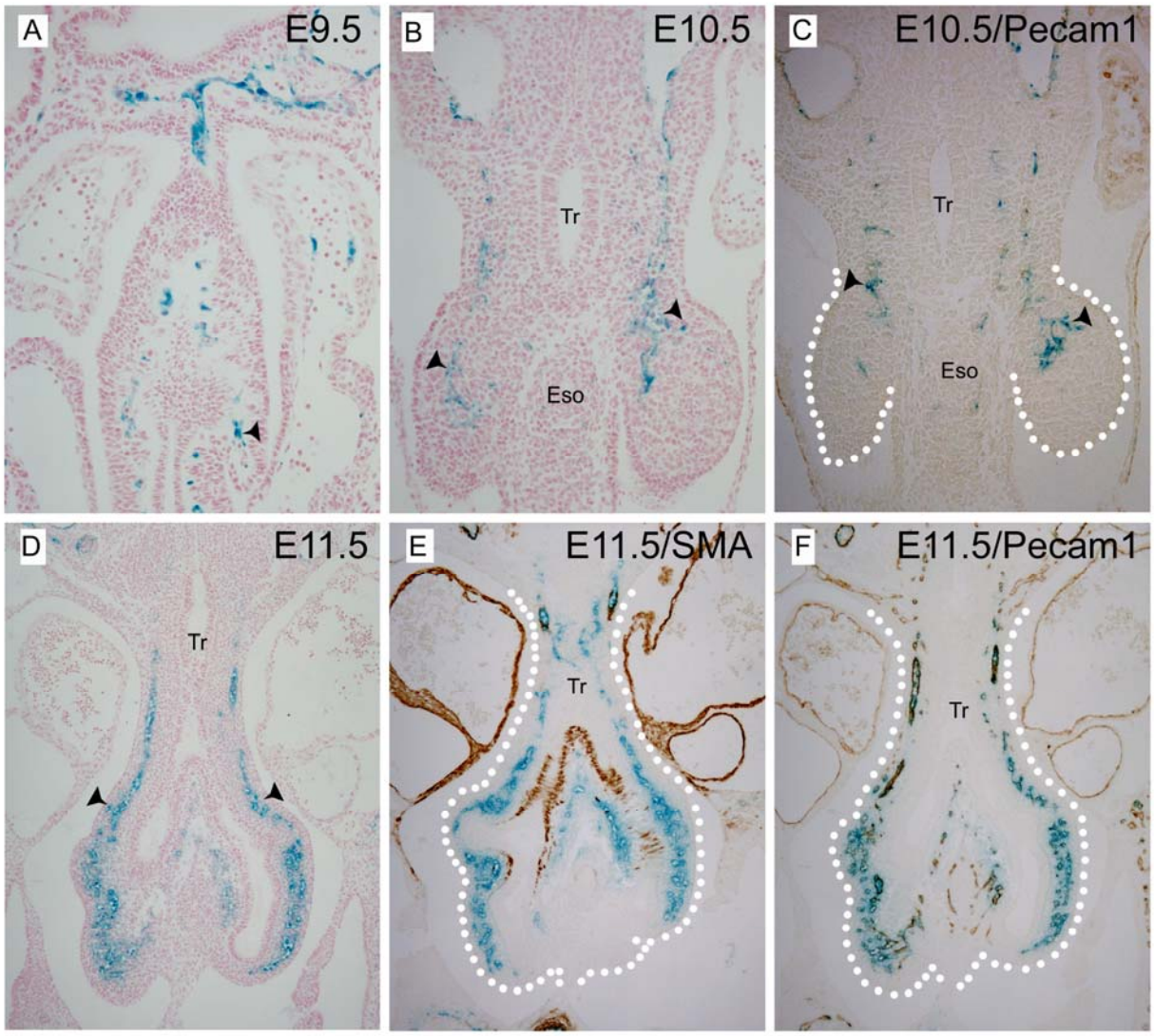

Figure 4-2. Ontogeny of Alk1 in the E9.5 - 11.5 lungs. A) The isolated Alk1-positive cells were readily detected in the primordial lung bud at E9.5 (arrow head). B) The branching of primordial lung to both left and right sides was obvious at E10.5. A continuous line of Alk1-positive cells were detected at the proximal part of lung (arrow head), whereas patchy Alk1-positive cells were detected at distal lung at E10.5. C) Most of Alk1-positive cells were colocalized with Pecam1 immunostaining. D) At E11.5, the Alk1-expressing cells were further extended to distal lung. E) Immunostaining with αSMA defines bronchial SMCs. Note that no αSMA-positive cells were detected in the vessels. F) Immunostaining with Pecam1 was completely overlapped with X-gal staining. Tr; trachea, Eso; esophagus.

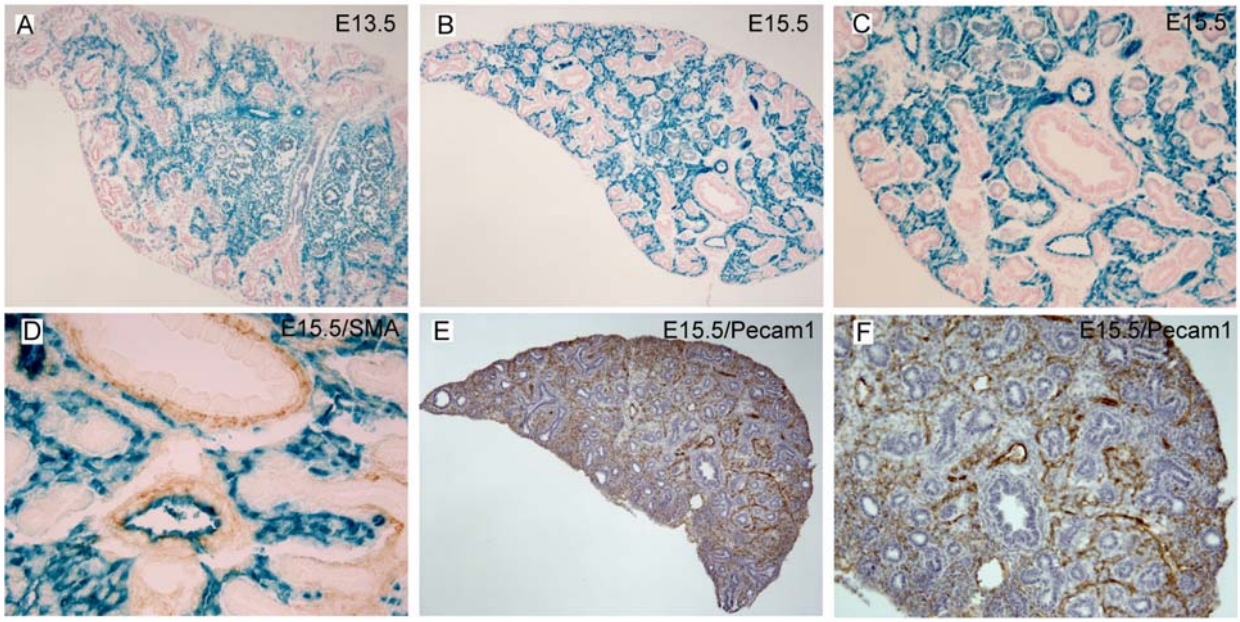

Figure 4-3. Ontogeny of Alk1 in the E13.5 and E15.5 lungs. A) and B) The Alk1-positive cells were further extended to distal lung during E13.5 - 15.5. C) A high magnification of view of E15.5 revealed the Alk1expression in the ECs. D) Immunohistochemistry with αSMA further confirmed that the Alk1 expression were limited in the ECs. E) and F) The pattern of immunostaining with Pecam1 was indistinguishable with the pattern of X-gal staining at E15.5.

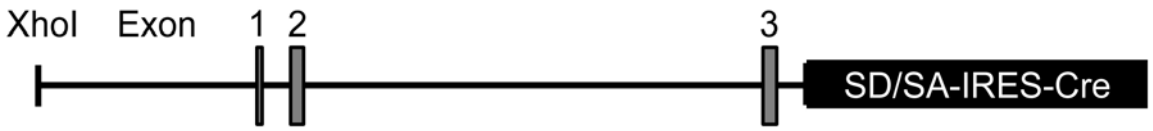

Figure 4-4. The *pAlk1-cre* construct. The 9.2 kb of *Alk1* promoter/enhancer is connected to Cre cassette. For proper splicing and transcription, the Cre cassette contains SV40 splicing donor/acceptor signals (SD/SA), internal ribosomal entry sequence (IRES), Cre gene and poly A signal.

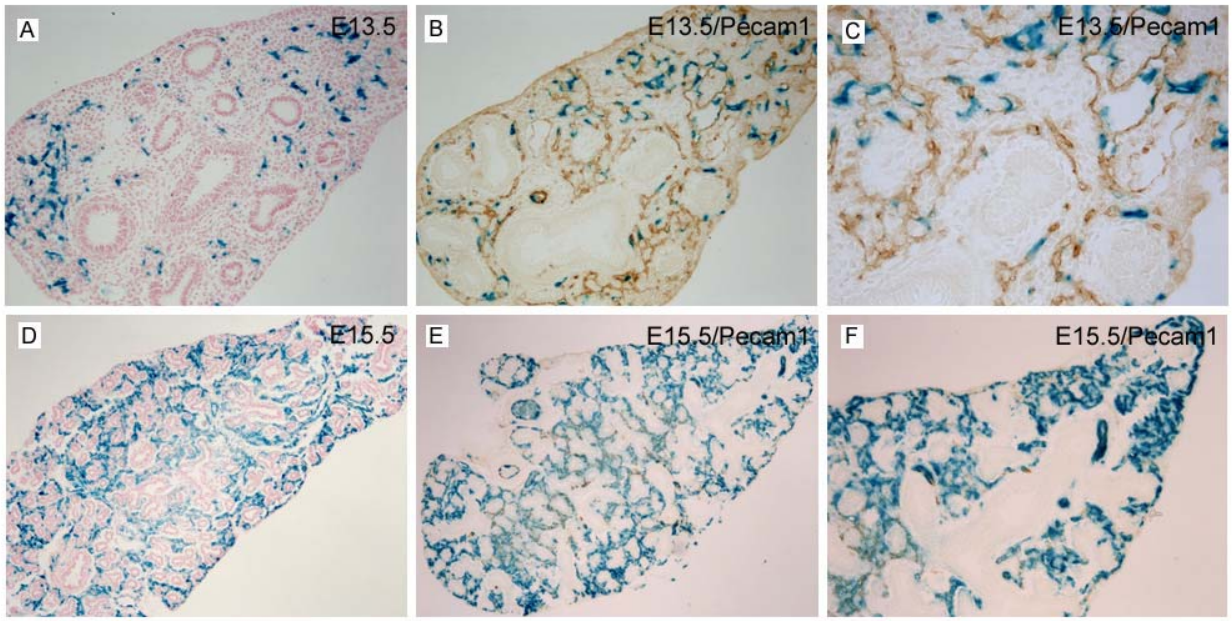

Figure 4-5. The pattern of Cre activity in the lung of Tg(*Alk1-cre*)-L1 line. A) At E13.5, a patchy Cre activity was detected in ECs. B) and C) Immunostaining with Pecam1 demonstrated colocalization of X-gal stained ECs. Note that a subset of pulmonary ECs exhibits Cre activity. D) - F) At E15.5, most of pulmonary ECs displayed Cre activity confirmed by Pecam1 immunostaining.

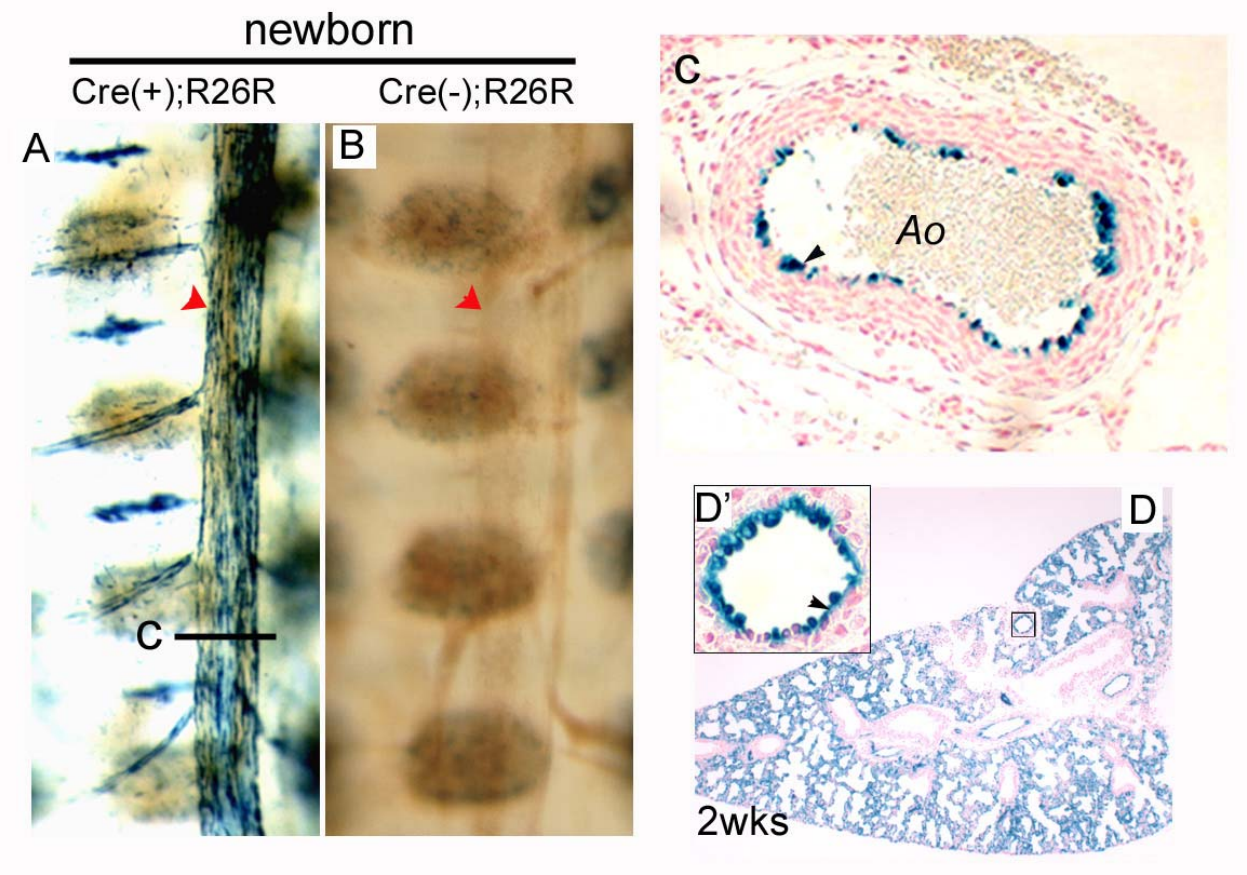

Figure 4-6. Cre activity in the Tg(*Alk1-cre*)-L1 line during postnatal stages. A) Whole mount X-gal staining showed Cre activities in the aorta (red arrowheads) and branching intercostal arteries in the *Alk1-cre(+)*;R26R bigenic mice, but not in the *Alk1-Cre(-)*;R26R monogenic mice B). C) Histology revealed a mosaic pattern of Cre activity in the aortic ECs. D) In the 2wks lung, a uniform pattern of Cre activity in the pulmonary ECs was detected. D') A high magnification view of one of pulmonary arteries. Black arrowheads represent ECs containing a recombined allele via Cre activity.

CHAPTER 5
DEVELOPMENT OF AN ANIMAL MODEL OF HUMAN PULMONARY ARTERIAL HYPERTENSION (PAH)

Note

The work presented in this chapter will be published in the "Genetic ablation of the *Bmpr2* gene in pulmonary endothelium is sufficient to predispose pulmonary arterial hypertension." by Hong KH, Lee YJ, Beppu H, Bloch K, Li E, Raizada MK, and Oh SP (in preparation)

Introduction

Pulmonary arterial hypertension (PAH) is a rare lung disorder (2-3 per million per year), in which pulmonary arterial mean pressure rises far above normal levels (25 mmHg at rest and 30 mmHg during exercise) (234-236). Pathological features of PAH include intimal fibrosis, medial hypertrophy, adventitial proliferation, plexiform lesions, and the obliteration of small arteries in the lung. Such alterations in precapillary pulmonary arteries cause increased pulmonary vascular resistance, which leads to right ventricular hypertrophy and eventually to heart failure. Prognosis of PAH is still poor, despite recent advances in therapeutics showing a beneficial effect on the survival rate of some PAH patients (8).

The pathogenesis of PAH is largely unknown, but there are ample evidence implicating the involvement of diverse vascular effectors. In general, pulmonary hypertension can be promoted by hormones, growth factors, neurotransmitters, and environmental stresses that induce pulmonary vascular constriction, cell proliferation, or vascular remodeling (1;6). Genetic studies have shown that impairment of bone morphogenic protein receptor type II (BMPR2) signaling plays a critical role in pathogenesis of PAH. Most cases of PAH are sporadic, but about 10% of them are inherited in an autosomal-dominant manner. Heterozygous mutations of the *BMPR2* gene were found in 70% of familial PAH cases (60;90;93;237). Furthermore, 26% of apparently sporadic PAH cases also contain germline *BMPR2* mutations (62). The characteristics

of *BMPR2* mutations indicate haploinsufficiency as the molecular mechanism of disease (14). In addition to the *BMPR2* gene, recent studies have shown that PAH also develops in hereditary hemorrhagic telangiectasia (HHT) patients with *ALK1* (Activin receptor Like Kinase-1) or *ENG* (ENDOGLIN) mutations (63;65;66).

Studies have shown that abut 20% of people harboring a heterozygous *BMPR2* mutation exhibit PAH phenotype, suggesting that the heterozygous *BMPR2* mutations are necessary, but by themselves insufficient, to account for the clinical manifestation of PAH (238). Environmental or genetic second hits may play a pivotal role in triggering the disease. Mononuclear cell infiltrations were often observed in the PAH vascular lesions, implicating inflammation as a potential environmental factor triggering PAH (14). Inflammation inflicted by viral transduction of 5-lipoxygenase (5LO), an inflammation mediator, in Bmpr2 hetrozygous mice ($Bmpr2^{+/-}$) mice displayed PAH phenotype (134). Serotonin also increased susceptibility to PAH in $Bmpr2^{+/-}$ mice by inhibiting BMP signaling in smooth muscle cells (135). In terms of genetic second hit, loss of heterozygosity (LOH) of *BMPR2* allele was investigated. A report showed that BMPR2 heterozygosity was retained in plexiform and concentric vascular lesions of 7 familial PAH patients harboring *BMPR2* mutations (172), demonstrating that BMPR2 LOH is not required for abnormal vascular remodeling in PAH. It remains unknown, however, whether or how homozygous *BMPR2* mutations impact on morphogenetic changes of pulmonary vessels pertinent to PAH.

The cellular origin critical for initiation of PAH pathogenesis has not been clearly demonstrated. Hyper-proliferation SMC layer is a key feature of PAH pathogenesis. Plexiform lesions consist of over-proliferating endothelial cells. Adventitial proliferation is also involved in PAH pathology. BMPR2 is expressed in multiple cell types in the lung. In blood vessels,

BMPR2 expression was observed in SMC and adventitial fibroblasts, as well as in ECs (14;239). Transgenic mice in which a dominant-negative form of Bmpr2 was expressed selectively in SMCs developed pulmonary hypertension (136), implicating perturbed BMPR2 signaling in SMCs for the pathobiology of PAH. It remains unknown, however, whether *BMPR2* mutations in pulmonary ECs can also trigger the disease.

Here we show using the *Cre/loxP* system that heterozygous *Bmpr2* deletion in pulmonary ECs can predispose to PAH. We also demonstrate that homozygous *Bmpr2* deletion in pulmonary ECs is insufficient to cause PAH, but increases susceptibility to PAH. This novel animal model will provide valuable resources with which to further our understanding of the etiology and pathogenesis of PAH.

Results

Bmpr2 Deletion in Pulmonary ECs by a Novel Cre Transgenic Mouse Line

To investigate the role of BMPR2 signaling in pulmonary vascular endothelium, we utilized a *Bmpr2* conditional knockout mouse strain (180) and a novel Cre transgenic mouse line, designated as Tg(*Alk1-cre*)-L1 (Park *et al*., unpublished). The Tg(*Alk1-cre*)-L1 line was established during the screening of multiple transgenic founder lines in which the Cre recombinase is driven by a 9.2 kb *Alk1* genomic fragment (240). Unlike other Tg(*Alk1-cre*) and known endothelium-specific Cre lines, Cre-mediated DNA excision (Cre activity, hereafter) was not detected in the endocardial cells and their progeny in Tg(*Alk1-cre*)-L1 mice. On the other hand, the Cre activity was observed in pulmonary ECs from its emergence during embryogenesis till adulthood. We have monitored the Cre activity of neonatal and adult Tg(*Alk1-cre*)-L1 mice by crossing them with R26R mice in which constitutive lacZ expression is designed to be activated by Cre. As shown in Figure 5-1A and 1B, the Cre activity was detected in vast areas of the lung of 5 month-old Tg(*Alk1-cre*)-L1;R26R mice. Histological sections showed that

pulmonary ECs were positive, whereas the bronchial epithelia and smooth muscle layers were negative for the Cre activity. We crossed Tg(*Alk1-cre*)-L1 mice with *Bmpr2*$^{f/f}$ females to generate *Bmpr2*$^{+/f}$;Tg(*Alk1*-cre)-L1 male mice, that were subsequently crossed with *Bmpr2*$^{f/f}$;R26R females.

The Cre(+);*Bmpr2*$^{f/f}$ mice were viable over 8 months. Genomic PCR analysis on multiple organs/tissues of two month-old Cre(+);*Bmpr2*$^{f/f}$ mice revealed that the Cre-mediated *Bmpr2* gene excision was detected only in the lung sample, indicating a lung-specific Cre expression in the L1 line (Figure 5-1C). Western blot analysis on whole lung extracts with anti-BMPR2 antibody revealed a reduced amount of BMPR2 protein in Cre(+);*Bmpr2*$^{+/f}$ and Cre(+);*Bmpr2*$^{f/f}$ lungs compared to Cre(-);*Bmpr2*$^{f/f}$ controls (Figure 5-1D).

***Bmpr2* Deletion in Pulmonary ECs Can Induce Elevation of RVSP and RV Hypertrophy**

To assess the pulmonary artery pressure, right ventricular pressure was measured by right heart catheterization through the right jugular vein. At 2-4 month-old ages, mean right ventricular systolic pressure (RVSP) of control [Cre(-);*Bmpr2*$^{f/f}$] mice was 23 ± 0.68 mmHg (n=11). The mean RVSP of Cre(+);*Bmpr2*$^{+/f}$ was not significantly higher than that of control, but one mouse had RVSP of 44 mmHg (Figure 5-2A). The mean RVSP of Cre(+);*Bmpr2*$^{f/f}$ was significantly higher (30.1 ± 2.1 mmHg; $p < 0.05$) than that of control (Figure 5-2A). Out of 24 Cre(+);*Bmpr2*$^{f/f}$ mice examined, 7 of them showed RVSP higher than 30 mmHg. This result indicates that endothelial heterozygous and homozygous *Bmpr2* deletion can elevate pulmonary arterial pressure in a gene-dosage dependent manner.

To determine whether the frequency or severity of pulmonary hypertension (PH) is affected by aging, we measured the RV pressure on 6 month-old mice. As shown in Figure 5-2B, the frequency of PH in Cre(+);*Bmpr2*$^{+/f}$ (3/10) and Cre(+);*Bmpr2*$^{f/f}$ (6/9) 6 month-old group was increased compared to that in 2-4 month-old corresponding genotype groups. There was no

significant difference in the systemic pressure among different genotype groups, nor between PH (i.e., above 30 mmHg RVSP) and non-PH (N-PH; below 30 mmHg RVSP) groups (Figure 5-2C). The RV/(LV+septum) ratio, an indicator of RV hypertrophy, was significantly higher in the PH group compared to the control or non-PH group, confirming the presence of sustained elevation of RV pressure (Figure 5-2D).

Increased Number and Medial Wall Thickness of Alpha-SMA-Positive Distal Arteries in the Mutant Mice with Elevated RVSP

To determine whether the elevation of RVSP and right ventricular hypertrophy were associated with pulmonary vascular remodeling, lung tissue sections were examined by H&E staining and immunohistochemistry. General aspects of lung development and morphology were indistinguishable among genotype groups and between the PH and non-PH groups. Immunostaining of the lung sections with αSMA antibodies revealed increased number of αSMA-positive small arteries and thickness of SMC layers of small arteries in the PH group compared to the non-PH group (Figure 5-3A and 3B). Quantitative morphometric analysis demonstrated that the percentages of αSMA-positive small arteries (30-70 μm outer diameter) in the PH group were significantly greater than those in the non-PH group in both Cre(+);*Bmpr2*$^{+/f}$ and Cre(+);*Bmpr2*$^{f/f}$ mice (Figure 5-3C). It is noteworthy that the percentage of αSMA-positive small arteries in the non-PH Cre(+);*Bmpr2*$^{f/f}$ mice was also significantly greater than that in the non-PH Cre(+);*Bmpr2*$^{+/f}$ mice (Figure 5-3C). The thickness of medial layer of αSMA-positive small arteries in the PH group was also significantly greater than that in the non-PH group (Figure 5-3D).

Pathohistological Features of PAH in the Mutant Mice with Elevated RVSP

Elevated serotonin signaling and tenascin-C (Tn-C) expression have been implicated in the pathogenesis of PAH. Transgenic mice overexpressing the 5-hydroxytryptamine transporter

(5HTT) gene in smooth muscles develop pulmonary hypertension (150). Tenascin-C (Tn-C) is an extracellular matrix glycoprotein induced in a number of experimental and clinical forms of PAH, including familial PAH, monocrotalin-induced PAH, and flow-induced vascular remodeling (241-243). Immunostaining with anti-5HTT and Tn-C antibodies visualized marked elevation of these proteins in the SMC layer of the PH lungs (Figure 5-4C and 4F).

We found a high incidence of focal leukocyte infiltrations at the periphery of pulmonary vessels of Cre(+);*Bmpr2*$^{+/f}$ (38%; 5/13) and Cre(+);*Bmpr2*$^{f/f}$ (44%; 11/25) mice compared to the control mice (0/11) (Figure 5-5A and 5B). Among Cre(+);*Bmpr2*$^{f/f}$ mice, frequency of the infiltration appeared to be higher in the PH group (8/14) than that in the N-PH (3/11) group. Most of the infiltrated cells were CD68-positive monocyte/macrophages (Figure 5-2B inset). Neointima formation in occlusive arteries was also observed in a limited number of the PH lungs (Figure 5-2C – 2E). *In situ* thrombosis of small muscular arteries was also observed in about 50% (9/18) of the PH lungs. As shown in Figure 5-5F, lumens of the affected vessels were partially or completely occluded by fibrin(ogen)-positive thrombi.

Discussion

We show here that some, but not all, mice having the genetic ablation of *Bmpr2* in pulmonary ECs exhibited an elevation of RVSP with various histopathological features reminiscent of human PAH lungs, demonstrating for the first time *in vivo* that *Bmpr2* mutation in endothelium is sufficient to predispose PAH. Homozygous *Bmpr2* deletion, by itself, was not sufficient to cause PAH, but increased the susceptibility to PAH.

PAH is a heterogeneous disorder, having multiple etiology. A mounting body of evidence, however, has shown that BMP signaling pathway plays a pivotal role in the pathogenesis of PAH. Genetic studies have demonstrated that heterozygous *BMPR2* mutations predispose PAH in sporadic as well as familial cases (60;62;90;93;237). In addition, recent

studies revealed that impaired BMPR2 signaling might be a central mechanism for PAH caused by hypoxia and MCT administration, two major experimental animal models for PAH (132;243).

Since the pathogenesis of PAH involves all vascular components, identity of the principal cell type for PAH pathogenesis has been investigated. West *et al.* have shown by an inducible transgenic approach that overexpression of a dominant-negative form of Bmpr2 resulted in elevation of pulmonary arterial pressure, suggesting that impairment of the Bmpr2 signal in SMC might be sufficient to cause PAH (136). Despite the lack of direct evidence, pulmonary ECs have been suspected as a primary cell type in which *BMPR2* mutations elicit PAH. Occurrence of plexiform, which consist of proliferative endothelial cells, in severe form of PAH, suggests that pulmonary ECs are the principal source of PAH pathogenesis. Predisposition of PAH by mutations in *ALK-1* or *ENG* genes (63;65;66), which express primarily in endothelial cells (117;244), also support this speculation. The data presented here is the first direct in vivo evidence, however, that endothelial Bmpr2 mutation is sufficient to predispose PAH.

Since familial PAH is a dominantly inherited disease and haploinsufficiency is a common mechanism for familial PAH, *Bmpr2*$^{+/-}$ mice received much attention as a genetic model. Although an initial report showed modest elevation of mean pulmonary arterial pressure in *Bmpr2*$^{+/-}$ mice (133), more recent studies using the same mouse strain showed no significant difference of RVSP between *Bmpr2*$^{+/-}$ and control mice (134;135). We showed here dichotomy of PAH phenotype among mice harboring heterozygous *Bmpr2* deletion in pECs: 1/11 (9%) in 2-4 month-old group and 3/9 (33%) in 6 month-old group. The reason for this discrepancy is unclear, but perhaps the differences in a number of experimental conditions used might have contributed to it. These include methods for hemodynamic study (*i.e*. direct cardiac puncture *vs*. cardiac catheterization), anesthesia conditions, and number, age and strain of mice.

We showed that endothelial *Bmpr2* deletion can cause muscularization of the medial layer of distal arteries. Since no Cre activity was detected in SMCs, the BMPR2 signaling must be intact in SMCs of these mice. Therefore, medial hypertrophy in the PH group mice is due to indirect effect of defects in endothelial cells. We observed a higher incidence of infiltration of CD68-positive mononuclear cells in the perivascular regions of Cre(+);*Bmpr2*$^{+/f}$ and Cre(+);*Bmpr2*$^{f/f}$ mice compared to Cre(-);*Bmpr2*$^{f/f}$ controls, and a higher frequency in the PH group than the N-PH group. This data suggests that *Bmpr2* deletion in pulmonary ECs may cause some forms of endothelial dysfunction, which makes the pulmonary vessels more susceptible to secondary triggers such as inflammation or thrombosis. This result is consistent with pathological findings in human PAH samples, and also consistent with the report demonstrating that *Bmpr2*$^{+/-}$ develop PAH upon treatment with pro-inflammatory reagents or serotonin (134;135). What remains to be investigated, however, is the nature of the 'endothelial dysfunction', and the underlying mechanism by which *Bmpr2* deletion in pulmonary ECs causes such a condition.

Based on the observation that cells in the plexiogenic lesion are monoclonal (12;171), LOH of the *BMPR2* gene in those cells has been suggested as a potential pathogenetic mechanism for PAH. Machado *et al.* investigated microsatellite instability in 5 loci including a *BMPR2* locus on DNA samples isolated from plexiform and concentric vascular lesions of 7 familial PAH patient lungs by laser microdissection technique, but heterozygosity of the *BMPR2* gene appeared to be maintained (172). This result demonstrated that LOH of BMPR2 is not necessary for the development of such vascular lesions. We demonstrated here that homozygous *Bmpr2* deletion in pulmonary ECs by itself is not sufficient to develop PAH. Our data showed, however, that homozygous *Bmpr2* deletion significantly increases the susceptibility to PAH,

compared to heterozygous *Bmpr2* deletion. We observed a high incidence of infiltration of CD68-positive mononuclear cells in the perivascular regions of PAH lungs, suggesting that *Bmpr2* deletion in pulmonary ECs may cause some forms of endothelial dysfunction, which makes the pulmonary vessels more susceptible to secondary triggers such as inflammation or thrombosis. This result is consistent with pathological findings in human PAH samples, and also consistent with the report demonstrating that *Bmpr2*$^{+/-}$ develop PAH upon treatment with pro-inflammatory reagents or serotonin (134;135). What remains to be investigated, however, is the nature of the 'endothelial dysfunction', and the underlying mechanism by which *Bmpr2* deletion in pulmonary ECs causes such a condition.

It is unclear why some, but not all, mutant mice develop PAH. There was no gender bias for the PAH phenotype in the mutant mice. To examine the possibility that the phenotypic variation resulted from variance of *Bmpr2* deletion in pulmonary ECs, we monitored the Cre activity by introducing the R26R allele. No differences in the intensity and pattern of X-gal staining were detected between PH and N-PH groups regardless of their genotypes, indicating that the phenotypic variation should not be attributed to incomplete excision of *Bmpr2* gene in pulmonary ECs. Also, the PAH phenotype had no correlation with the presence of R26R allele. We showed here that about 30% of Cre(+);*Bmpr2*$^{+/f}$ mice showed PAH phenotype at 6 months of age. This statistic result is similar to human studies showing that about 20% of people harboring *BMPR2* mutations develop PAH (238). Since mice used in this present study were on 129Sv, C57BL/6, and FVB mixed background, strain-specific genetic modifiers might have played a role for controlling the susceptibility to the second hit.

The underlying pathogenetic mechanisms for PAH is poorly understood. One of the major impediments for this task is limited access to biological samples. PAH is a rare disease, and only

available pathological samples are from lung transplantation patients, at the very last stage of the disease. The animal models for PAH will therefore provide relevant pathological samples from early to late stages of PAH. Once established, these animals can also be used to test the efficacy of novel therapeutic drugs. Tg(*Alk1-cre*)-L1 as well as Cre(+);*Bmpr2*$^{f/f}$ mouse lines presented here will be useful genetic resources to further our knowledge about PAH pathogenesis, specifically for the role of BMPR2 signaling in pulmonary endothelium.

Currently available endothelial Cre lines, including Tg(*Tie1-cre*), Tg(*Tie2-cre*), *Flk1*$^{+/cre}$, and Tg(*Vecad-cre*) lines, express the Cre recombinase in the endocardial cells, progeny of which constitute atrioventricular cushions (217;225;226;245). Conditional deletion of several TGF/BMP receptors using these Cre lines appeared to have some form of cardiac malformations, such as cardiac valve or ventricular septal defects (221;227;246). When we deleted the *Bmpr2* gene using Tg(*Tie2-cre*) mice, most Tg(*Tie2-cre*);*Bmpr2*$^{f/-}$ mice died before the weaning age because of the presence of cardiac malformations (unpublished; Beppu *et al*.). In this regard, the Tg(*Alk1-cre*)-L1 line is superior to these known endothelial Cre lines for evaluating the impact of a gene deletion in pulmonary ECs because Cre is not expressed in the endocardial cells and their progeny during cardiogenesis stages (Park *et al*. unpublished). The Tg(*Alk1-cre*)-L1 line will also be useful to assess the role of other BMPR2 signaling partners (e.g BMPR1A and SMAD1) or of potential downstream mediators in PAH pathogenesis of PAH.

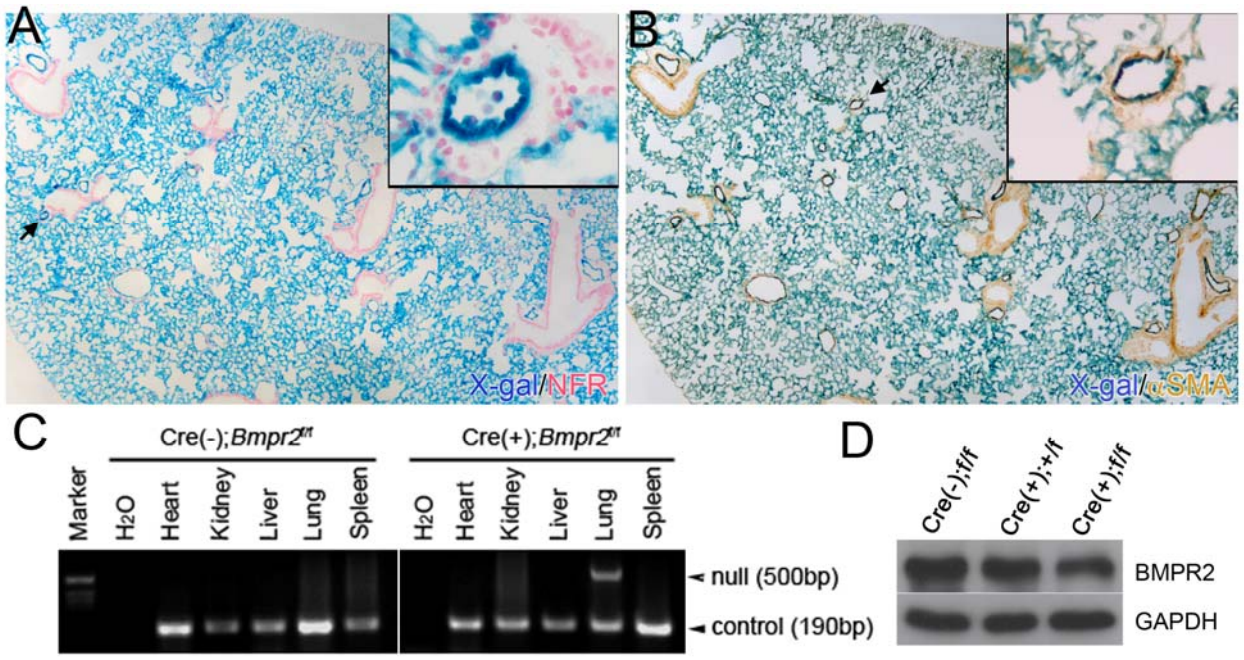

Figure 5-1. Tg(*Alk1-cre*)-L1 mice express the Cre recombinase in the pulmonary vascular endothelial cells. A) and B) The cells in which Cre-mediated recombination has occurred were visualized by staining the lungs of 5-month-old Tg(*Alk1-cre*)-L1;R26R bigenic mice with X-gal for the lacZ expression. Sections of whole mount X-gal stained lungs were counter stained with nuclear fast red (NFR; A), or with αSMA antibody. Insets are magnified views of the area indicated by arrows. Note that X-gal positive cells resided in vascular ECs, but neither in airway epithelial cells nor smooth muscle cells. C) PCR detection of the $Bmpr2^{\Delta Ex4,5}$ allele (i.e., deletion of exons 4 and 5 of *Bmpr2* by Cre) from genomic DNA isolated from multiple organs/tissues of 2-month-old Cre(-);$Bmpr2^{f/f}$ (left) and Cre(+);$Bmpr2^{f/f}$ (right), demonstrating a lung-specific Cre activity. A primer set amplifying an Alk1 locus (~190 bps) was used as a control for PCR reaction. D) Western blotting analysis with BMPR2 antibody on whole lung lysate shows reduced levels of BMPR2 protein (~120 kd) in Cre(+);$Bmpr2^{+/f}$ and Cre(+);$Bmpr2^{f/f}$ lungs compared to Cre(-);$Bmpr2^{f/f}$ lungs. GAPDH (~36 kd) was used as a loading control.

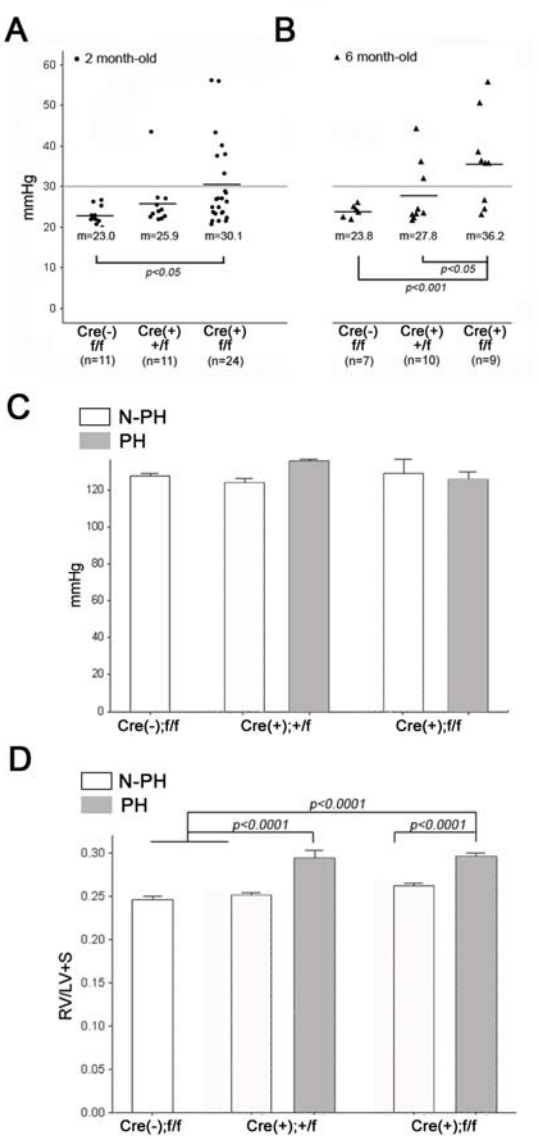

Figure 5-2. Endothelial *Bmpr2* deletion resulted in elevation of RVSP and RV hypertrophy in gene dosage and age dependent manners. A) and B) RV pressure of control, Cre(+);*Bmpr2*$^{+/f}$ and Cre(+);*Bmpr2*$^{f/f}$ mice was measured at 2-4 and 6 months of age. Each dot represents RVSP of an individual mouse. Mean value (m) of RVSP of each genotype group was given and indicated by horizontal bars. Pulmonary hypertensive (PH) group (i.e. RVSP greater than 30 mmHg; open bar) and none-PH (N-PH; solid bar) group were separated in each genotype in C) and D). C) Systolic systemic pressure was recoded by an indirect tail cuff method. There was no significant difference among any comparisons. D) The RV/(LV+S) ratios in PH groups were significantly greater than that in N-PH groups regardless of their genotypes. Levels of statistical significance are indicated.

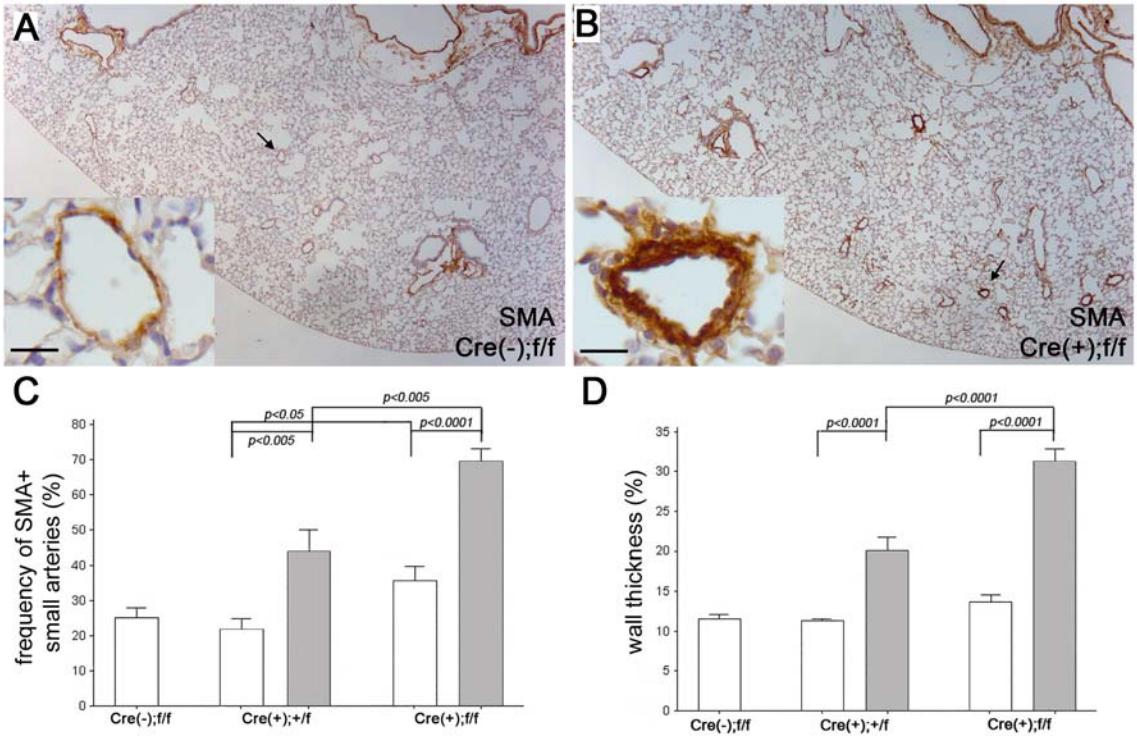

Figure 5-3. Mice in the PH group exhibited increased number of muscularized distal arteries and thickening of medial layers. A) and B) Representative histological sections of control and PH lungs, stained with αSMA antibody. Insets in A) and B) are magnified views of the areas indicated by arrows. Note readily identifiable strong αSMA-positive small arteries in the PH group lungs, and thickening of arterial walls (inset in B). Scale bars in insets represent 25 μm. C) and D) Percentages of small arteries positive for αSMA staining and medical thickness of distal arteries were compared among five groups, i.e. control, PH and N-PH groups in each mutant genotype. Mice in PH group in either genotype showed significant increases in number of αSMA-positive small arteries and in thickness of medial layers.

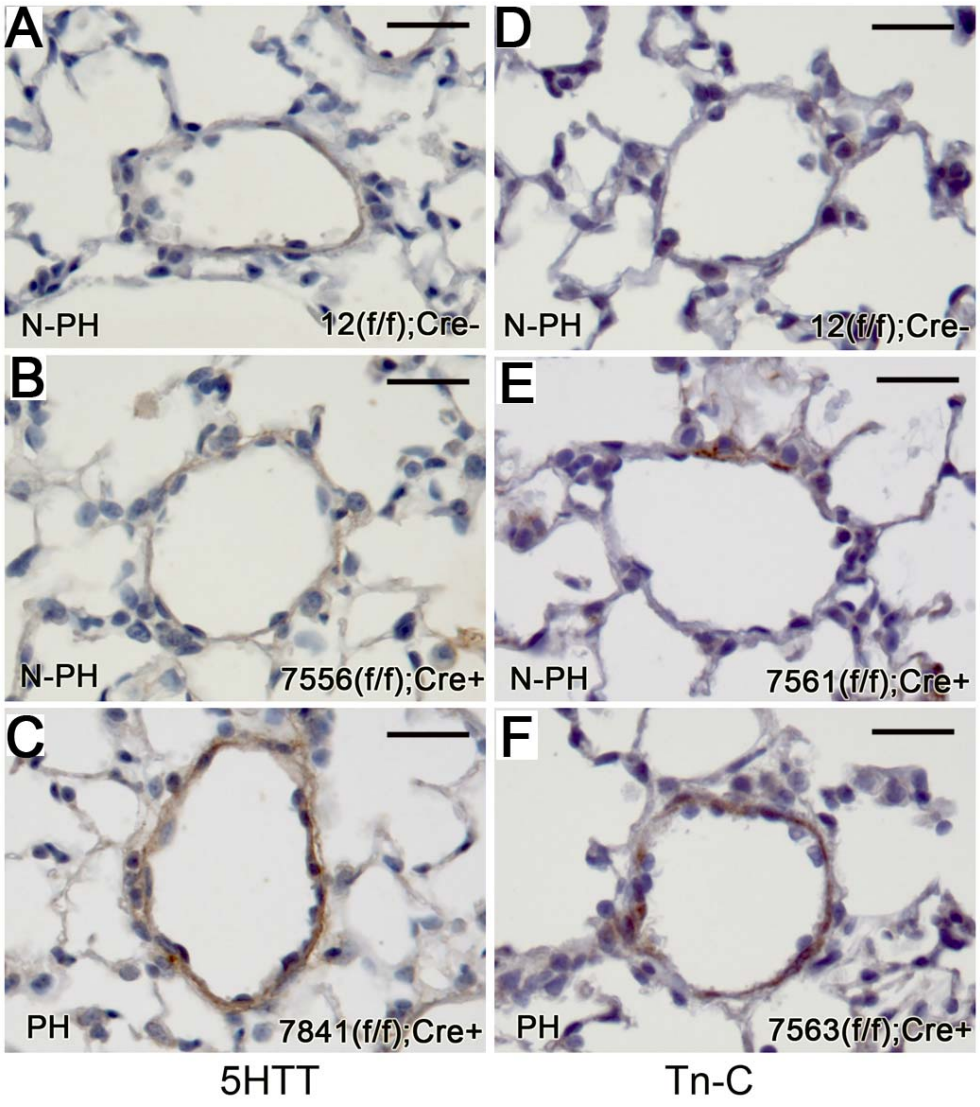

Figure 5-4. Previously identified PAH-associated protein expressions were elevated in SMC layers of PH mouse lungs. A) - F) Immunostaining of control and mutant lungs with antibodies against serotonin transporter (5HTT) and tenascin-C (Tn-C) revealed elevated expression of both 5HTT and Tn-C in SMC layers of PH group samples compared to control and N-PH group samples. Representative areas containing similar sized vessels were shown. Scale bars represent 25 μm.

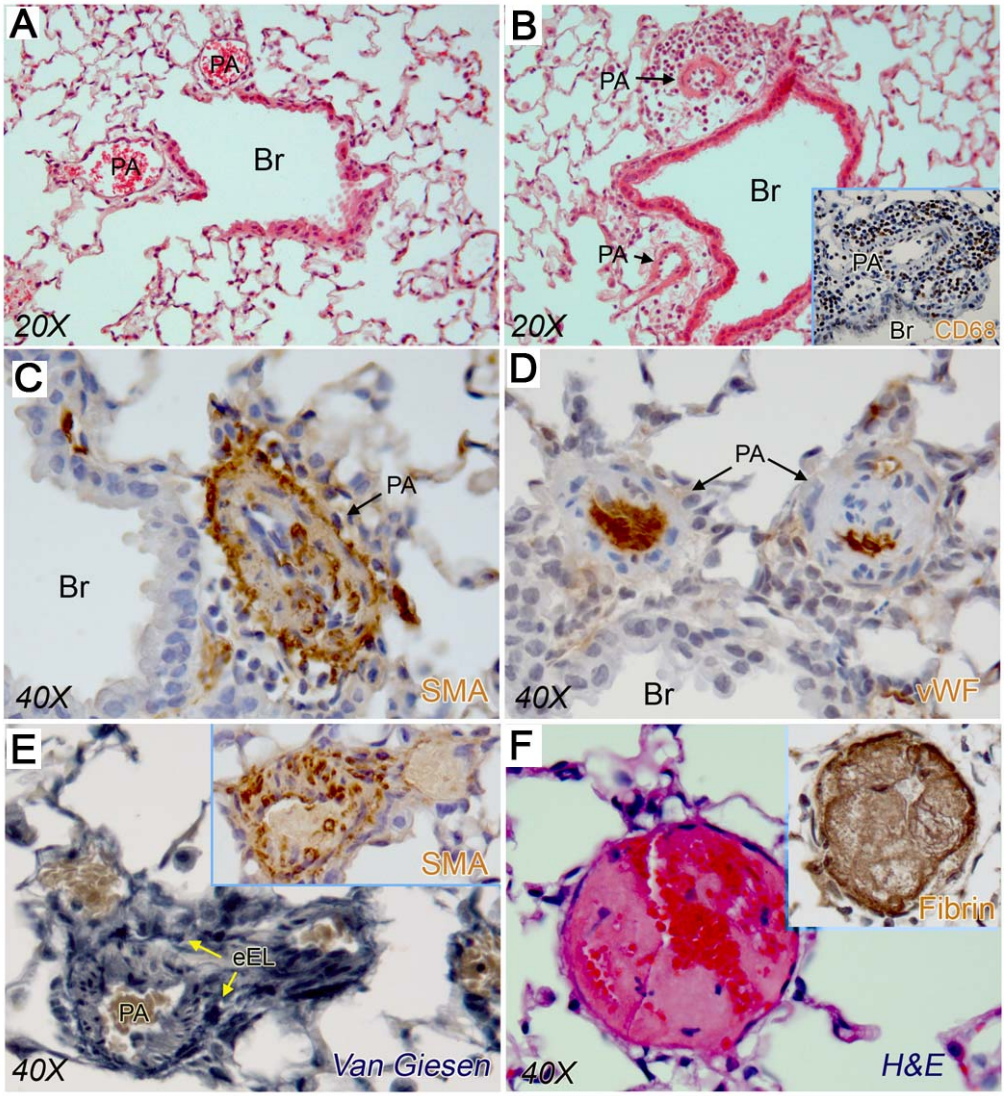

Figure 5-5. Vascular lesions of the PH lungs mimic some pathological features of human PAH. A) and B) H&E staining of control and PH lungs, showing focal leukocyte infiltration around pulmonary arteries of PH lungs of Cre(+);*Bmpr2*$^{f/+}$ or Cre(+);*Bmpr2*$^{f/f}$ mice. Immunohistochemical studies revealed what the infiltrated cells were mostly CD68-positive mononuclear cells (inset in B). Br, Bronchus; PA, pulmonary artery. C) and D) Immunostaining with αSMA and von Willebrand factor (vWF) antibodies showed occlusive arteries with neointima formation in a PH lung. E) Elastic van Geison staining showed neointima formation. Most cells in neointima were αSMA-positive. eEL, external elastic lamina. F, H&E staining showing a representative *in situ* thrombotic lesion in a PH lung. Lumen of the affected vessel was occluded by formation of fibrin(ogen)-positive thrombus (inset).

CHAPTER 6
CONCLUSION AND PERSPECTIVES

In the presented studies, two distinct TGF-β receptors linked to inherited cardiovascular diseases, *i.e* HHT2 and PAH, were studied. Although the biological significance of TGF-β has been implicated in a variety of biological processes for decades, multiple debatable and unknown issues regarding the role of the receptors in the vascular biology are yet to be answered. Throughout the studies, most of the work has been engaged in elucidating the physiologic or pathogenic roles of the receptors in the endothelial biology.

In Chapter 3, we sought to characterize the regulatory mechanism of dynamic pattern of Alk1 expression via *in vivo* analysis of the *Alk1* promoter and intron 2 regions. In Chapter 4, we developed and characterized a novel Tg(*Alk1-cre*)-L1 line displaying a unique pattern of Cre activity in the pulmonary ECs. Finally, in Chapter 5, using the Tg(*Alk1-cre*)-L1 line we sought to test a long-awaited and evidence-based hypothesis in the PAH field by selectively deleting *Bmpr2* in the pulmonary ECs.

The 9.2 kb of *Alk1* Promoter As a Driver of Spatiotemporal Pattern of *Alk1* Expression

The *in silico* approach used to analyze the *Alk1* promoter revealed highly homologous regions between mouse and human ALK1 in the promoter and intron 2 regions. Based on the data, the Alk1 promoter was further dissected in order to determine what the key regulator/enhancer for Alk1 expression. Because, as noted in Chapter 1, Alk1 exhibits a heterogeneity in the tissue-specificity of expression, the well-established *in vivo* transgenesis approach was employed to bypass any disagreement that may have been caused by an *in vitro* culture of the ECs. To our surprise, the 9.2 kb of pXh4.5-in2-SIB construct, containing whole homologous sequences in intron 2, precisely recapitulated the endogenous Alk1 expression, whereas the two other constructs failed to show an Alk1-specific expression pattern. The X-gal

staining in the Tg(*Alk1-lacZ*) (from the pXh4.5-in2-SIB construct) was predominantly limited in the arterial ECs of large vessels and perineural and pulmonary capillaries during development. As expected, Alk1 expression was greatly diminished during the adult stage, but could be induced with wound challenge. However, the inducibility of Alk1 during wound-healing was not as robust as in $Alk1^{+/lacZ}$ mice. The difference between the lines is most likely caused by a lack of an additional regulatory element(s) which would be necessary for precise induciblity of the Alk1 gene in adult. Consistent with the phenotype displaying excessive dilation/fusion in embryonic vessels of $Alk1^{lacZ/lacZ}$, null mutation of Alk1 also caused the malformation of umbilical vessels. The phenotype includes dilation of the vessels at E9.5, followed by fusion of the vessels at E10.5. Of interest, although the Alk1 expression was detected in both umbilical arterial and umbilical venous ECs, the Alk1 expression in the umbilical arterial ECs is still dominant. The data indicates that because partial pressure of oxygen in the umbilical vein is higher than that in the umbilical artery, the level of oxygen does not seem to be a direct mechanism in the regulation of the Alk1 expression. Supporting this view, a recent microarray analysis showed that no significant changes of oxygen-sensitive genes in the blood outgrowth endothelial cells (BOECs) isolated from HHT patients were detected (247).

HHT is a vascular disease caused by a mutation in the TGF-β type receptor (Eng or ALK1) or in a cytoplasmic mediator (SMAD4). Most of the diagnostic screening for this mutation has been carried out with direct sequencing of coding exons. It has been shown that 60% of HHT cases are caused by such exonic mutations, however, the types of mutations in the rest of the cases are still inexplicable (189). The presented results are the first to demonstrate the potential role of intronic sequence in the regulation of Alk1 expression. Thus, the results from the study

may provide genomic sequence information for screening non-exonic mutations of *ALK1* in HHT2 patients.

A future prospect would be follow-up studies on further dissecting and defining the homologous regions in intron 2. To directly determine whether the homologous sequence in intron 2 does function as a true enhancer element governing EC-dominant expression, an *in vivo* transient transgenic approach would be a beneficial tool. According to this method, various transgenic constructs containing a minimal *Alk1* promoter, intron 2 sequence with or without homologous region along with the *lacZ* reporter gene would be designed, introduced into fertilized mouse eggs and embryos would be harvested to visualize the transgenic constructs' expression through X-gal staining. The confirmed promoter and homologous sequence would be a useful resource for a viral vector system. Furthermore, the *in vivo* dissection of the homologous region would provide us sequence information for the identification of trans-acting factors in the regulation of dynamic pattern of Alk1 expression.

A Novel Tg(*Alk1-Cre*)-L1 Line As a Pulmonary EC-Dominant Cre Deleter

Using the 9.2 kb Alk1 fragment, a novel Tg(*Alk1-cre*)-L1 line was developed. In the line, uniform Cre activity was persistently observed in pulmonary ECs from E15.5 on. On the other hand, the ECs of systemic vessels displayed mosaic Cre activity. Consistent with the pattern of Alk1 expression in pulmonary vessels, pulmonary Cre activity in the line was shown in almost all of the pulmonary ECs during embryonic and early postnatal stages. In the Tg(*Alk1-lacZ*) line, however, the X-gal staining was mostly limited to small vessels, such as small arteries and capillaries, during the adult stage. As discussed in Chapter 4, once an allele is recombined by Cre in a cell, progenitor cells from the cell also contain the recombined allele. This is most likely the reason why the homogeneous pattern of X-gal staining in all pulmonary ECs persisted through the late embryonic and in the adult stages of the Tg(*Alk1-cre*)-L1;R26R bigenic mice. More

importantly, unlike any other pan-endothelium-specific Cre lines, the Tg(*Alk1-cre*)-L1 line exhibited minimal Cre activity in the ECs of the coronary vessel and capillaries in the heart and no endocardial Cre activity. As discussed in Chapter 1, based on the trace of X-gal staining pattern in the Tg(*Alk1-cre*);R26R bigenic mice, the turnover rate for pulmonary EC seems to be very slow in adults.

Alk1-Cre(+);Bmpr2$^{f/f}$ Mice As an Unique Model System of PAH

In Chapter 5, the pathogenic role of perturbed endothelial Bmpr2 signaling in the development of PAH was highlighted. Based on the pathohistological evidence of endothelial dysfunction and low disease penetrance in PAH individuals, we hypothesized that the homozygous deletion of *Bmpr2* in the pulmonary ECs increases the genetic susceptibility to PAH. Indeed, endothelial *Bmpr2* deletion could predispose elevation of RVSP, muscularization of small arteries and right ventricular hypertrophy. Although the disease penetrance was still incomplete in our mouse model, homozygous deletion of *Bmpr2* in ECs led to higher frequency of PAH than heterozygous deletion with an age-dependent manner. The data suggests that the factors altering gene dosage of Bmpr2 play a pathogenic role in the development of PAH. Certainly, none of the mutant mice appeared to display congenital heart defects such as septal defects or valvular pulmonary stenosis. This result was possibly achieved due to the lack of endocardial Cre activity in the Tg(*Alk1-cre*)-L1 line. Our initial attempt with collaboration was to conditionally delete *Bmpr2* in ECs by using the Tg(*Tie2-cre*). However, the *Tie2-cre(+);Bmpr2$^{f/f}$* mice displayed postnatal anomalies including heart defect. The result further indicates that unlike any other EC-specific Cre lines, the Tg(*Alk1-cre*)-L1 line is a unique line as a pulmonary EC-dominant Cre deleter without causing heart defect. The *Tie2-cre(+);Bmpr2$^{f/f}$* mice would be a useful resource for studying other types of PH such as persistent PH caused by congenital heart defects. Interestingly, the subset of hypertensive mice exhibited signs of

endothelial dysfunction such as perivascular infiltration and *in situ* thrombosis. Although the subset of PAH individuals also exhibit the signs of endothelial dysfunction, the mechanism underlying such dysfunctions is still open to question. It is tempting to speculate that the Bmpr2 signal plays a protective role in the endothelium from injuries such as inflammation responses and mechanical forces such as flow shear stress.

Perspectives

Although our murine models have helped to explain some critical issues in the etiology of PAH, a number of mechanistic questions are still unanswered. For subsequent examination of inflammatory responses as one of the multiple hits in our model system, a chronic infusion of inflammatory cytokine such as IL-1β, IL-6 or MCP-1 into *Alk1-cre(+);Bmpr2*$^{+/f}$ and *Alk1-cre(+);Bmpr2*$^{f/f}$ mice would be a useful approach to resolving this possibility. Because the mouse model we used in the PAH study harbors mixed genetic backgrounds (*i.e.* 129Sv/J, C57BL/6 and FVB), strain-specific modifier gene(s) might play a role in the development of pathophysiological manifestation in the *Alk1-cre(+);Bmpr2*$^{+/f}$ or *Alk1-cre(+);Bmpr2*$^{f/f}$ mice. Therefore, PCR-based genome-wide scan for the identification of potential quantitative trait loci (QTL) linked to PAH in the hypertensive mice would be useful approach to test this possibility.

As discussed in Chapter 1, PAH is known to exhibit opposite vascular phenotypes of HHT. It has been demonstrated that the subset of HHT individuals with the *ALK1* mutation also displayed clinical manifestations of PAH. Therefore, one of the fundamental questions in the genetics of PAH would be how the *ALK1* mutation genocopies the BMPR2 deficiency. A recent study suggests that in the presence of BMP9, BMPR2 can preferentially interact with ALK1 in ECs and inhibit growth factors stimulated-cell migration and proliferation (99). Moreover, Yu *et al.* demonstrated that loss of the BMPR2 function can be compensated by another TGF-β type II

receptor, ActRIIa, in SMCs (108). Therefore, to further test the mechanistic role of the interactions between the receptors, some genetic compound mice such as *Alk1-cre(+);Bmpr2$^{f/f}$;ActRIIa$^{-/-}$* or *Alk1-cre(+);Bmpr2$^{f/f}$;Alk1$^{+/f}$* would provide a direct answer for the questions. Follow-up studies with the mouse strains would help to explain the incomplete disease penetrance in our mouse model and *BMPR2* mutation carrier as well. Because the *Alk1-cre(+);Alk1$^{f/f}$* mice exhibit postnatal lethality with malformation in the pulmonary vessels, the *Alk1-cre(+);Bmpr2$^{f/f}$;Alk1$^{+/f}$* mice would at least in part provide answers for the interwoven link among the receptors as a disease-causing mechanism. Furthermore, the mouse line would be a useful genetic resource to study a decision-point of the two distinct diseases, *i.e.* HHT and PAH, caused by *ALK1* mutation.

Another intriguing question in the PAH field is whether PAH as a consequence of the *BMPR2* mutation is mediated by a SMAD-dependent signaling mechanism. To investigate the pathogenic significance of SMAD-dependent signaling as a downstream contributor to the development of PAH, the conditional deletion of endothelial Smad1 in compound *Alk1-cre(+);Smad1$^{f/f}$* mice would be worthy. A recent study showed that homozygous inactivation of endothelial Smad5 in *Tie2-cre(+);Smad5$^{-/f}$* mice did not impair blood vessel formation, suggesting SMAD1 to be a main downstream mediator of BMPR2 in ECs (248). Indeed, reduced levels of phosphorylated SMAD1 was observed in the pulmonary vessels in PAH individuals with a heterozygous *BMPR2* mutation (169). Thus, the *Alk1-cre(+);Smad1$^{f/f}$* mice would further provide evidence of the dependence of SMAD1 signaling in the development of PAH.

The isolated pulmonary EC would be a good research resource to investigate the impact of endothelial *BMPR2* mutation *in vitro*. To nullify the *Bmpr2* allele, ROSA26-*creER(+);Bmpr2$^{f/f}$* mice would be generated, the pulmonary ECs can be isolated from the mouse strain, and

tamoxifen would be treated to the isolated ECs. Because the CreER efficiently becomes active by tamoxifen, the system would provide sets of experiments to test the impaired Bmpr2 function in the endothelial biology under various conditions. The isolated ECs would be a useful resource to investigate questions regarding the perturbed trafficking of mutant Bmpr2 to membrane, and desensitization of mutant Bmpr2 to ligands. It has been shown that BMPR2 containing some types of mutation fail to reach the cell membrane (249). The data suggests that the failure in targeting BMPR2 to membrane might be one of the disease-causing mechanisms with or without heterozygous *BMPR2* mutation. The functional significance of membrane trafficking of BMPR2 was recently reviewed (250). Morrell *et al.* showed that SMCs isolated from the pulmonary artery of individuals with IPAH exhibited altered growth responses to the BMP-2, -4, and -7, as compared with SMCs isolated from controls (251). The dynamics of BMPR2 on the plasma membrane seem to be a complex system (252). Currently it is unknown how the mutant BMPR2 desensitizes the ligands; thus, it would be worthy to test the possible involvement of the receptor desensitization in ECs containing mutant Bmpr2.

In conclusion, using genetically modified mice we have demonstrated that the endothelial deletion of *Bmpr2* can predispose PAH. The mouse lines, as powerful research resources, have the potential to be used in the isolation of new therapeutic targets and discovery of target drug(s) for PAH. The presented data also will meet our common endeavor in the improvement of public health.

APPENDIX A

Publications

1. Seki,T., Hong,K.H., Yun,J., Kim,S.J., and Oh,S.P. 2004. Isolation of a regulatory region of activin receptor-like kinase 1 gene sufficient for arterial endothelium-specific expression. *Circ.Res.* 94:e72-e77.

2. Park,S., Lee,Y.J., Lee,H.J., Seki,T., Hong,K.H., Park,J., Beppu,H., Lim,I.K., Yoon,J.W., Li,E. *et al*. 2004. B-cell translocation gene 2 (Btg2) regulates vertebral patterning by modulating bone morphogenetic protein/smad signaling. *Mol.Cell Biol.* 24:10256-10262.

3. Seki,T.*, Hong,K.H.*, and Oh,S.P. 2006. Nonoverlapping expression patterns of ALK1 and ALK5 reveal distinct roles of each receptor in vascular development. *Lab Invest* 86:116-129. (* equally contributed)

4. Lee,Y.J., Hong,K.H., Yun,J., and Oh,S.P. 2006. Generation of activin receptor type IIB isoform-specific hypomorphic alleles. *Genesis.* 44:487-494.

5. Hong,K.H., Seki,T., and Oh,S.P. 2007. Activin receptor-like kinase 1 is essential for placental vascular development in mice. *Lab Invest* 87:670-679.

LIST OF REFERENCES

1. Farber,H.W. and Loscalzo,J. 2004. Pulmonary arterial hypertension. *N.Engl.J.Med.* 351:1655-1665.

2. Nauser,T.D. and Stites,S.W. 2001. Diagnosis and treatment of pulmonary hypertension. *Am.Fam.Physician* 63:1789-1798.

3. Fuster,V., Steele,P.M., Edwards,W.D., Gersh,B.J., McGoon,M.D., and Frye,R.L. 1984. Primary pulmonary hypertension: natural history and the importance of thrombosis. *Circulation* 70:580-587.

4. Schwenke,D.O., Pearson,J.T., Mori,H., and Shirai,M. 2006. Long-term monitoring of pulmonary arterial pressure in conscious, unrestrained mice. *J.Pharmacol.Toxicol.Methods* 53:277-283.

5. Humbert,M., Sitbon,O., and Simonneau,G. 2004. Treatment of Pulmonary Arterial Hypertension. *N Engl J Med* 351:1425-1436.

6. Newman,J.H., Fanburg,B.L., Archer,S.L., Badesch,D.B., Barst,R.J., Garcia,J.G., Kao,P.N., Knowles,J.A., Loyd,J.E., McGoon,M.D. *et al*. 2004. Pulmonary arterial hypertension: future directions: report of a National Heart, Lung and Blood Institute/Office of Rare Diseases workshop. *Circulation* 109:2947-2952.

7. Rich,S., Dantzker,D.R., Ayres,S.M., Bergofsky,E.H., Brundage,B.H., Detre,K.M., Fishman,A.P., Goldring,R.M., Groves,B.M., Koerner,S.K. *et al*. 1987. Primary pulmonary hypertension. A national prospective study. *Ann.Intern.Med.* 107:216-223.

8. McLaughlin,V.V., Presberg,K.W., Doyle,R.L., Abman,S.H., McCrory,D.C., Fortin,T., and Ahearn,G. 2004. Prognosis of pulmonary arterial hypertension: ACCP evidence-based clinical practice guidelines. *Chest* 126:78S-92S.

9. Yi,E.S., Kim,H., Ahn,H., Strother,J., Morris,T., Masliah,E., Hansen,L.A., Park,K., and Friedman,P.J. 2000. Distribution of obstructive intimal lesions and their cellular phenotypes in chronic pulmonary hypertension. A morphometric and immunohistochemical study. *Am.J.Respir.Crit Care Med.* 162:1577-1586.

10. Morrell,N.W., Upton,P.D., Kotecha,S., Huntley,A., Yacoub,M.H., Polak,J.M., and Wharton,J. 1999. Angiotensin II activates MAPK and stimulates growth of human pulmonary artery smooth muscle via AT1 receptors. *Am.J.Physiol* 277:L440-L448.

11. Tuder,R.M., Groves,B., Badesch,D.B., and Voelkel,N.F. 1994. Exuberant endothelial cell growth and elements of inflammation are present in plexiform lesions of pulmonary hypertension. *Am.J.Pathol.* 144:275-285.

12. Lee,S.D., Shroyer,K.R., Markham,N.E., Cool,C.D., Voelkel,N.F., and Tuder,R.M. 1998. Monoclonal endothelial cell proliferation is present in primary but not secondary pulmonary hypertension. *J.Clin.Invest* 101:927-934.

13. Pietra,G.G., Edwards,W.D., Kay,J.M., Rich,S., Kernis,J., Schloo,B., Ayres,S.M., Bergofsky,E.H., Brundage,B.H., Detre,K.M. *et al*. 1989. Histopathology of primary pulmonary hypertension. A qualitative and quantitative study of pulmonary blood vessels from 58 patients in the National Heart, Lung, and Blood Institute, Primary Pulmonary Hypertension Registry. *Circulation* 80:1198-1206.

14. Atkinson,C., Stewart,S., Upton,P.D., Machado,R., Thomson,J.R., Trembath,R.C., and Morrell,N.W. 2002. Primary pulmonary hypertension is associated with reduced pulmonary vascular expression of type II bone morphogenetic protein receptor. *Circulation* 105:1672-1678.

15. Pietra,G.G. 1994. Histopathology of primary pulmonary hypertension. *Chest* 105:2S-6S.

16. Teichert-Kuliszewska,K., Kutryk,M.J., Kuliszewski,M.A., Karoubi,G., Courtman,D.W., Zucco,L., Granton,J., and Stewart,D.J. 2006. Bone morphogenetic protein receptor-2 signaling promotes pulmonary arterial endothelial cell survival: implications for loss-of-function mutations in the pathogenesis of pulmonary hypertension. *Circ.Res.* 98:209-217.

17. Stenmark,K.R. and Mecham,R.P. 1997. Cellular and molecular mechanisms of pulmonary vascular remodeling. *Annu.Rev.Physiol* 59:89-144.

18. Meyrick,B. and Reid,L. 1978. The effect of continued hypoxia on rat pulmonary arterial circulation. An ultrastructural study. *Lab Invest* 38:188-200.

19. Jones,R., Jacobson,M., and Steudel,W. 1999. alpha-smooth-muscle actin and microvascular precursor smooth-muscle cells in pulmonary hypertension. *Am.J.Respir.Cell Mol.Biol.* 20:582-594.

20. Frid,M.G., Brunetti,J.A., Burke,D.L., Carpenter,T.C., Davie,N.J., Reeves,J.T., Roedersheimer,M.T., van Rooijen,N., and Stenmark,K.R. 2006. Hypoxia-induced pulmonary vascular remodeling requires recruitment of circulating mesenchymal precursors of a monocyte/macrophage lineage. *Am.J.Pathol.* 168:659-669.

21. Minamino,T., Christou,H., Hsieh,C.M., Liu,Y., Dhawan,V., Abraham,N.G., Perrella,M.A., Mitsialis,S.A., and Kourembanas,S. 2001. Targeted expression of heme oxygenase-1 prevents the pulmonary inflammatory and vascular responses to hypoxia. *Proc.Natl.Acad.Sci.U.S.A* 98:8798-8803.

22. McLaughlin,V.V. and McGoon,M.D. 2006. Pulmonary arterial hypertension. *Circulation* 114:1417-1431.

23. Weiss,B.M., Zemp,L., Seifert,B., and Hess,O.M. 1998. Outcome of pulmonary vascular disease in pregnancy: a systematic overview from 1978 through 1996. *J.Am.Coll.Cardiol.* 31:1650-1657.

24. Golovina,V.A., Platoshyn,O., Bailey,C.L., Wang,J., Limsuwan,A., Sweeney,M., Rubin,L.J., and Yuan,J.X. 2001. Upregulated TRP and enhanced capacitative Ca(2+)

entry in human pulmonary artery myocytes during proliferation. *Am.J.Physiol Heart Circ.Physiol* 280:H746-H755.

25. Somlyo,A.P. and Somlyo,A.V. 1994. Signal transduction and regulation in smooth muscle. *Nature* 372:231-236.

26. Rich,S., Kaufmann,E., and Levy,P.S. 1992. The effect of high doses of calcium-channel blockers on survival in primary pulmonary hypertension. *N.Engl.J.Med.* 327:76-81.

27. Clapp,L.H., Finney,P., Turcato,S., Tran,S., Rubin,L.J., and Tinker,A. 2002. Differential effects of stable prostacyclin analogs on smooth muscle proliferation and cyclic AMP generation in human pulmonary artery. *Am.J.Respir.Cell Mol.Biol.* 26:194-201.

28. Christman,B.W., McPherson,C.D., Newman,J.H., King,G.A., Bernard,G.R., Groves,B.M., and Loyd,J.E. 1992. An imbalance between the excretion of thromboxane and prostacyclin metabolites in pulmonary hypertension. *N.Engl.J.Med.* 327:70-75.

29. Higenbottam,T., Wheeldon,D., Wells,F., and Wallwork,J. 1984. Long-term treatment of primary pulmonary hypertension with continuous intravenous epoprostenol (prostacyclin). *Lancet* 1:1046-1047.

30. McLaughlin,V.V., Shillington,A., and Rich,S. 2002. Survival in primary pulmonary hypertension: the impact of epoprostenol therapy. *Circulation* 106:1477-1482.

31. Sitbon,O., Humbert,M., Nunes,H., Parent,F., Garcia,G., Herve,P., Rainisio,M., and Simonneau,G. 2002. Long-term intravenous epoprostenol infusion in primary pulmonary hypertension: prognostic factors and survival. *J.Am.Coll.Cardiol.* 40:780-788.

32. Barst,R.J., Rubin,L.J., Long,W.A., McGoon,M.D., Rich,S., Badesch,D.B., Groves,B.M., Tapson,V.F., Bourge,R.C., Brundage,B.H. *et al*. 1996. A comparison of continuous intravenous epoprostenol (prostacyclin) with conventional therapy for primary pulmonary hypertension. The Primary Pulmonary Hypertension Study Group. *N.Engl.J.Med.* 334:296-302.

33. Sitbon,O., Humbert,M., and Simonneau,G. 2002. Primary pulmonary hypertension: Current therapy. *Prog.Cardiovasc.Dis.* 45:115-128.

34. Humbert,M., Sanchez,O., Fartoukh,M., Jagot,J.L., Sitbon,O., and Simonneau,G. 1998. Treatment of severe pulmonary hypertension secondary to connective tissue diseases with continuous IV epoprostenol (prostacyclin). *Chest* 114:80S-82S.

35. Okano,Y., Yoshioka,T., Shimouchi,A., Satoh,T., and Kunieda,T. 1997. Orally active prostacyclin analogue in primary pulmonary hypertension. *Lancet* 349:1365.

36. Hoeper,M.M., Schwarze,M., Ehlerding,S., Adler-Schuermeyer,A., Spiekerkoetter,E., Niedermeyer,J., Hamm,M., and Fabel,H. 2000. Long-term treatment of primary pulmonary hypertension with aerosolized iloprost, a prostacyclin analogue. *N.Engl.J.Med.* 342:1866-1870.

37. Alberts,G.F., Peifley,K.A., Johns,A., Kleha,J.F., and Winkles,J.A. 1994. Constitutive endothelin-1 overexpression promotes smooth muscle cell proliferation via an external autocrine loop. *J.Biol.Chem.* 269:10112-10118.

38. Rich,S. and McLaughlin,V.V. 2003. Endothelin receptor blockers in cardiovascular disease. *Circulation* 108:2184-2190.

39. Hosoda,K., Nakao,K., Hiroshi,A., Suga,S., Ogawa,Y., Mukoyama,M., Shirakami,G., Saito,Y., Nakanishi,S., and Imura,H. 1991. Cloning and expression of human endothelin-1 receptor cDNA. *FEBS Lett.* 287:23-26.

40. Ogawa,Y., Nakao,K., Arai,H., Nakagawa,O., Hosoda,K., Suga,S., Nakanishi,S., and Imura,H. 1991. Molecular cloning of a non-isopeptide-selective human endothelin receptor. *Biochem.Biophys.Res.Commun.* 178:248-255.

41. Giaid,A., Yanagisawa,M., Langleben,D., Michel,R.P., Levy,R., Shennib,H., Kimura,S., Masaki,T., Duguid,W.P., and Stewart,D.J. 1993. Expression of endothelin-1 in the lungs of patients with pulmonary hypertension. *N.Engl.J.Med.* 328:1732-1739.

42. Wagner,O.F., Vierhapper,H., Gasic,S., Nowotny,P., and Waldhausl,W. 1992. Regional effects and clearance of endothelin-1 across pulmonary and splanchnic circulation. *Eur.J.Clin.Invest* 22:277-282.

43. Channick,R.N., Simonneau,G., Sitbon,O., Robbins,I.M., Frost,A., Tapson,V.F., Badesch,D.B., Roux,S., Rainisio,M., Bodin,F. *et al*. 2001. Effects of the dual endothelin-receptor antagonist bosentan in patients with pulmonary hypertension: a randomised placebo-controlled study. *Lancet* 358:1119-1123.

44. Rubin,L.J., Badesch,D.B., Barst,R.J., Galie,N., Black,C.M., Keogh,A., Pulido,T., Frost,A., Roux,S., Leconte,I. *et al*. 2002. Bosentan therapy for pulmonary arterial hypertension. *N.Engl.J.Med.* 346:896-903.

45. Barst,R.J., Rich,S., Widlitz,A., Horn,E.M., McLaughlin,V., and McFarlin,J. 2002. Clinical efficacy of sitaxsentan, an endothelin-A receptor antagonist, in patients with pulmonary arterial hypertension: open-label pilot study. *Chest* 121:1860-1868.

46. Barst,R.J., Langleben,D., Frost,A., Horn,E.M., Oudiz,R., Shapiro,S., McLaughlin,V., Hill,N., Tapson,V.F., Robbins,I.M. *et al*. 2004. Sitaxsentan therapy for pulmonary arterial hypertension. *Am.J.Respir.Crit Care Med.* 169:441-447.

47. Griffiths,M.J. and Evans,T.W. 2005. Inhaled nitric oxide therapy in adults. *N.Engl.J.Med.* 353:2683-2695.

48. Mehta,S. 2003. Sildenafil for pulmonary arterial hypertension: exciting, but protection required. *Chest* 123:989-992.

49. Giaid,A. and Saleh,D. 1995. Reduced expression of endothelial nitric oxide synthase in the lungs of patients with pulmonary hypertension. *N.Engl.J.Med.* 333:214-221.

50. Ghofrani,H.A., Pepke-Zaba,J., Barbera,J.A., Channick,R., Keogh,A.M., Gomez-Sanchez,M.A., Kneussl,M., and Grimminger,F. 2004. Nitric oxide pathway and phosphodiesterase inhibitors in pulmonary arterial hypertension. *J.Am.Coll.Cardiol.* 43:68S-72S.

51. Cohen,A.H., Hanson,K., Morris,K., Fouty,B., McMurty,I.F., Clarke,W., and Rodman,D.M. 1996. Inhibition of cyclic 3'-5'-guanosine monophosphate-specific phosphodiesterase selectively vasodilates the pulmonary circulation in chronically hypoxic rats. *J.Clin.Invest* 97:172-179.

52. Jernigan,N.L. and Resta,T.C. 2002. Chronic hypoxia attenuates cGMP-dependent pulmonary vasodilation. *Am.J.Physiol Lung Cell Mol.Physiol* 282:L1366-L1375.

53. Frostell,C.G., Blomqvist,H., Hedenstierna,G., Lundberg,J., and Zapol,W.M. 1993. Inhaled nitric oxide selectively reverses human hypoxic pulmonary vasoconstriction without causing systemic vasodilation. *Anesthesiology* 78:427-435.

54. Frostell,C., Fratacci,M.D., Wain,J.C., Jones,R., and Zapol,W.M. 1991. Inhaled nitric oxide. A selective pulmonary vasodilator reversing hypoxic pulmonary vasoconstriction. *Circulation* 83:2038-2047.

55. Galie,N., Ghofrani,H.A., Torbicki,A., Barst,R.J., Rubin,L.J., Badesch,D., Fleming,T., Parpia,T., Burgess,G., Branzi,A. *et al*. 2005. Sildenafil citrate therapy for pulmonary arterial hypertension. *N.Engl.J.Med.* 353:2148-2157.

56. Nishimura,T., Vaszar,L.T., Faul,J.L., Zhao,G., Berry,G.J., Shi,L., Qiu,D., Benson,G., Pearl,R.G., and Kao,P.N. 2003. Simvastatin rescues rats from fatal pulmonary hypertension by inducing apoptosis of neointimal smooth muscle cells. *Circulation* 108:1640-1645.

57. Kao,P.N. 2005. Simvastatin treatment of pulmonary hypertension: an observational case series. *Chest* 127:1446-1452.

58. Schermuly,R.T., Dony,E., Ghofrani,H.A., Pullamsetti,S., Savai,R., Roth,M., Sydykov,A., Lai,Y.J., Weissmann,N., Seeger,W. *et al*. 2005. Reversal of experimental pulmonary hypertension by PDGF inhibition. *J.Clin.Invest* 115:2811-2821.

59. Ghofrani,H.A., Seeger,W., and Grimminger,F. 2005. Imatinib for the treatment of pulmonary arterial hypertension. *N.Engl.J.Med.* 353:1412-1413.

60. Lane,K.B., Machado,R.D., Pauciulo,M.W., Thomson,J.R., Phillips,J.A., III, Loyd,J.E., Nichols,W.C., and Trembath,R.C. 2000. Heterozygous germline mutations in BMPR2, encoding a TGF-beta receptor, cause familial primary pulmonary hypertension. The International PPH Consortium. *Nat.Genet.* 26:81-84.

61. Deng,Z., Morse,J.H., Slager,S.L., Cuervo,N., Moore,K.J., Venetos,G., Kalachikov,S., Cayanis,E., Fischer,S.G., Barst,R.J. *et al*. 2000. Familial primary pulmonary hypertension

(gene PPH1) is caused by mutations in the bone morphogenetic protein receptor-II gene. *Am.J.Hum.Genet.* 67:737-744.

62. Thomson,J.R., Machado,R.D., Pauciulo,M.W., Morgan,N.V., Humbert,M., Elliott,G.C., Ward,K., Yacoub,M., Mikhail,G., Rogers,P. *et al*. 2000. Sporadic primary pulmonary hypertension is associated with germline mutations of the gene encoding BMPR-II, a receptor member of the TGF-beta family. *J.Med.Genet.* 37:741-745.

63. Trembath,R.C., Thomson,J.R., Machado,R.D., Morgan,N.V., Atkinson,C., Winship,I., Simonneau,G., Galie,N., Loyd,J.E., Humbert,M. *et al*. 2001. Clinical and molecular genetic features of pulmonary hypertension in patients with hereditary hemorrhagic telangiectasia. *N.Engl.J.Med.* 345:325-334.

64. Olivieri,C., Mira,E., Delu,G., Pagella,F., Zambelli,A., Malvezzi,L., Buscarini,E., and Danesino,C. 2002. Identification of 13 new mutations in the ACVRL1 gene in a group of 52 unselected Italian patients affected by hereditary haemorrhagic telangiectasia. *J.Med.Genet.* 39:E39.

65. Harrison,R.E., Flanagan,J.A., Sankelo,M., Abdalla,S.A., Rowell,J., Machado,R.D., Elliott,C.G., Robbins,I.M., Olschewski,H., McLaughlin,V. *et al*. 2003. Molecular and functional analysis identifies ALK-1 as the predominant cause of pulmonary hypertension related to hereditary haemorrhagic telangiectasia. *J.Med.Genet.* 40:865-871.

66. Abdalla,S.A., Gallione,C.J., Barst,R.J., Horn,E.M., Knowles,J.A., Marchuk,D.A., Letarte,M., and Morse,J.H. 2004. Primary pulmonary hypertension in families with hereditary haemorrhagic telangiectasia. *Eur.Respir.J.* 23:373-377.

67. Chaouat,A., Coulet,F., Favre,C., Simonneau,G., Weitzenblum,E., Soubrier,F., and Humbert,M. 2004. Endoglin germline mutation in a patient with hereditary haemorrhagic telangiectasia and dexfenfluramine associated pulmonary arterial hypertension. *Thorax* 59:446-448.

68. Harrison,R.E., Berger,R., Haworth,S.G., Tulloh,R., Mache,C.J., Morrell,N.W., Aldred,M.A., and Trembath,R.C. 2005. Transforming growth factor-beta receptor mutations and pulmonary arterial hypertension in childhood. *Circulation* 111:435-441.

69. McAllister,K.A., Grogg,K.M., Johnson,D.W., Gallione,C.J., Baldwin,M.A., Jackson,C.E., Helmbold,E.A., Markel,D.S., McKinnon,W.C., Murrell,J. *et al*. 1994. Endoglin, a TGF-beta binding protein of endothelial cells, is the gene for hereditary haemorrhagic telangiectasia type 1. *Nat.Genet.* 8:345-351.

70. McDonald,M.T., Papenberg,K.A., Ghosh,S., Glatfelter,A.A., Biesecker,B.B., Helmbold,E.A., Markel,D.S., Zolotor,A., McKinnon,W.C., Vanderstoep,J.L. *et al*. 1994. A disease locus for hereditary haemorrhagic telangiectasia maps to chromosome 9q33-34. *Nat.Genet.* 6:197-204.

71. Shovlin,C.L., Hughes,J.M., Tuddenham,E.G., Temperley,I., Perembelon,Y.F., Scott,J., Seidman,C.E., and Seidman,J.G. 1994. A gene for hereditary haemorrhagic telangiectasia maps to chromosome 9q3. *Nat.Genet.* 6:205-209.

72. Johnson,D.W., Berg,J.N., Baldwin,M.A., Gallione,C.J., Marondel,I., Yoon,S.J., Stenzel,T.T., Speer,M., Pericak-Vance,M.A., Diamond,A. *et al*. 1996. Mutations in the activin receptor-like kinase 1 gene in hereditary haemorrhagic telangiectasia type 2. *Nat.Genet.* 13:189-195.

73. Kim,I.Y., Lee,D.H., Lee,D.K., Ahn,H.J., Kim,M.M., Kim,S.J., and Morton,R.A. 2004. Loss of expression of bone morphogenetic protein receptor type II in human prostate cancer cells. *Oncogene* 23:7651-7659.

74. Shi,Y. and Massague,J. 2003. Mechanisms of TGF-beta signaling from cell membrane to the nucleus. *Cell* 113:685-700.

75. Massague,J. 2000. How cells read TGF-beta signals. *Nat.Rev.Mol.Cell Biol.* 1:169-178.

76. Derynck,R. and Zhang,Y.E. 2003. Smad-dependent and Smad-independent pathways in TGF-beta family signalling. *Nature* 425:577-584.

77. De Larco,J.E. and Tadaro,G.J. 1978. A human fibrosarcoma cell line producing multiplication stimulating activity (MSA)-related peptides. *Nature* 272:356-358.

78. Roberts,A.B., Lamb,L.C., Newton,D.L., Sporn,M.B., De Larco,J.E., and Todaro,G.J. 1980. Transforming growth factors: isolation of polypeptides from virally and chemically transformed cells by acid/ethanol extraction. *Proc.Natl.Acad.Sci.U.S.A* 77:3494-3498.

79. Roberts,A.B., Anzano,M.A., Lamb,L.C., Smith,J.M., and Sporn,M.B. 1981. New class of transforming growth factors potentiated by epidermal growth factor: isolation from non-neoplastic tissues. *Proc.Natl.Acad.Sci.U.S.A* 78:5339-5343.

80. Oh,S.P., Yeo,C.Y., Lee,Y., Schrewe,H., Whitman,M., and Li,E. 2002. Activin type IIA and IIB receptors mediate Gdf11 signaling in axial vertebral patterning. *Genes Dev.* 16:2749-2754.

81. Seki,T., Hong,K.H., and Oh,S.P. 2006. Nonoverlapping expression patterns of ALK1 and ALK5 reveal distinct roles of each receptor in vascular development. *Lab Invest* 86:116-129.

82. Rosenzweig,B.L., Imamura,T., Okadome,T., Cox,G.N., Yamashita,H., ten Dijke,P., Heldin,C.H., and Miyazono,K. 1995. Cloning and characterization of a human type II receptor for bone morphogenetic proteins. *Proc.Natl.Acad.Sci.U.S.A* 92:7632-7636.

83. Kawabata,M., Chytil,A., and Moses,H.L. 1995. Cloning of a novel type II serine/threonine kinase receptor through interaction with the type I transforming growth factor-beta receptor. *J.Biol.Chem.* 270:5625-5630.

84. Liu,F., Ventura,F., Doody,J., and Massague,J. 1995. Human type II receptor for bone morphogenic proteins (BMPs): extension of the two-kinase receptor model to the BMPs. *Mol.Cell Biol.* 15:3479-3486.

85. Wong,W.K., Morse,J.H., and Knowles,J.A. 2006. Evolutionary conservation and mutational spectrum of BMPR2 gene. *Gene* 368:84-93.

86. Beppu,H., Minowa,O., Miyazono,K., and Kawabata,M. 1997. cDNA cloning and genomic organization of the mouse BMP type II receptor. *Biochem.Biophys.Res.Commun.* 235:499-504.

87. Wong,W.K., Knowles,J.A., and Morse,J.H. 2005. Bone morphogenetic protein receptor type II C-terminus interacts with c-Src: implication for a role in pulmonary arterial hypertension. *Am.J.Respir.Cell Mol.Biol.* 33:438-446.

88. Cogan,J.D., Pauciulo,M.W., Batchman,A.P., Prince,M.A., Robbins,I.M., Hedges,L.K., Stanton,K.C., Wheeler,L.A., Phillips,J.A., III, Loyd,J.E. *et al*. 2006. High frequency of BMPR2 exonic deletions/duplications in familial pulmonary arterial hypertension. *Am.J.Respir.Crit Care Med.* 174:590-598.

89. Aldred,M.A., Vijayakrishnan,J., James,V., Soubrier,F., Gomez-Sanchez,M.A., Martensson,G., Galie,N., Manes,A., Corris,P., Simonneau,G. *et al*. 2006. BMPR2 gene rearrangements account for a significant proportion of mutations in familial and idiopathic pulmonary arterial hypertension. *Hum.Mutat.* 27:212-213.

90. Machado,R.D., Aldred,M.A., James,V., Harrison,R.E., Patel,B., Schwalbe,E.C., Gruenig,E., Janssen,B., Koehler,R., Seeger,W. *et al*. 2006. Mutations of the TGF-beta type II receptor BMPR2 in pulmonary arterial hypertension. *Hum.Mutat.* 27:121-132.

91. Ramos,M., Lame,M.W., Segall,H.J., and Wilson,D.W. 2006. The BMP type II receptor is located in lipid rafts, including caveolae, of pulmonary endothelium in vivo and in vitro. *Vascul.Pharmacol.* 44:50-59.

92. Nohe,A., Keating,E., Knaus,P., and Petersen,N.O. 2004. Signal transduction of bone morphogenetic protein receptors. *Cell Signal.* 16:291-299.

93. Machado,R.D., Pauciulo,M.W., Thomson,J.R., Lane,K.B., Morgan,N.V., Wheeler,L., Phillips,J.A., III, Newman,J., Williams,D., Galie,N. *et al*. 2001. BMPR2 haploinsufficiency as the inherited molecular mechanism for primary pulmonary hypertension. *Am.J.Hum.Genet.* 68:92-102.

94. Loyd,J.E., Primm,R.K., and Newman,J.H. 1984. Familial primary pulmonary hypertension: clinical patterns. *Am.Rev.Respir.Dis.* 129:194-197.

95. Beppu,H., Kawabata,M., Hamamoto,T., Chytil,A., Minowa,O., Noda,T., and Miyazono,K. 2000. BMP type II receptor is required for gastrulation and early development of mouse embryos. *Dev.Biol.* 221:249-258.

96. Delot,E.C., Bahamonde,M.E., Zhao,M., and Lyons,K.M. 2003. BMP signaling is required for septation of the outflow tract of the mammalian heart. *Development* 130:209-220.

97. Katoh,Y. and Katoh,M. 2006. Comparative integromics on BMP/GDF family. *Int.J.Mol.Med.* 17:951-955.

98. Shimasaki,S., Moore,R.K., Otsuka,F., and Erickson,G.F. 2004. The bone morphogenetic protein system in mammalian reproduction. *Endocr.Rev.* 25:72-101.

99. Scharpfenecker,M., van Dinther,M., Liu,Z., van Bezooijen,R.L., Zhao,Q., Pukac,L., Lowik,C.W., and ten Dijke,P. 2007. BMP-9 signals via ALK1 and inhibits bFGF-induced endothelial cell proliferation and VEGF-stimulated angiogenesis. *J.Cell Sci.* 120:964-972.

100. Mazerbourg,S., Klein,C., Roh,J., Kaivo-Oja,N., Mottershead,D.G., Korchynskyi,O., Ritvos,O., and Hsueh,A.J. 2004. Growth differentiation factor-9 signaling is mediated by the type I receptor, activin receptor-like kinase 5. *Mol.Endocrinol.* 18:653-665.

101. David,L., Mallet,C., Mazerbourg,S., Feige,J.J., and Bailly,S. 2006. Identification of BMP9 and BMP10 as functional activators of the orphan activin receptor-like kinase 1 (ALK1) endothelial cells. *Blood*.

102. Nie,X., Luukko,K., and Kettunen,P. 2006. BMP signalling in craniofacial development. *Int.J.Dev.Biol.* 50:511-521.

103. van Wijk,B., Moorman,A.F., and van den Hoff,M.J. 2007. Role of bone morphogenetic proteins in cardiac differentiation. *Cardiovasc.Res.* 74:244-255.

104. Chen,D., Zhao,M., and Mundy,G.R. 2004. Bone morphogenetic proteins. *Growth Factors* 22:233-241.

105. Zhang,S., Fantozzi,I., Tigno,D.D., Yi,E.S., Platoshyn,O., Thistlethwaite,P.A., Kriett,J.M., Yung,G., Rubin,L.J., and Yuan,J.X. 2003. Bone morphogenetic proteins induce apoptosis in human pulmonary vascular smooth muscle cells. *Am.J.Physiol Lung Cell Mol.Physiol* 285:L740-L754.

106. Lagna,G., Nguyen,P.H., Ni,W., and Hata,A. 2006. BMP-dependent activation of caspase-9 and caspase-8 mediates apoptosis in pulmonary artery smooth muscle cells. *Am.J.Physiol Lung Cell Mol.Physiol* 291:L1059-L1067.

107. Frank,D.B., Abtahi,A., Yamaguchi,D.J., Manning,S., Shyr,Y., Pozzi,A., Baldwin,H.S., Johnson,J.E., and de Caestecker,M.P. 2005. Bone morphogenetic protein 4 promotes pulmonary vascular remodeling in hypoxic pulmonary hypertension. *Circ.Res.* 97:496-504.

108. Yu,P.B., Beppu,H., Kawai,N., Li,E., and Bloch,K.D. 2005. Bone morphogenetic protein (BMP) type II receptor deletion reveals BMP ligand-specific gain of signaling in pulmonary artery smooth muscle cells. *J.Biol.Chem.* 280:24443-24450.

109. Eddahibi,S., Guignabert,C., Barlier-Mur,A.M., Dewachter,L., Fadel,E., Dartevelle,P., Humbert,M., Simonneau,G., Hanoun,N., Saurini,F. *et al*. 2006. Cross talk between endothelial and smooth muscle cells in pulmonary hypertension: critical role for serotonin-induced smooth muscle hyperplasia. *Circulation* 113:1857-1864.

110. Fernandez,L., Sanz-Rodriguez,F., Blanco,F.J., Bernabeu,C., and Botella,L.M. 2006. Hereditary hemorrhagic telangiectasia, a vascular dysplasia affecting the TGF-beta signaling pathway. *Clin.Med.Res.* 4:66-78.

111. Abdalla,S.A. and Letarte,M. 2006. Hereditary haemorrhagic telangiectasia: current views on genetics and mechanisms of disease. *J.Med.Genet.* 43:97-110.

112. Guttmacher,A.E., Marchuk,D.A., and White,R.I., Jr. 1995. Hereditary hemorrhagic telangiectasia. *N.Engl.J.Med.* 333:918-924.

113. Oh,S.P., Seki,T., Goss,K.A., Imamura,T., Yi,Y., Donahoe,P.K., Li,L., Miyazono,K., ten Dijke,P., Kim,S. *et al*. 2000. Activin receptor-like kinase 1 modulates transforming growth factor-beta 1 signaling in the regulation of angiogenesis. *Proc.Natl.Acad.Sci.U.S.A* 97:2626-2631.

114. Urness,L.D., Sorensen,L.K., and Li,D.Y. 2000. Arteriovenous malformations in mice lacking activin receptor-like kinase-1. *Nat.Genet.* 26:328-331.

115. Srinivasan,S., Hanes,M.A., Dickens,T., Porteous,M.E., Oh,S.P., Hale,L.P., and Marchuk,D.A. 2003. A mouse model for hereditary hemorrhagic telangiectasia (HHT) type 2. *Hum.Mol.Genet.* 12:473-482.

116. Torsney,E., Charlton,R., Diamond,A.G., Burn,J., Soames,J.V., and Arthur,H.M. 2003. Mouse model for hereditary hemorrhagic telangiectasia has a generalized vascular abnormality. *Circulation* 107:1653-1657.

117. Seki,T., Yun,J., and Oh,S.P. 2003. Arterial endothelium-specific activin receptor-like kinase 1 expression suggests its role in arterialization and vascular remodeling. *Circ.Res.* 93:682-689.

118. Stenmark,K.R., Fagan,K.A., and Frid,M.G. 2006. Hypoxia-induced pulmonary vascular remodeling: cellular and molecular mechanisms. *Circ.Res.* 99:675-691.

119. Penaloza,D. and Arias-Stella,J. 2007. The heart and pulmonary circulation at high altitudes: healthy highlanders and chronic mountain sickness. *Circulation* 115:1132-1146.

120. Mauban,J.R., Remillard,C.V., and Yuan,J.X. 2005. Hypoxic pulmonary vasoconstriction: role of ion channels. *J.Appl.Physiol* 98:415-420.

121. Waypa,G.B. and Schumacker,P.T. 2005. Hypoxic pulmonary vasoconstriction: redox events in oxygen sensing. *J.Appl.Physiol* 98:404-414.

122. Waypa,G.B., Marks,J.D., Mack,M.M., Boriboun,C., Mungai,P.T., and Schumacker,P.T. 2002. Mitochondrial reactive oxygen species trigger calcium increases during hypoxia in pulmonary arterial myocytes. *Circ.Res.* 91:719-726.

123. Mandegar,M., Fung,Y.C., Huang,W., Remillard,C.V., Rubin,L.J., and Yuan,J.X. 2004. Cellular and molecular mechanisms of pulmonary vascular remodeling: role in the development of pulmonary hypertension. *Microvasc.Res.* 68:75-103.

124. Takahashi,H., Goto,N., Kojima,Y., Tsuda,Y., Morio,Y., Muramatsu,M., and Fukuchi,Y. 2006. Downregulation of type II bone morphogenetic protein receptor in hypoxic pulmonary hypertension. *Am.J.Physiol Lung Cell Mol.Physiol* 290:L450-L458.

125. Young,K.A., Ivester,C., West,J., Carr,M., and Rodman,D.M. 2006. BMP signaling controls PASMC KV channel expression in vitro and in vivo. *Am.J.Physiol Lung Cell Mol.Physiol* 290:L841-L848.

126. Rondelet,B., Kerbaul,F., Motte,S., Van Beneden,R., Remmelink,M., Brimioulle,S., McEntee,K., Wauthy,P., Salmon,I., Ketelslegers,J.M. *et al*. 2003. Bosentan for the prevention of overcirculation-induced experimental pulmonary arterial hypertension. *Circulation* 107:1329-1335.

127. Rondelet,B., Kerbaul,F., Van Beneden,R., Motte,S., Fesler,P., Hubloue,I., Remmelink,M., Brimioulle,S., Salmon,I., Ketelslegers,J.M. *et al*. 2004. Signaling molecules in overcirculation-induced pulmonary hypertension in piglets: effects of sildenafil therapy. *Circulation* 110:2220-2225.

128. Copple,B.L., Ganey,P.E., and Roth,R.A. 2003. Liver inflammation during monocrotaline hepatotoxicity. *Toxicology* 190:155-169.

129. Mukhopadhyay,S. and Sehgal,P.B. 2006. Discordant regulatory changes in monocrotaline-induced megalocytosis of lung arterial endothelial and alveolar epithelial cells. *Am.J.Physiol Lung Cell Mol.Physiol* 290:L1216-L1226.

130. Mathew,R., Huang,J., Shah,M., Patel,K., Gewitz,M., and Sehgal,P.B. 2004. Disruption of endothelial-cell caveolin-1alpha/raft scaffolding during development of monocrotaline-induced pulmonary hypertension. *Circulation* 110:1499-1506.

131. Wilson,D.W., Lame,M.W., Dunston,S.K., Taylor,D.W., and Segall,H.J. 1998. Monocrotaline pyrrole interacts with actin and increases thrombin-mediated permeability in pulmonary artery endothelial cells. *Toxicol.Appl.Pharmacol.* 152:138-144.

132. Morty,R.E., Nejman,B., Kwapiszewska,G., Hecker,M., Zakrzewicz,A., Kouri,F.M., Peters,D.M., Dumitrascu,R., Seeger,W., Knaus,P. *et al*. 2007. Dysregulated bone morphogenetic protein signaling in monocrotaline-induced pulmonary arterial hypertension. *Arterioscler.Thromb.Vasc.Biol.* 27:1072-1078.

133. Beppu,H., Ichinose,F., Kawai,N., Jones,R.C., Yu,P.B., Zapol,W.M., Miyazono,K., Li,E., and Bloch,K.D. 2004. BMPR-II heterozygous mice have mild pulmonary hypertension and an impaired pulmonary vascular remodeling response to prolonged hypoxia. *Am.J Physiol Lung Cell Mol.Physiol*.

134. Song,Y., Jones,J.E., Beppu,H., Keaney,J.F., Jr., Loscalzo,J., and Zhang,Y.Y. 2005. Increased susceptibility to pulmonary hypertension in heterozygous BMPR2-mutant mice. *Circulation* 112:553-562.

135. Long,L., MacLean,M.R., Jeffery,T.K., Morecroft,I., Yang,X., Rudarakanchana,N., Southwood,M., James,V., Trembath,R.C., and Morrell,N.W. 2006. Serotonin increases susceptibility to pulmonary hypertension in BMPR2-deficient mice. *Circ.Res.* 98:818-827.

136. West,J., Fagan,K., Steudel,W., Fouty,B., Lane,K., Harral,J., Hoedt-Miller,M., Tada,Y., Ozimek,J., Tuder,R. *et al*. 2004. Pulmonary hypertension in transgenic mice expressing a dominant-negative BMPRII gene in smooth muscle. *Circ.Res.* 94:1109-1114.

137. Martin,K.B., Klinger,J.R., and Rounds,S.I. 2006. Pulmonary arterial hypertension: new insights and new hope. *Respirology.* 11:6-17.

138. De Caestecker,M. 2006. Serotonin signaling in pulmonary hypertension. *Circ.Res.* 98:1229-1231.

139. Fanburg,B.L. and Lee,S.L. 1997. A new role for an old molecule: serotonin as a mitogen. *Am.J.Physiol* 272:L795-L806.

140. Weir,E.K., Hong,Z., and Varghese,A. 2004. The serotonin transporter: a vehicle to elucidate pulmonary hypertension? *Circ.Res.* 94:1152-1154.

141. Ni,W. and Watts,S.W. 2006. 5-hydroxytryptamine in the cardiovascular system: focus on the serotonin transporter (SERT). *Clin.Exp.Pharmacol.Physiol* 33:575-583.

142. Lesch,K.P., Bengel,D., Heils,A., Sabol,S.Z., Greenberg,B.D., Petri,S., Benjamin,J., Muller,C.R., Hamer,D.H., and Murphy,D.L. 1996. Association of anxiety-related traits with a polymorphism in the serotonin transporter gene regulatory region. *Science* 274:1527-1531.

143. Eddahibi,S., Hanoun,N., Lanfumey,L., Lesch,K.P., Raffestin,B., Hamon,M., and Adnot,S. 2000. Attenuated hypoxic pulmonary hypertension in mice lacking the 5-hydroxytryptamine transporter gene. *J.Clin.Invest* 105:1555-1562.

144. Eddahibi,S., Humbert,M., Fadel,E., Raffestin,B., Darmon,M., Capron,F., Simonneau,G., Dartevelle,P., Hamon,M., and Adnot,S. 2001. Serotonin transporter overexpression is responsible for pulmonary artery smooth muscle hyperplasia in primary pulmonary hypertension. *J.Clin.Invest* 108:1141-1150.

145. Willers,E.D., Newman,J.H., Loyd,J.E., Robbins,I.M., Wheeler,L.A., Prince,M.A., Stanton,K.C., Cogan,J.A., Runo,J.R., Byrne,D. *et al*. 2006. Serotonin transporter polymorphisms in familial and idiopathic pulmonary arterial hypertension. *Am.J.Respir.Crit Care Med.* 173:798-802.

146. Machado,R.D., Koehler,R., Glissmeyer,E., Veal,C., Suntharalingam,J., Kim,M., Carlquist,J., Town,M., Elliott,C.G., Hoeper,M. *et al*. 2006. Genetic association of the serotonin transporter in pulmonary arterial hypertension. *Am.J.Respir.Crit Care Med.* 173:793-797.

147. Marcos,E., Fadel,E., Sanchez,O., Humbert,M., Dartevelle,P., Simonneau,G., Hamon,M., Adnot,S., and Eddahibi,S. 2004. Serotonin-induced smooth muscle hyperplasia in various forms of human pulmonary hypertension. *Circ.Res.* 94:1263-1270.

148. Guignabert,C., Raffestin,B., Benferhat,R., Raoul,W., Zadigue,P., Rideau,D., Hamon,M., Adnot,S., and Eddahibi,S. 2005. Serotonin transporter inhibition prevents and reverses monocrotaline-induced pulmonary hypertension in rats. *Circulation* 111:2812-2819.

149. MacLean,M.R., Deuchar,G.A., Hicks,M.N., Morecroft,I., Shen,S., Sheward,J., Colston,J., Loughlin,L., Nilsen,M., Dempsie,Y. *et al*. 2004. Overexpression of the 5-hydroxytryptamine transporter gene: effect on pulmonary hemodynamics and hypoxia-induced pulmonary hypertension. *Circulation* 109:2150-2155.

150. Guignabert,C., Izikki,M., Tu,L.I., Li,Z., Zadigue,P., Barlier-Mur,A.M., Hanoun,N., Rodman,D., Hamon,M., Adnot,S. *et al*. 2006. Transgenic mice overexpressing the 5-hydroxytryptamine transporter gene in smooth muscle develop pulmonary hypertension. *Circ.Res.* 98:1323-1330.

151. Steudel,W., Ichinose,F., Huang,P.L., Hurford,W.E., Jones,R.C., Bevan,J.A., Fishman,M.C., and Zapol,W.M. 1997. Pulmonary vasoconstriction and hypertension in mice with targeted disruption of the endothelial nitric oxide synthase (NOS 3) gene. *Circ.Res.* 81:34-41.

152. Miller,A.A., Hislop,A.A., Vallance,P.J., and Haworth,S.G. 2005. Deletion of the eNOS gene has a greater impact on the pulmonary circulation of male than female mice. *Am.J.Physiol Lung Cell Mol.Physiol* 289:L299-L306.

153. Fagan,K.A., Morrissey,B., Fouty,B.W., Sato,K., Harral,J.W., Morris,K.G., Jr., Hoedt-Miller,M., Vidmar,S., McMurtry,I.F., and Rodman,D.M. 2001. Upregulation of nitric oxide synthase in mice with severe hypoxia-induced pulmonary hypertension. *Respir.Res.* 2:306-313.

154. Le Cras,T.D. and McMurtry,I.F. 2001. Nitric oxide production in the hypoxic lung. *Am.J.Physiol Lung Cell Mol.Physiol* 280:L575-L582.

155. Khoo,J.P., Zhao,L., Alp,N.J., Bendall,J.K., Nicoli,T., Rockett,K., Wilkins,M.R., and Channon,K.M. 2005. Pivotal role for endothelial tetrahydrobiopterin in pulmonary hypertension. *Circulation* 111:2126-2133.

156. Nandi,M., Miller,A., Stidwill,R., Jacques,T.S., Lam,A.A., Haworth,S., Heales,S., and Vallance,P. 2005. Pulmonary hypertension in a GTP-cyclohydrolase 1-deficient mouse. *Circulation* 111:2086-2090.

157. Yang,S., Lee,Y.J., Kim,J.M., Park,S., Peris,J., Laipis,P., Park,Y.S., Chung,J.H., and Oh,S.P. 2006. A murine model for human sepiapterin-reductase deficiency. *Am.J.Hum.Genet.* 78:575-587.

158. Klinger,J.R., Warburton,R.R., Pietras,L.A., Smithies,O., Swift,R., and Hill,N.S. 1999. Genetic disruption of atrial natriuretic peptide causes pulmonary hypertension in normoxic and hypoxic mice. *Am.J.Physiol* 276:L868-L874.

159. Leitman,D.C., Andresen,J.W., Catalano,R.M., Waldman,S.A., Tuan,J.J., and Murad,F. 1988. Atrial natriuretic peptide binding, cross-linking, and stimulation of cyclic GMP accumulation and particulate guanylate cyclase activity in cultured cells. *J.Biol.Chem.* 263:3720-3728.

160. Onoue,S., Ohmori,Y., Endo,K., Yamada,S., Kimura,R., and Yajima,T. 2004. Vasoactive intestinal peptide and pituitary adenylate cyclase-activating polypeptide attenuate the cigarette smoke extract-induced apoptotic death of rat alveolar L2 cells. *Eur.J.Biochem.* 271:1757-1767.

161. Said,S.I. and Dickman,K.G. 2000. Pathways of inflammation and cell death in the lung: modulation by vasoactive intestinal peptide. *Regul.Pept.* 93:21-29.

162. Said,S.I., Hamidi,S.A., Dickman,K.G., Szema,A.M., Lyubsky,S., Lin,R.Z., Jiang,Y.P., Chen,J.J., Waschek,J.A., and Kort,S. 2007. Moderate pulmonary arterial hypertension in male mice lacking the vasoactive intestinal peptide gene. *Circulation* 115:1260-1268.

163. Ambartsumian,N., Klingelhofer,J., Grigorian,M., Christensen,C., Kriajevska,M., Tulchinsky,E., Georgiev,G., Berezin,V., Bock,E., Rygaard,J. *et al*. 2001. The metastasis-associated Mts1(S100A4) protein could act as an angiogenic factor. *Oncogene* 20:4685-4695.

164. Kriajevska,M., Tarabykina,S., Bronstein,I., Maitland,N., Lomonosov,M., Hansen,K., Georgiev,G., and Lukanidin,E. 1998. Metastasis-associated Mts1 (S100A4) protein modulates protein kinase C phosphorylation of the heavy chain of nonmuscle myosin. *J.Biol.Chem.* 273:9852-9856.

165. Greenway,S., van Suylen,R.J., Du Marchie,S.G., Kwan,E., Ambartsumian,N., Lukanidin,E., and Rabinovitch,M. 2004. S100A4/Mts1 produces murine pulmonary artery changes resembling plexogenic arteriopathy and is increased in human plexogenic arteriopathy. *Am.J.Pathol.* 164:253-262.

166. Dorfmuller,P., Zarka,V., Durand-Gasselin,I., Monti,G., Balabanian,K., Garcia,G., Capron,F., Coulomb-Lhermine,A., Marfaing-Koka,A., Simonneau,G. *et al*. 2002. Chemokine RANTES in severe pulmonary arterial hypertension. *Am.J.Respir.Crit Care Med.* 165:534-539.

167. Damas,J.K., Otterdal,K., Yndestad,A., Aass,H., Solum,N.O., Froland,S.S., Simonsen,S., Aukrust,P., and Andreassen,A.K. 2004. Soluble CD40 ligand in pulmonary arterial hypertension: possible pathogenic role of the interaction between platelets and endothelial cells. *Circulation* 110:999-1005.

168. Caslin,A.W., Heath,D., Madden,B., Yacoub,M., Gosney,J.R., and Smith,P. 1990. The histopathology of 36 cases of plexogenic pulmonary arteriopathy. *Histopathology* 16:9-19.

169. Yang,X., Long,L., Southwood,M., Rudarakanchana,N., Upton,P.D., Jeffery,T.K., Atkinson,C., Chen,H., Trembath,R.C., and Morrell,N.W. 2005. Dysfunctional Smad signaling contributes to abnormal smooth muscle cell proliferation in familial pulmonary arterial hypertension. *Circ.Res.* 96:1053-1063.

170. Massague,J. 2003. Integration of Smad and MAPK pathways: a link and a linker revisited. *Genes Dev.* 17:2993-2997.

171. Tuder,R.M., Radisavljevic,Z., Shroyer,K.R., Polak,J.M., and Voelkel,N.F. 1998. Monoclonal endothelial cells in appetite suppressant-associated pulmonary hypertension. *Am.J.Respir.Crit Care Med.* 158:1999-2001.

172. Machado,R.D., James,V., Southwood,M., Harrison,R.E., Atkinson,C., Stewart,S., Morrell,N.W., Trembath,R.C., and Aldred,M.A. 2005. Investigation of second genetic hits at the BMPR2 locus as a modulator of disease progression in familial pulmonary arterial hypertension. *Circulation* 111:607-613.

173. Cowan,K.N., Heilbut,A., Humpl,T., Lam,C., Ito,S., and Rabinovitch,M. 2000. Complete reversal of fatal pulmonary hypertension in rats by a serine elastase inhibitor. *Nat.Med.* 6:698-702.

174. McMurtry,M.S., Archer,S.L., Altieri,D.C., Bonnet,S., Haromy,A., Harry,G., Bonnet,S., Puttagunta,L., and Michelakis,E.D. 2005. Gene therapy targeting survivin selectively induces pulmonary vascular apoptosis and reverses pulmonary arterial hypertension. *J.Clin.Invest* 115:1479-1491.

175. Hayashida,K., Fujita,J., Miyake,Y., Kawada,H., Ando,K., Ogawa,S., and Fukuda,K. 2005. Bone marrow-derived cells contribute to pulmonary vascular remodeling in hypoxia-induced pulmonary hypertension. *Chest* 127:1793-1798.

176. Zhao,Y.D., Courtman,D.W., Deng,Y., Kugathasan,L., Zhang,Q., and Stewart,D.J. 2005. Rescue of monocrotaline-induced pulmonary arterial hypertension using bone marrow-derived endothelial-like progenitor cells: efficacy of combined cell and eNOS gene therapy in established disease. *Circ.Res.* 96:442-450.

177. Sahara,M., Sata,M., Morita,T., Nakamura,K., Hirata,Y., and Nagai,R. 2007. Diverse contribution of bone marrow-derived cells to vascular remodeling associated with pulmonary arterial hypertension and arterial neointimal formation. *Circulation* 115:509-517.

178. Raoul,W., Wagner-Ballon,O., Saber,G., Hulin,A., Marcos,E., Giraudier,S., Vainchenker,W., Adnot,S., Eddahibi,S., and Maitre,B. 2007. Effects of bone marrow-derived cells on monocrotaline- and hypoxia-induced pulmonary hypertension in mice. *Respir.Res.* 8:8.

179. Shalaby,F., Rossant,J., Yamaguchi,T.P., Gertsenstein,M., Wu,X.F., Breitman,M.L., and Schuh,A.C. 1995. Failure of blood-island formation and vasculogenesis in Flk-1-deficient mice. *Nature* 376:62-66.

180. Beppu,H., Lei,H., Bloch,K.D., and Li,E. 2005. Generation of a floxed allele of the mouse BMP type II receptor gene. *Genesis.* 41:133-137.

181. Lawson,N.D. and Weinstein,B.M. 2002. Arteries and veins: making a difference with zebrafish. *Nat.Rev.Genet.* 3:674-682.

182. Wang,H.U., Chen,Z.F., and Anderson,D.J. 1998. Molecular distinction and angiogenic interaction between embryonic arteries and veins revealed by ephrin-B2 and its receptor Eph-B4. *Cell* 93:741-753.

183. Zhong,T.P., Childs,S., Leu,J.P., and Fishman,M.C. 2001. Gridlock signalling pathway fashions the first embryonic artery. *Nature* 414:216-220.

184. Gerety,S.S., Wang,H.U., Chen,Z.F., and Anderson,D.J. 1999. Symmetrical mutant phenotypes of the receptor EphB4 and its specific transmembrane ligand ephrin-B2 in cardiovascular development. *Mol.Cell* 4:403-414.

185. Krebs,L.T., Xue,Y., Norton,C.R., Shutter,J.R., Maguire,M., Sundberg,J.P., Gallahan,D., Closson,V., Kitajewski,J., Callahan,R. *et al*. 2000. Notch signaling is essential for vascular morphogenesis in mice. *Genes Dev.* 14:1343-1352.

186. Goumans,M.J., Valdimarsdottir,G., Itoh,S., Rosendahl,A., Sideras,P., and ten Dijke,P. 2002. Balancing the activation state of the endothelium via two distinct TGF-beta type I receptors. *EMBO J.* 21:1743-1753.

187. Abdalla,S.A., Pece-Barbara,N., Vera,S., Tapia,E., Paez,E., Bernabeu,C., and Letarte,M. 2000. Analysis of ALK-1 and endoglin in newborns from families with hereditary hemorrhagic telangiectasia type 2. *Hum.Mol.Genet.* 9:1227-1237.

188. van den,D.S., Mummery,C.L., and Westermann,C.J. 2003. Hereditary hemorrhagic telangiectasia: an update on transforming growth factor beta signaling in vasculogenesis and angiogenesis. *Cardiovasc.Res.* 58:20-31.

189. Lesca,G., Plauchu,H., Coulet,F., Lefebvre,S., Plessis,G., Odent,S., Riviere,S., Leheup,B., Goizet,C., Carette,M.F. *et al*. 2004. Molecular screening of ALK1/ACVRL1 and ENG genes in hereditary hemorrhagic telangiectasia in France. *Hum.Mutat.* 23:289-299.

190. Berg,J., Porteous,M., Reinhardt,D., Gallione,C., Holloway,S., Umasunthar,T., Lux,A., McKinnon,W., Marchuk,D., and Guttmacher,A. 2003. Hereditary haemorrhagic

telangiectasia: a questionnaire based study to delineate the different phenotypes caused by endoglin and ALK1 mutations. *J.Med.Genet.* 40:585-590.

191. Marchuk,D.A., Srinivasan,S., Squire,T.L., and Zawistowski,J.S. 2003. Vascular morphogenesis: tales of two syndromes. *Hum.Mol.Genet.* 12 Spec No 1:R97-112.

192. Roman,B.L., Pham,V.N., Lawson,N.D., Kulik,M., Childs,S., Lekven,A.C., Garrity,D.M., Moon,R.T., Fishman,M.C., Lechleider,R.J. *et al*. 2002. Disruption of acvrl1 increases endothelial cell number in zebrafish cranial vessels. *Development* 129:3009-3019.

193. Rossant,J. and Cross,J.C. 2001. Placental development: lessons from mouse mutants. *Nat.Rev.Genet.* 2:538-548.

194. Adamson,S.L., Lu,Y., Whiteley,K.J., Holmyard,D., Hemberger,M., Pfarrer,C., and Cross,J.C. 2002. Interactions between trophoblast cells and the maternal and fetal circulation in the mouse placenta. *Dev.Biol.* 250:358-373.

195. Downs,K.M. 2002. Early placental ontogeny in the mouse. *Placenta* 23:116-131.

196. Shin,D., Garcia-Cardena,G., Hayashi,S., Gerety,S., Asahara,T., Stavrakis,G., Isner,J., Folkman,J., Gimbrone,M.A., Jr., and Anderson,D.J. 2001. Expression of ephrinB2 identifies a stable genetic difference between arterial and venous vascular smooth muscle as well as endothelial cells, and marks subsets of microvessels at sites of adult neovascularization. *Dev.Biol.* 230:139-150.

197. Gale,N.W., Baluk,P., Pan,L., Kwan,M., Holash,J., DeChiara,T.M., McDonald,D.M., and Yancopoulos,G.D. 2001. Ephrin-B2 selectively marks arterial vessels and neovascularization sites in the adult, with expression in both endothelial and smooth-muscle cells. *Dev.Biol.* 230:151-160.

198. Shutter,J.R., Scully,S., Fan,W., Richards,W.G., Kitajewski,J., Deblandre,G.A., Kintner,C.R., and Stark,K.L. 2000. Dll4, a novel Notch ligand expressed in arterial endothelium. *Genes Dev.* 14:1313-1318.

199. Villa,N., Walker,L., Lindsell,C.E., Gasson,J., Iruela-Arispe,M.L., and Weinmaster,G. 2001. Vascular expression of Notch pathway receptors and ligands is restricted to arterial vessels. *Mech.Dev.* 108:161-164.

200. Kokubo,H., Miyagawa-Tomita,S., and Johnson,R.L. 2005. Hesr, a mediator of the Notch signaling, functions in heart and vessel development. *Trends Cardiovasc.Med.* 15:190-194.

201. Levine,R.J., Lam,C., Qian,C., Yu,K.F., Maynard,S.E., Sachs,B.P., Sibai,B.M., Epstein,F.H., Romero,R., Thadhani,R. *et al*. 2006. Soluble endoglin and other circulating antiangiogenic factors in preeclampsia. *N.Engl.J.Med.* 355:992-1005.

202. Venkatesha,S., Toporsian,M., Lam,C., Hanai,J., Mammoto,T., Kim,Y.M., Bdolah,Y., Lim,K.H., Yuan,H.T., Libermann,T.A. *et al*. 2006. Soluble endoglin contributes to the pathogenesis of preeclampsia. *Nat.Med.* 12:642-649.

203. Noris,M., Perico,N., and Remuzzi,G. 2005. Mechanisms of disease: Pre-eclampsia. *Nat.Clin.Pract.Nephrol.* 1:98-114.

204. Redman,C.W. and Sargent,I.L. 2005. Latest advances in understanding preeclampsia. *Science* 308:1592-1594.

205. Hirashima,M., Lu,Y., Byers,L., and Rossant,J. 2003. Trophoblast expression of fms-like tyrosine kinase 1 is not required for the establishment of the maternal-fetal interface in the mouse placenta. *Proc.Natl.Acad.Sci.U.S.A* 100:15637-15642.

206. St Jacques,S., Forte,M., Lye,S.J., and Letarte,M. 1994. Localization of endoglin, a transforming growth factor-beta binding protein, and of CD44 and integrins in placenta during the first trimester of pregnancy. *Biol.Reprod.* 51:405-413.

207. Lebrin,F., Goumans,M.J., Jonker,L., Carvalho,R.L., Valdimarsdottir,G., Thorikay,M., Mummery,C., Arthur,H.M., and Dijke,P.T. 2004. Endoglin promotes endothelial cell proliferation and TGF-beta/ALK1 signal transduction. *EMBO J* 23:4018-4028.

208. Sauer,B. and Henderson,N. 1988. Site-specific DNA recombination in mammalian cells by the Cre recombinase of bacteriophage P1. *Proc.Natl.Acad.Sci.U.S.A* 85:5166-5170.

209. Moore,M.A. and Owen,J.J. 1965. Chromosome marker studies on the development of the haemopoietic system in the chick embryo. *Nature* 208:956.

210. Garcia-Porrero,J.A., Godin,I.E., and Dieterlen-Lievre,F. 1995. Potential intraembryonic hemogenic sites at pre-liver stages in the mouse. *Anat.Embryol.(Berl)* 192:425-435.

211. Alvarez-Silva,M., Belo-Diabangouaya,P., Salaun,J., and Dieterlen-Lievre,F. 2003. Mouse placenta is a major hematopoietic organ. *Development* 130:5437-5444.

212. Ema,M. and Rossant,J. 2003. Cell fate decisions in early blood vessel formation. *Trends Cardiovasc.Med.* 13:254-259.

213. Shalaby,F., Ho,J., Stanford,W.L., Fischer,K.D., Schuh,A.C., Schwartz,L., Bernstein,A., and Rossant,J. 1997. A requirement for Flk1 in primitive and definitive hematopoiesis and vasculogenesis. *Cell* 89:981-990.

214. Kattman,S.J., Huber,T.L., and Keller,G.M. 2006. Multipotent flk-1+ cardiovascular progenitor cells give rise to the cardiomyocyte, endothelial, and vascular smooth muscle lineages. *Dev.Cell* 11:723-732.

215. Cai,C.L., Liang,X., Shi,Y., Chu,P.H., Pfaff,S.L., Chen,J., and Evans,S. 2003. Isl1 identifies a cardiac progenitor population that proliferates prior to differentiation and contributes a majority of cells to the heart. *Dev.Cell* 5:877-889.

216. Moretti,A., Caron,L., Nakano,A., Lam,J.T., Bernshausen,A., Chen,Y., Qyang,Y., Bu,L., Sasaki,M., Martin-Puig,S. *et al*. 2006. Multipotent embryonic isl1+ progenitor cells lead to cardiac, smooth muscle, and endothelial cell diversification. *Cell* 127:1151-1165.

217. Kisanuki,Y.Y., Hammer,R.E., Miyazaki,J., Williams,S.C., Richardson,J.A., and Yanagisawa,M. 2001. Tie2-Cre transgenic mice: a new model for endothelial cell-lineage analysis in vivo. *Dev.Biol.* 230:230-242.

218. de Lange,F.J., Moorman,A.F., Anderson,R.H., Manner,J., Soufan,A.T., Gier-de Vries,C., Schneider,M.D., Webb,S., van den Hoff,M.J., and Christoffels,V.M. 2004. Lineage and morphogenetic analysis of the cardiac valves. *Circ.Res.* 95:645-654.

219. Armstrong,E.J. and Bischoff,J. 2004. Heart valve development: endothelial cell signaling and differentiation. *Circ.Res.* 95:459-470.

220. Garry,D.J. and Olson,E.N. 2006. A common progenitor at the heart of development. *Cell* 127:1101-1104.

221. Park,C., Lavine,K., Mishina,Y., Deng,C.X., Ornitz,D.M., and Choi,K. 2006. Bone morphogenetic protein receptor 1A signaling is dispensable for hematopoietic development but essential for vessel and atrioventricular endocardial cushion formation. *Development* 133:3473-3484.

222. Nanba,D., Kinugasa,Y., Morimoto,C., Koizumi,M., Yamamura,H., Takahashi,K., Takakura,N., Mekada,E., Hashimoto,K., and Higashiyama,S. 2006. Loss of HB-EGF in smooth muscle or endothelial cell lineages causes heart malformation. *Biochem.Biophys.Res.Commun.* 350:315-321.

223. Lincoln,J., Kist,R., Scherer,G., and Yutzey,K.E. 2007. Sox9 is required for precursor cell expansion and extracellular matrix organization during mouse heart valve development. *Dev.Biol.* 305:120-132.

224. Licht,A.H., Raab,S., Hofmann,U., and Breier,G. 2004. Endothelium-specific Cre recombinase activity in flk-1-Cre transgenic mice. *Dev.Dyn.* 229:312-318.

225. Motoike,T., Markham,D.W., Rossant,J., and Sato,T.N. 2003. Evidence for novel fate of Flk1+ progenitor: contribution to muscle lineage. *Genesis.* 35:153-159.

226. Gustafsson,E., Brakebusch,C., Hietanen,K., and Fassler,R. 2001. Tie-1-directed expression of Cre recombinase in endothelial cells of embryoid bodies and transgenic mice. *J.Cell Sci.* 114:671-676.

227. Song,L., Fassler,R., Mishina,Y., Jiao,K., and Baldwin,H.S. 2007. Essential functions of Alk3 during AV cushion morphogenesis in mouse embryonic hearts. *Dev.Biol.* 301:276-286.

228. Have-Opbroek,A.A. 1991. Lung development in the mouse embryo. *Exp.Lung Res.* 17:111-130.

229. Cardoso,W.V. 2000. Lung morphogenesis revisited: old facts, current ideas. *Dev.Dyn.* 219:121-130.

230. Schachtner,S.K., Wang,Y., and Scott,B.H. 2000. Qualitative and quantitative analysis of embryonic pulmonary vessel formation. *Am.J.Respir.Cell Mol.Biol.* 22:157-165.

231. Parera,M.C., van Dooren,M., van Kempen,M., de Krijger,R., Grosveld,F., Tibboel,D., and Rottier,R. 2005. Distal angiogenesis: a new concept for lung vascular morphogenesis. *Am.J.Physiol Lung Cell Mol.Physiol* 288:L141-L149.

232. deMello,D.E., Sawyer,D., Galvin,N., and Reid,L.M. 1997. Early fetal development of lung vasculature. *Am.J.Respir.Cell Mol.Biol.* 16:568-581.

233. Soriano,P. 1999. Generalized lacZ expression with the ROSA26 Cre reporter strain. *Nat.Genet.* 21:70-71.

234. Gaine,S.P. and Rubin,L.J. 1998. Primary pulmonary hypertension. *Lancet* 352:719-725.

235. Archer,S. and Rich,S. 2000. Primary pulmonary hypertension: a vascular biology and translational research "Work in progress". *Circulation* 102:2781-2791.

236. Rudarakanchana,N., Trembath,R.C., and Morrell,N.W. 2001. New insights into the pathogenesis and treatment of primary pulmonary hypertension. *Thorax* 56:888-890.

237. Nichols,W.C., Koller,D.L., Slovis,B., Foroud,T., Terry,V.H., Arnold,N.D., Siemieniak,D.R., Wheeler,L., Phillips,J.A., III, Newman,J.H. *et al*. 1997. Localization of the gene for familial primary pulmonary hypertension to chromosome 2q31-32. *Nat.Genet.* 15:277-280.

238. Loyd,J.E. 2002. Genetics and pulmonary hypertension. *Chest* 122:284S-286S.

239. Zakrzewicz,A., Hecker,M., Marsh,L.M., Kwapiszewska,G., Nejman,B., Long,L., Seeger,W., Schermuly,R.T., Morrell,N.W., Morty,R.E. *et al*. 2007. Receptor for activated C-kinase 1, a novel interaction partner of type II bone morphogenetic protein receptor, regulates smooth muscle cell proliferation in pulmonary arterial hypertension. *Circulation* 115:2957-2968.

240. Seki,T., Hong,K.H., Yun,J., Kim,S.J., and Oh,S.P. 2004. Isolation of a regulatory region of activin receptor-like kinase 1 gene sufficient for arterial endothelium-specific expression. *Circ.Res.* 94:e72-e77.

241. Ivy,D.D., McMurtry,I.F., Colvin,K., Imamura,M., Oka,M., Lee,D.S., Gebb,S., and Jones,P.L. 2005. Development of occlusive neointimal lesions in distal pulmonary arteries of endothelin B receptor-deficient rats: a new model of severe pulmonary arterial hypertension. *Circulation* 111:2988-2996.

242. Ihida-Stansbury,K., McKean,D.M., Lane,K.B., Loyd,J.E., Wheeler,L.A., Morrell,N.W., and Jones,P.L. 2006. Tenascin-C is induced by mutated BMP type II receptors in familial

forms of pulmonary arterial hypertension. *Am.J.Physiol Lung Cell Mol.Physiol* 291:L694-L702.

243. Jones,P.L., Chapados,R., Baldwin,H.S., Raff,G.W., Vitvitsky,E.V., Spray,T.L., and Gaynor,J.W. 2002. Altered hemodynamics controls matrix metalloproteinase activity and tenascin-C expression in neonatal pig lung. *Am.J.Physiol Lung Cell Mol.Physiol* 282:L26-L35.

244. Jonker,L. and Arthur,H.M. 2002. Endoglin expression in early development is associated with vasculogenesis and angiogenesis. *Mech.Dev.* 110:193-196.

245. Alva,J.A., Zovein,A.C., Monvoisin,A., Murphy,T., Salazar,A., Harvey,N.L., Carmeliet,P., and Iruela-Arispe,M.L. 2006. VE-Cadherin-Cre-recombinase transgenic mouse: a tool for lineage analysis and gene deletion in endothelial cells. *Dev.Dyn.* 235:759-767.

246. Jiao,K., Langworthy,M., Batts,L., Brown,C.B., Moses,H.L., and Baldwin,H.S. 2006. Tgfbeta signaling is required for atrioventricular cushion mesenchyme remodeling during in vivo cardiac development. *Development* 133:4585-4593.

247. Fernandez-Lopez,A., Garrido-Martin,E.M., Sanz-Rodriguez,F., Pericacho,M., Rodriguez-Barbero,A., Eleno,N., Lopez-Novoa,J.M., Duwell,A., Vega,M.A., Bernabeu,C. *et al*. 2007. Gene expression fingerprinting for human hereditary hemorrhagic telangiectasia. *Hum.Mol.Genet.* 16:1515-1533.

248. Umans,L., Cox,L., Tjwa,M., Bito,V., Vermeire,L., Laperre,K., Sipido,K., Moons,L., Huylebroeck,D., and Zwijsen,A. 2007. Inactivation of Smad5 in endothelial cells and smooth muscle cells demonstrates that Smad5 is required for cardiac homeostasis. *Am.J.Pathol.* 170:1460-1472.

249. Rudarakanchana,N., Flanagan,J.A., Chen,H., Upton,P.D., Machado,R., Patel,D., Trembath,R.C., and Morrell,N.W. 2002. Functional analysis of bone morphogenetic protein type II receptor mutations underlying primary pulmonary hypertension. *Hum.Mol.Genet.* 11:1517-1525.

250. Sehgal,P.B. and Mukhopadhyay,S. 2007. Dysfunctional intracellular trafficking in the pathobiology of pulmonary arterial hypertension. *Am.J.Respir.Cell Mol.Biol.* 37:31-37.

251. Morrell,N.W., Yang,X., Upton,P.D., Jourdan,K.B., Morgan,N., Sheares,K.K., and Trembath,R.C. 2001. Altered growth responses of pulmonary artery smooth muscle cells from patients with primary pulmonary hypertension to transforming growth factor-beta(1) and bone morphogenetic proteins. *Circulation* 104:790-795.

252. Hartung,A., Bitton-Worms,K., Rechtman,M.M., Wenzel,V., Boergermann,J.H., Hassel,S., Henis,Y.I., and Knaus,P. 2006. Different routes of bone morphogenic protein (BMP) receptor endocytosis influence BMP signaling. *Mol.Cell Biol.* 26:7791-7805.

BIOGRAPHICAL SKETCH

Kwon-Ho Hong was born in Naju city of Jeonnam province, Korea. Then he moved to Seoul when he was 10 years-old, and grew up there. Following graduation from the Gyeongseong high school, he went to the KONKUK University in Seoul where he earned a Bachelor of Science degree in animal science in 1997. He went to the Korean Army in 1991 and served for 28 months. During his college years, he enjoyed an extracurricular activity in a club named "The Workshop" where his passion for the biological science was built up. In 1997, he joined Prof. Hoon-Taek Lee's laboratory at the same university and studied the biological function of Leptin using transgenic mice. He received a Master of Science degree in 1999. In 2000, he originally started a Ph.D. program in the department of Animal Sciences, University of Florida. After two semesters in the department, he moved to Dr. S. Paul Oh's laboratory in the department of Physiology & Functional Genomics in 2001. After one year of working in his laboratory as a research assistant, he reentered the Interdisciplinary Program (IDP) in Biomedical Sciences, University of Florida in 2002. He rejoined Dr. S. Paul Oh's laboratory in 2003. During Ph.D. degree, the majority of his work was engaged in the studies of the *in vivo* role of TGF-β receptors in the vascular biology.